

https://dspace.org/

Characterizing the influence of a prosthesis on the shot put movement

Boulle, Nathanael

2021
https://hdl.handle.net/10539/33001

Downloaded from a DSpace repository. https://dspace.org/



UNIVERSITY OF THE
WITWATERSRAND,
JOHANNESBURG

Characterizing the influence of a prosthesis on the shot put movement

Nathanael Boulle

School of Mechanical, Industrial and Aeronautical Engineering
University of Witwatersrand
Johannesburg, South Africa

Supervisor:
Taahirah Mangera
Co-Supervisor:
Frank Kienhöfer

A dissertation submitted to the Faculty of Engineering and the Built Environment, University of the Witwatersrand, Johannesburg, in fulfilment of the requirements for the degree of Master of Science in Engineering.

October 2020

SCHOOL OF MECHANICAL, INDUSTRIAL & AERONAUTICAL ENGINEERING

PLAGIARISM DECLARATION TO BE SIGNED BY ALL HIGHER DEGREE STUDENTS

SENATE PLAGIARISM POLICY: APPENDIX ONE

I, Nathanael Boulle (Student number: 1914053) am a student registered for the degree of Msc Mechanical Engineering.

I hereby declare the following:

I am aware that plagiarism (the use of someone else's work without their permission and/or without acknowledging the original source) is wrong.

I confirm that the work submitted for assessment for the above degree is my own unaided work except where I have explicitly indicated otherwise.

I have followed the required conventions in referencing the thoughts and ideas of others.

I understand that the University of the Witwatersrand may take disciplinary action against me if there is a belief that this is not my own unaided work or that I have failed to acknowledge the source of the ideas or words in my writing.

Signature: 

Acknowledgements

This project would truly not have been completed successfully without the influence of a number of individuals in my life.

First among these incredible people I must thank my supervisor, Taahirah Mangera, for the patient guidance that she has given me during the challenging circumstances of this year in particular. I am grateful to be her student.

My co-supervisor, Prof. Kienhöfer, I thank you for the expertise and experience you brought to the research which gave it legitimacy far beyond what I could have provided. I am appreciative of your support, most notably in the proposal and editing phases of the dissertation.

Prof. Olivier, you provided assistance which made the experimental section of this project possible. You are an inspiration to me and all of your students. Your enthusiasm for biomechanical research is immense and I am fortunate to have worked with you. Thank you.

To my research participant, without you this dissertation would have no content. Meeting you and working with you has been a highlight of the experience and I am continually motivated by the example you have set by your life.

To my parents, Robert and Janine, I thank you for your dependable love throughout this journey. I am fortunate to be your son and I share any success that I have with you. My brothers, you have kept me grounded and provided me with more support than you know. I am thankful for the presence of each of you in my life.

Abstract

Competitive able-bodied athletes have shown to benefit from biomechanical analysis. However, there is a paucity of research into the movement science of disabled athletes and uncertainty as to whether the biomechanical principles of able-bodied athletes can be applied to disabled athletes. This is true for competitive shot put, which is the focus of this study. This investigation seeks to provide principles for improved shot put outcomes for an athlete using a lower limb prosthesis, and determine whether able-bodied literature can be applied to disabled movement science for the shot put movement. The main biomechanical principles of able-bodied shot put athletes are concerned with segment velocity, centre of gravity (CG) profile, feet sequencing and trunk rotation. Motion data was collected using a Xsens MVN Analyze motion capture system and ground reaction force data was collected using a FDM pressure walkway. The captured data was used to articulate and validate a rigid multibody model developed in Simscape Multibody, a simulation environment provided by MATLAB. The model was lower body specific and computed results including combined segmental velocity data, joint torques, normal forces and frictional forces which were not offered by the motion capture system. The simulation was validated using measured displacements from the Xsens motion capture system as well as measured ground reaction forces measured using the pressure walkway. The principle investigation (Section 7) emphasizes the importance of, and provided mathematical parameters for, the initial glide of the preamble as well as the delivery stride, which are the two primary movements in shot put. Significant areas of influence for the prosthesis are characterized by a reduced delivery stride width, impaired sequential muscle activation and difficulty in providing an effective base from which the upper body segments can extend. The evidence of the investigation indicates that the utilization of able-bodied movement principles is useful in disabled sports science. Moreover, due to this correlation of the the disabled athlete with able-bodied counterparts, the shot put principles can be observed as fundamental theory for any given shot putter, or by extension any projectile based sport.

Contents

1 Introduction **1**
1.1 Background and motivation . . . 1
1.2 Problem statement . . . 2
1.3 Objectives . . . 2
1.4 Delineations and limitations . . . 2
1.5 Plan of development . . . 3
1.6 Nomenclature . . . 4

2 Literature review **6**
2.1 Shot put principles . . . 6
2.1.1 Shot put movement deconstruction . . . 6
2.1.2 Integration of segments . . . 8
2.1.3 Extension of lower extremities and trunk . . . 9
2.1.4 Primary variables . . . 10
2.1.5 CG profile . . . 12
2.1.6 Feet placement . . . 13
2.1.7 Shot put principles summary . . . 14
2.2 Experimental measurement techniques . . . 15
2.2.1 Measurement using video . . . 15
2.2.2 Motion capture (mocap) measurement . . . 16
2.2.3 Force plates and pressure walkways . . . 17
2.2.4 EMG data . . . 17
2.2.5 Experimental measurement summary . . . 18
2.3 Multibody simulation . . . 20
2.3.1 Simplifications . . . 20
2.3.2 Body segment properties . . . 22
2.3.3 Anatomical planes of reference . . . 24
2.3.4 Body joint properties . . . 25
2.3.5 Segment hierarchy . . . 27
2.3.6 Simulation kinematics . . . 28
2.3.7 Simulation dynamics . . . 29
2.3.8 Multibody modelling systems . . . 31
2.3.9 Multibody simulation summary . . . 32
2.4 Literature search summary . . . 33

3 Methodology **34**
3.1 Research design . . . 34
3.2 Data collection . . . 35
3.2.1 Xsens MVN Analyze . . . 35
3.2.2 FDM pressure walkway . . . 35
3.2.3 Data processing and analysis . . . 36
3.3 Rigid multibody model . . . 38
3.3.1 Segment hierarchy . . . 38
3.3.2 Segment properties . . . 39
3.3.3 Joint properties . . . 40
3.3.4 Contact plane . . . 41
3.4 Simulation actuation . . . 41
3.4.1 Simscape Multibody . . . 42
3.4.2 Actuation and validation data . . . 42
3.4.3 Actuation validation and analysis . . . 43
3.5 Principle investigation . . . 44
3.5.1 Simulation results . . . 45
3.5.2 Parametric study . . . 45
3.5.3 Principle investigation summary . . . 50
3.6 Limitations and ethical considerations . . . 51
3.6.1 Ethical considerations . . . 51
3.7 Conclusion . . . 52

4 Data collection **53**
4.1 Movement timescale analysis . . . 53
4.2 Joint trajectory analysis . . . 54
4.3 Data collection conclusion . . . 58

5 Rigid multibody model **60**
5.1 Anthropometric measurements . . . 60
5.2 Segment geometries . . . 61
5.2.1 Definitions . . . 61
5.3 Inertial properties . . . 62
5.4 Joint properties . . . 62
5.5 Rigid multibody model conclusion . . . 63

6 Simulation actuation and validation **65**
6.1 Joint trajectory comparison . . . 65
6.1.1 Right leg joints . . . 65
6.1.2 Left hip and trunk joint motion . . . 67
6.2 Normal force validation . . . 68
6.3 Displacement validation . . . 70
6.4 Actuation and validation conclusion . . . 72

7 Principle investigation **73**
7.1 Simulation results . . . 73
7.1.1 Segment velocity . . . 73
7.1.2 CG displacement profiles . . . 75
7.2 Parametric results analysis . . . 76
7.2.1 Knee flexion during initial glide . . . 76
7.2.2 Hip abduction for delivery stance . . . 79
7.2.3 Trunk rotation for release velocity . . . 81
7.2.4 Prosthesis property parameters . . . 83
7.3 Principle investigation conclusions . . . 85

8 Conclusion **88**
8.1 Summary of investigation . . . 88
8.2 Summary of findings . . . 89
8.3 Conclusions . . . 90
8.3.1 Recommendations for future work . . . 91

9 Appendices **98**
9.1 Appendix A - Regression equations for inertial properties . . . 98
9.2 Appendix B - General model parameters . . . 103
9.3 Appendix C - Simscape Multibody block diagram interface . . . 108
9.3.1 World plane . . . 109
9.3.2 Torso subsystem . . . 110
9.3.3 Right leg subsystem . . . 111
9.3.4 Left leg subsystem . . . 112
9.4 Appendix D - Ethical clearance . . . 113

List of Figures

1 Movement deconstruction with time intervals . . . 7
2 Graph displaying velocities of individual segments . . . 9
3 Visual depiction of the primary variables for an efficient shot put throw . . . 11
4 Visual depiction of the CG profile, give in the XZ plane . . . 12
5 CG profile from the Coh et al. analysis on the rotational technique . . . 12
6 Visual depiction of the feet placement during the movement preamble . . . 13
7 Figure showing the raw output of an EMG . . . 18
8 Opensim gait analysis . . . 21
9 Diagram underlining the need for increased segments if the model is going to align accurately with real joints and segments . . . 21
10 Diagram describing the different geometries of body segments when developing a model . . . 23
11 Diagram illustrating the anatomical frames of reference . . . 24
12 Diagram describing the joint angle categorization and the joint/segment organization for the methodology . . . 26
13 Diagram underlining the complexity of the shoulder joint . . . 27
14 Diagram showing the options when modelling a lower body specific model. . . 28
15 Flow diagrams describing the distinction between forward and inverse dynamics . . . 29
16 Figure depicting the type of normal forces when developing foot contact in a model . . . 30
17 Flow diagram describing Opensim modelling process . . . 31
18 Flow diagram describing the framework used generically for simulation based studies. . . . 34
19 Diagram describing the flow of data gathered from the experiments and simulation. . . . 36
20 Simscape flow diagram for developing a biomechanical model . . . 42
21 Schematic describing the knee flexion parameter . . . 46
22 Schematic describing the trunk rotation velocity parameter . . . 47
23 Contact surface parameter . . . 48
24 Structure of the results and analysis section . . . 52
25 Graph displaying the right foot displacement and velocity metrics. . . . 53
26 Graph displaying acceleration data for relevant segments. . . . 53
27 Graph displaying the filtered data collected for the right ankle. . . . 55

28 Graph displaying the filtered data collected for the right knee. 55
29 Graph displaying the filtered data collected for the right hip. 55
30 Graph displaying the filtered data collected for the left hip. 56
31 Graph displaying the filtered data collected for the pelvis segment. 57
32 Diagram detailing the geometries of relevant segments 61
33 Diagram detailing type and location of joints in the rigid multibody model . 63
34 Right ankle motion trajectory 65
35 Right knee motion trajectory 66
36 Right hip motion trajectory 66
37 Left hip motion trajectory 67
38 Graph displaying the computed normal force in comparison to one of the experimental data sets. 68
39 Graph displaying x displacement comparison 70
40 Graph displaying z displacement comparison 71
41 Right leg segments velocity 73
42 Left leg and trunk segment velocity 74
43 CG profile depicted in the XZ plane 75
44 CG x displacement 75
45 Graph displaying knee flexion trajectories used for the knee flexion parameter. 76
46 Graph displaying friction forces for varying knee flexion angles. 77
47 Graph displaying knee joint torque required for varying knee flexion angles. . 78
48 Graph displaying the combined hip abduction angles used in the hip abduction parameter 79
49 Trunk rotational trajectories used for the trunk rotation parameter 81
50 Graph displaying the trunk angular velocity for differing trunk rotation . . . 82
51 Graph displaying the friction force variance for differing prosthesis surface areas. * legend units: x$10^{-3}m^2$ 84
52 Graph displaying the friction force variance for differing prosthesis friction properties 84

List of Tables

1 Table summarizing the shot put principles identified in able-bodied literature 14
2 Significant joint properties* 25

3 Table detailing the approach used to identify significant landmarks of the shot put movement. 37
4 Xsens measurement descriptions 39
5 Simulation joint types 40
6 Lower body joint data comparison 43
7 Table of prescribed angles used for the hip abduction parameter 47
8 Table detailing geometries of contact surface used 48
9 Table of the friction coefficients to be used for the friction parameter 49
10 Table summarizing investigation approach using the simulation. 50
11 Timescale empirical values 54
12 Waypoint data 58
13 Table detailing the values for the anthropometric measurements used 60
14 Table of inertial properties of segments. * CoM taken from the proximal end of a segment ** Rod moment of inertia about proximal end 62
15 Normal forces at significant landmarks. 69
16 Timescale of significant landmarks in the shot put movement 70
17 Table detailing results based on a varying knee flexion range during the initial glide movement. * indicates the generic flexion used by the athlete. 78
18 Table detailing the results of the hip abduction parameter taken at the left foot landing (LFL) landmark, approximately 0.49 s. 80
19 Table of local maximums denoting throw landmarks for varying trunk rotations. FF = Friction force, AV = Angular velocity 82
20 Prosthesis parameters. *denotes the generic geometry and friction coefficients used. 83
21 Table highlighting the influence of the prosthesis for individual principles. . . 86

1 Introduction

1.1 Background and motivation

Disabled sport offers a unique opportunity for disabled individuals to pursue athletic goals. Such opportunities are important because they showcase the perseverance and courage necessary to overcome mental and physical obstacles. Disabled sport is also an opportunity to raise awareness and dismantle barriers for individuals that are often marginalized by the public. As such, inequality that people with disabilities often need to accept as an unfortunate component of the infrastructure of society has fortunately been addressed in the sporting world. However, there are many ways in which this inclusiveness can be extended to further equalize the professional outcomes of disabled athletes. One such way is the extending the range of implementation of biomechanical sporting analyses to include not only able-bodied athletes, but disabled athletes too. One such way is extending the range of implementation for biomechanical sporting analyses to include not only able-bodied athletes, but disabled athletes too.

Extensive coaching, training and analysis is required for all athletes to excel at a professional level. For many professional athletes, this is guided by biomechanical research. Biomechanical research includes motion analysis and multibody simulation which can facilitate the improvement of athletic performance [1]. In literature, able-bodied shot put analysis has benefited from techniques including video analysis, motion capture and simulated models. In an able-bodied context, biomechanical investigations have been beneficial due to the significant sample set of athletes available which is advantageous when developing empirical results. Such studies have developed principles which reliably improve the performance of able-bodied shot putters.

No published evidence exists verifying whether these principles also extend to disabled athletes. This is largely due to the unique movement as a result of the limitations applied by the prosthesis. Most evident in the nerve damage and differing centers of gravity (CGs) of body segments as a result of the disability. It is also challenging to develop this depth of research for disabled athletes as the empirical results used in able-bodied literature require numerous tests with a large sample to develop suitable accuracy or understanding. In a disabled context, it is challenging to collect a large enough sample to develop analysis which is meaningful. Each individuals movement is unique insofar as no two disabilities are completely the same. This is coupled with a comparatively small amount of funding available for disabled athletes, which means that reliable bespoke investigations are not common.

Due to the modified movement as a result of prostheses, a thorough investigation to understand the effect of prostheses on performance and if principles derived from testing and modeling able-bodied athletes can be applied to disabled athletes is required. This approach will profit from the depth of able-bodied research and apply this to address the paucity of disabled shot put research.

1.2 Problem statement

An evaluation of the applicability of able-bodied biomechanical principles to improve the performance of disabled athletes is required to determine if able-bodied research can benefit disabled athletes or else if new models of the different and unique movement is required.

1.3 Objectives

1. Determine the relevance of able-bodied shot put biomechanical principles on a shot put movement influenced by a lower limb prosthesis
2. Determine the benefit of multibody simulation for a disabled athlete's movement which is not aided by the depth of research from able-bodied literature.
3. Investigate the influence of the prosthesis. In particular, the manner in which the movement has had to be adapted when compared to the movement used by able-bodied athletes.

1.4 Delineations and limitations

Despite the obvious limitation of the loss of a limb, there is substantial room for innovation and a wide range of disabled athletes are able to perform at a highly competitive level with the help of a high performance sports prosthesis.

Should an athlete wish to officially compete, there are regulations limiting the design of the prosthesis. The most pertinent of which is under Section 7 of the World Para Athletics rules and regulations. In sub Section 7.2.1.3 it is stated that all equipment and prosthesis components need to be commercially available to all athletes [2]. Furthermore, a thorough

investigation into the design of the prosthesis is challenging due to intellectual property commitments made by the athlete to the prosthesis design company. This investigation will not attempt to scrutinize the design of the prosthesis.

Sports prostheses are designed to be highly effective in a limited range of movement, where aesthetics and functional movement are not the primary concern. The primary focus is movement that supports performance. Therefore, the current research is focused on a specific athlete with a lower limb prosthesis.

Key simplifications for the modelling phase of the investigation are found in the mechanical properties of the representation. These are detailed in Section 2.3.1. This does present a decrease in the accuracy of the results, however the goal is to accurately represent the movement which would not be possible should these mechanical properties be overly scrutinized.

The study was subject to limited contact time with the athlete in question. This is as a result of time and location constraints on the athlete. An implication of this is that there was only one experimental phase. There was no opportunity for further experiments after the simulation.

1.5 Plan of development

The plan of development describes the investigation sequentially, collecting the relevant sections into understandable portions. This aids in the understanding of the research approach used for the investigation.

The aim for the literature search in Section 2 was to investigate able-bodied shot put principles, experimental measurement techniques and multibody simulations. This provided understanding and substantiation to the movement investigation. The strategy for the research is outlined in the methodology (Section 3), which details the research design, including the approach for simulation actuation and principle investigation.

The body of the report begins with the data collection process described in Section 4. This includes details of the results for data acquisition as well as the processing of the data necessary for simulation actuation and validation. Details of the preparation for simulation are continued in Section 5 with the development of the rigid multibody model. This section

describes the simplifications for the respective segments of the human body to be included in the multibody simulation.

The final two sections of the body detail the strategy concerning the simulation and validation of the multibody model and it's implementation for the purposes of the investigation. The validation process (Section 6) investigated simulated data against experimentally acquired data in order to verify the accuracy of the simulation. The crux of the dissertation is the principle investigation (Section 7), where pertinent able-bodied principles were scrutinized in the simulated movement. The research is summarized in the conclusion and significant results are clarified along with recommendations for future work.

1.6 Nomenclature

Detailed below are terms referenced in the report. These expressions are important for an understanding of the movement and investigation strategies used.

Acceleration path: The preamble to the shot put throw where the shot is being accelerated with a velocity of zero, relative to the athlete.

Adduction: Movement of a segment toward the midline of the body.

Abduction: Movement of a segment away from the midline of the body.

Anthropometric measurements: Body measurements for segment dimensions.

Delivery stance: A movement parameter that is also a principle of able-bodied literature. Takes place as the left foot lands and offers a foundation from which release takes place.

Distal: Further away from the center of gravity. Opposite of proximal.

Extension: Increase of angle between two segments.

Flexion: Decrease of angle between two segments.

Initial glide: A movement parameter where the athlete jumps and lands on the right foot to gain momentum for rotation and increase the acceleration path of the shot.

Joint trajectory: Profile of a given angle during a movement, plotted against time.

Movement landmark: Significant points in the movement preamble. Including:

- TO (take off) - the athlete begins the initial glide movement whilst balancing on the right foot by flexing the right knee and jumping toward the center of the shot put circle.
- RFL (right foot lands) - the athlete completes the initial glide jump by landing on the right foot. It is here that the trunk rotation is initiated.
- LFL (left foot lands) - halfway through the rotation the left foot lands for the first time and the delivery stance is formed, with both feet on the ground. This is the base from which the lower body segments extend.
- SR (shot release) - building on top of the trunk rotation, the upper body segments extend resulting in the release of the shot put.

These movement landmarks are detailed in Section 2.1.1.

Multibody simulation: Numerical simulation where a system of connected bodies are actuated.

Parameter: Significant characteristic of the shot put movement that is measurable and lends itself to experimentation.

Principle: Significant 'rules of thumb' for shot put provided by able-bodied literature.

Proximal: Closer toward the center of gravity. Opposite of distal.

Segment: Singular component of multibody system.

Segment hierarchy: Organization and ordering of segments used to model a multibody simulation.

Waypoint: One of nine points in a given joint trajectory where motion is prescribed for actuation in the simulation.

2 Literature review

2.1 Shot put principles

The shot put has been an Olympic event since the first modern Olympics in 1896. The aim can be simply defined as propelling a mass as far as possible. In the 18th century the sport evolved from throwing stones to throwing cannonballs and hence the name 'shot' was derived [3]. Crucially, the propelling technique is described as a 'put' rather than a 'throw'. When considering a throw, the mass would start behind the line of the shoulders whereas in the putting technique the mass starts in line or in front of the shoulders.

When concerning shot put technique, the rotational technique was developed in the mid 20th century and is used today. This involves facing opposite to the required direction and rotating to gain speed and momentum prior to the throw. Prior to the rotation technique, the simpler 'glide' technique was used and is still used in some cases. This technique is used by the athlete in question and is described in further sections [4].

In all descriptions below a right handed shot putter is described. Should the shot putter be left handed, then the movement phases are inverted suitably. For the sake of eloquence, in the following sections, a shot put 'throw' and a 'put' will be used interchangeably.

The purpose of this section is to provide context and understanding to the movement for reference in further sections. In addition, able-bodied shot put principles or 'rules of thumb' are highlighted.

2.1.1 Shot put movement deconstruction

The shot put is released through the sequencing of distinct body segments and joints, performing individually or simultaneously to accomplish the task of propelling the shot . Within able-bodied literature, an investigation by Lanka [4], deconstructed the glide technique into phases. These phases are delineated by movement landmarks, which have been adopted by this research. The movement landmarks are significant components of the movement which have a fundamental impact on the outcome of the throw. These are detailed in Figure 1 followed by a description.

Movement landmarks

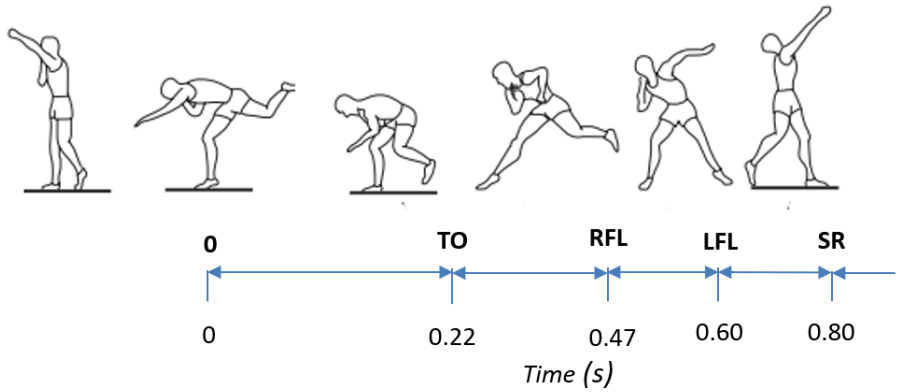


Figure 1: Movement deconstruction with time intervals

Take off (TO) - is the phase prior to the first glide movement and involves the activation of the muscular resources in the right leg and the extension of the knee angle to jump toward the center of the shot put circle. There is debate on the function of this phase, however the kinematics of the glide phase is integral to an efficient throw.

Right foot lands (RFL) - the right foot lands and initiates the rotation that extends through the hips. This rotation generates angular momentum until the eventual release. Simultaneously, the hips direct the next phase which is the left foot landing and delivery stance.

Left foot landing (LFL) - the transition in this phase is from a singularly supported position to one that is double supported for the first time in the throw. This is known as the delivery stance. After the left foot lands, the right leg extends for the second time and the CG is shifted onto the left leg. It is at this phase of the movement where the prosthesis has the most significant influence.

Shot put release (SR) - the culmination of all prior movement ends in a powerful release. This phase is initiated by the rotation of the hips through 90° which is followed by the subsequent rotation of the trunk, shoulders and the extension of the upper extremities [7].

This deconstruction is important, not only for the understanding of the movement, but also for reference in further sections of the report.

2.1.2 Integration of segments

During the shot put movement, there is crucial integration of the segments available which results in a powerful release. In interpretation of the glide technique, a powerful movement depends on:

1. Extension of lower extremities and trunk,
2. Rotation of the trunk, and
3. Extension of the throwing arm [4].

The synthesis of these movements is fundamental to increasing the release velocity. Broer [8] raised three important points for an idealized integration of these systems:

1. If release velocity is to be maximized, the articulation of an arbitrary body segment should start at the moment the segment immediately prior reaches maximum speed. This is described in Figure 2 from a shot put study by Zatsiorsky et al. [9] where the velocity of segments cascades (up the body) until release takes place.
2. It is not efficient to engage weak segments in preference to stronger ones.
3. At the point of release, the segments of the lower extremities and trunk should remain fixed, allowing for the extension of the upper extremities to have a stable base. This is also depicted in Figure 2, where the knee and hip segments both decrease to a lower velocity at release [8].

A further principle, underlined by Coh et al. [10], is that the activation (velocity) of segments begins far away (distally) from the point of release and 'cascades' through the intervening segments during the movement. This principle is known as the proximal-distal sequence of muscle chains [10]. This theory is illustrated in Figure 2 and holds true for motion in other sports. For example, in soccer, when kicking, the upper limbs provide momentum in the preamble to the kick, followed by the fixing of non-kicking foot finishing in a powerful kick by the kicking leg [11].

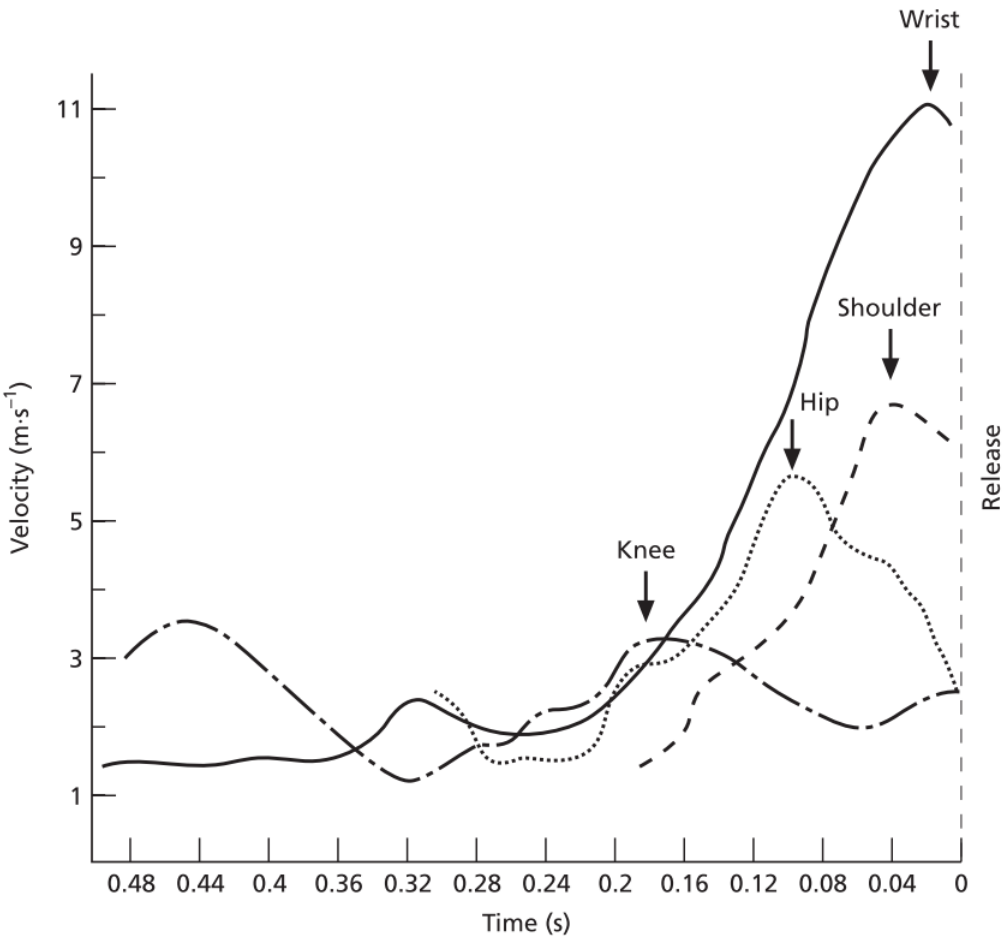


Figure 2: Graph displaying velocities of individual segments

2.1.3 Extension of lower extremities and trunk

The prosthesis interfaces with the ground and uses the reaction forces in the recruitment of the lower body. The recruitment of the lower body and trunk are important in many projectile sports such as cricket, baseball, javelin and discus. The same movement is significantly less effective in any one of these sports without preamble such as a run up or crouch [12]. When considering shot put, the shot (mass) remains stationary relative to the thrower until the eventual release, the upper body activates at the final moment for the throw. For the movements entire preamble, the lower body and trunk are generating momentum and a foundation for a powerful release. When considering the influence of the prosthesis on the movement, it is in this extension where the modifications would need to take place and where meaningful investigation is focused.

Benefits of the left knee and ankle joints

Most notably for the athlete in question, the flexion and extension of the left knee and ankle are not present. The flexion and extension of the knee is small during the shot put movement and remains rigid and is relatively inconsequential compared to the ankle. [13].

The ankle is a complex joint that allows the foot to be able to function both as a rigid lever arm during propulsion and as a mobile adapter during weight acceptance. Mobility is important for absorbing the ground reaction force (GRF) as well as propulsion of the body. Stability is necessary to provide a balanced base for the function to take place [14]. The left foot and ankle have this influence in the final 10% of the movement where the throw takes place. It is critical that the left foot and lower limb provide stability for a powerful release.

Estimated influence of prosthesis

Using the information discussed, concerning the benefits of the left knee and ankle joints, an estimation for the influence of the prosthesis could be made prior to the investigation.

The influence of the prosthesis on the movement is most notable in the second half of the movement at LFL (0.3 s). At this point the left foot of the athlete encounters the ground and the delivery stride is established. It is expected that the stability and width of the delivery stride will be influenced at this point of the movement.

Further in the movement (0.5 s) the right foot leaves the ground and the athlete is entirely supported by the left leg (and the prosthesis). Here, the rotation needs to be concluded by a powerful release and it was expected that the rotation velocity and size would be hindered by the stability (or lack thereof) of the prosthesis.

2.1.4 Primary variables

The flight of a shot directly after release is accurately described by projectile motion theory which yields important variables for the shot put movement. These variables are the release velocity, angle and height, illustrated in Figure 3 [15].

Of these variables, the magnitude of release velocity or simply the release velocity, is the most important as the distance of the projectile is directly proportional to the velocity squared.

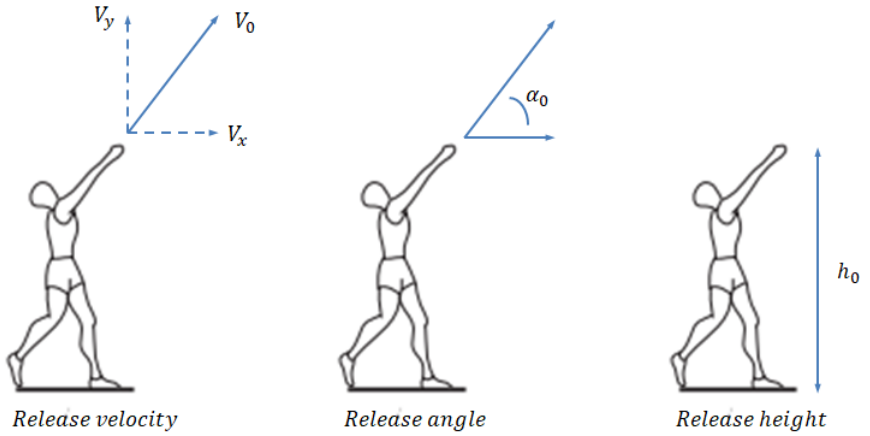


Figure 3: Visual depiction of the primary variables for an efficient shot put throw

This is evident in literature where Lanka quotes results of an increase in shot length by as much as a factor of 2.5 in some cases [4]. The release velocity is dependent on the velocity of the movement preamble. The angular velocity of the trunk is converted into translational velocity at release through the extension of the upper body (throwing arm). Typically when concerning elite throwers, the release velocity tends to be in the range of 12.5 m/s to 14 m/s, resulting in distances of +/- 20 m [4].

When concerning the release angle, there has been much debate in literature concerning an optimal value, particularly as it is arguably the easiest parameter to manipulate. This value has been quoted as between 37° to 41° in Lankas report [4] and +/- 35° in the Coh et al. study [10]. However, a report by Bartonietz [16] on the 1995 World Championships largely negated the effect of significant deviations of the optimal release angle. In the report, a range of 29° to 41° was quoted without correlation to an increased shot distance [16].

Through a comparative study of two different shot put athletes, Coh et al.[10] drew the conclusion that anthropometric measurements, such as overall height and throwing arm length, have the most significant effect on the release height.

The variables highlighted above are not strictly shot put principles. The distinction being that principles, described further sections, are components of the movement used for the increase of any of the aforementioned variables, ultimately increasing shot distance.

2.1.5 CG profile

The CG profile refers to the principles of the movement which govern the trajectory of the center of gravity of the athlete.

This can be perceived in the XY, or XZ plane. The CG profile has been investigated in the shot put reports by Lanka [4] and Coh et al. [10]. Furthermore, it has been referred to in biomechanical research of other projectile sports, notably referenced in reports by Worthington [17] and Mero et al. [18] on bowling and javelin respectively.

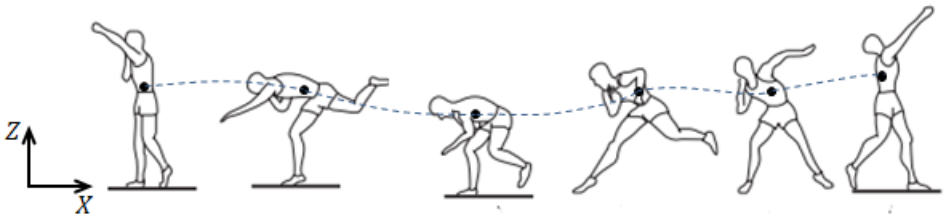


Figure 4: Visual depiction of the CG profile, give in the XZ plane

XZ plane: In literature an 'S' shaped or sinusoidal profile has been seen to be beneficial, where the 'height' or maximum displacement in the z axis, takes place at release to maximize that variable (release height) [19]. This is illustrated in Figure 4 from a study on the shot put technique by Coh et al.[10].

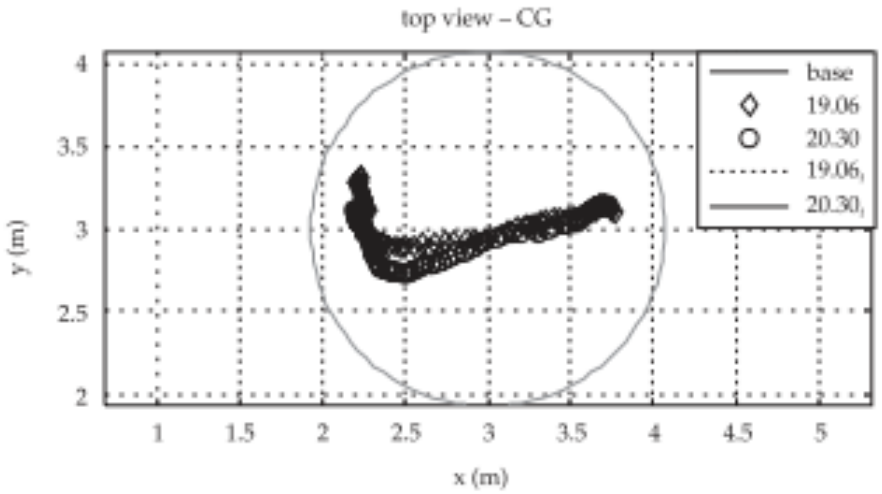


Figure 5: CG profile from the Coh et al. analysis on the rotational technique

XY plane: The profile or trajectory of the CG in the XY plane is expected to maintain a uniform direction in the lead up to release. Irrespective of the recruitment of the various muscular resources in the build up, the CG should maintain directional uniformity to ensure that the shot is aimed efficiently. This is described in Figure 5 from the report on Coh et al. [10] describing the rotational shot put technique.

2.1.6 Feet placement

The following principles refer to the base of the footwork and sequencing of the movement. These are drawn from studies by Zatsiorsky et al. [9] and Lanka [4]. There are two significant feet placements in the movement, separated by a rotation.

- Initial glide (TO-RFL) - taken as the displacement from take-off (TO) to right foot landing (RFL). This moves the athlete toward the middle of the circle as shown in Figure 6.
- Rotation phase (RFL - LFL) - here the athlete rotates, starting from the right foot through the hips, eventually to the shoulders and right arm where the release takes place.
- Delivery stance (LFL) - measured as the displacement between the left and right feet upon left foot landing. It is significantly influenced by the prosthesis, illustrated in Figure 6.

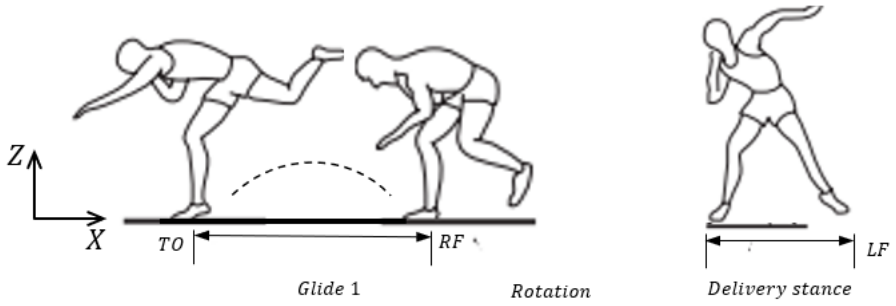


Figure 6: Visual depiction of the feet placement during the movement preamble

The purpose of the feet sequencing preamble is to increase the path of the acceleration of the shot put using the entire body [9]. The path of acceleration is the profile that the shot takes in the preamble of the movement where the activation of the muscles of the athlete

is applying acceleration to the shot. This ensures that whilst the relative velocity of the shot put is still zero, the release velocity is increased substantially. All of the above feet placement phases are important principles of the shot put movement and are well accepted by able-bodied literature.

2.1.7 Shot put principles summary

A summary of principles which improve shot put performance is given in Table 1. It is through the principle investigation that these principles are evaluated with respect to the athlete in question.

Table 1: Table summarizing the shot put principles identified in able-bodied literature

Principle	**Description**	**Relevance**	**References**
Segment velocity sequencing	The articulation of an arbitrary body segment should start at the moment the segment immediately prior reaches maximum speed. At the point of release, the segments of the lower extremities and trunk should remain fixed, allowing the extension of the upper extremities to have a stable base.	Integration of segments	Broer [8]
'S' shaped z displacement profile	In literature an 'S' shaped or sinusoidal profile has been seen to be beneficial, where the 'height' or maximum displacement in the z axis, takes place at release in order to maximize the release height.	CG displacement, release height	Lanka [4] Coh et al. [10] Terzis et al. [20]
x displacement profile uniformity	The CG should maintain uniformity in direction in order to ensure that the shot is directed efficiently in the correct direction.	CG displacement	Coh et al. [10]
Initial glide activation	This principle involves the activation of the muscular resources in the right leg and the extension of the knee to jump on the right leg toward the center of the shot put circle.	Feet placement	Terzis et al. [20] Lanka [4] Sugumar [21]
Delivery stance activation	This principle is measured as the displacement between the left and right feet upon the left foot landing. It is here that lower extremities are activated immediately before the release.	Feet placement	Lanka [4] Schaa [10]
Trunk rotation	Through the majority of the second half of the movement, the athlete rotates through almost 180°s. This angular velocity is converted into the linear velocity required for release.	Feet placement, release velocity	Zatsiosky et al. [9] Sugumar [21] Terzis et al. [20]

The next section discusses relevant experimental measurement techniques used by previous movement investigations.

2.2 Experimental measurement techniques

For professional athletes, using experimental measurement has proven to be invaluable and can support coaching by providing objective feedback. The systems described in this section are summarized below:

- Measurement using video
- Motion capture using high speed cameras or inertial sensors
- Force plates and pressure walkways
- EMG data acquisition

The aim for this section is to provide context to the system which supported the multibody simulation.

2.2.1 Measurement using video

Since its inception, movement experimentation using video analysis has played an important role in the coaching and development of athletic technique. This is due to the ease at which it can be paused, replayed and slowed down, allowing both the athlete and coach an opportunity to observe a given movement without requiring the athlete to recreate it repeatedly. A limitation of video analysis is that kinematic data cannot be computed accurately.

If kinematic data is to be approximated, the video can be altered or filtered in order be observed more simply. It is distinct from motion capture as motion capture typically involves back end algorithms that will further process the data into useful metrics such as joint angles, segment velocity and acceleration. Video analysis in this context refers to the simplifying of videos into component parts to focus on the important parameters of the technique. This is done using filtering techniques after the video has been taken [22]. These techniques however also do not provide outputs that are sufficiently accurate and there is limited evidence of them being reliably used in literature.

2.2.2 Motion capture (mocap) measurement

Motion capture has proven to be the foundation for much research concerning human movement science and is widely used in the athletic community. It achieves invaluable experimental measurement by extracting a mathematical representation for a given movement. Typical uses of motion capture include sports movement science, rehabilitation, robotics and ergonomics [23]. The following sections describe types of motion capture systems available.

High speed camera systems

Also known as optical systems, high speed camera systems operate by identifying alternate contrasts that are produced by reflective markers attached to the subject. Kinematic information must be inferred through the relative position of the markers [17].

Systems using optical means provide an accurate representation for the movement of a marker on a given anatomical landmark. The primary limitations for these systems are as follows:

- Resolution. An increased camera resolution results in more detail being ascertained of the marker. This is essential if the markers are close together, or challenging to distinguish.
- Marker adhesion. This refers to the means by which the markers are located on the subject. An adhesive is required which does not obscure the reflective marker. Miller [24] and Tranberg [25] both highlight the limitation of ensuring that adhesives don't move relative to the bony landmark being tracked.
- Testing infrastructure. The apparatus is limited to environments where cameras can be fixed in the required positions. This infrastructure can prove to be extensive, with numerous cameras at regular locations around the activity.
- Expense. Most fundamentally, these systems are limited by expense. Not only is the hardware costly, the data is needed to be processed into useful metrics which requires additional software licensing .

Sensor based motion capture analysis

Motion capture systems using inertial measurement units (IMUs) approximate the position and orientation of each segment by applying the result of a sensor-to-segment calibration

procedure to an estimate of sensor orientation [26]. Built in algorithms infer kinematic results from the sensor feedback when implemented in conjunction with the calibrated biomechanical model. Three-axis sensors placed on the body each include:

- Accelerometers which measure the translational acceleration vector of individual sensors.
- Gyroscopes that determine angular position and change in position of sensors relative to one another.
- Magnetometers which measure the magnetic field vector for wireless acquisition of the data [27].

There has been limited investigation of detailed biomechanical modelling when using kinematic inputs from IMUs. IMU based systems are not heavily dependent on external infrastructure such as cameras which allows athletes to be tested in a training environment [28].

2.2.3 Force plates and pressure walkways

Force plates/platforms measure the ground reaction force using either piezoelectric transducers or strain gauges. An important metric when using the force plate, other than the generic vectors F_z, F_y and F_x is the center of pressure (CoP). The center of pressure mirrors the center of mass on the force plate and thus is a good measure of the variation of the center of mass (CoM) in the X/Y plane [29].

Force plates and pressure walkways are used in numerous applications, including gait analysis investigations. A gait analysis by Fry et al. (2016) analyzed force plate data in order to validate a motion capture system [30]. This aligns with studies using force plates with motion capture systems to present a more thorough understanding of the movement.

2.2.4 EMG data

Electromyograms (EMGs) refer to the measurement of electromyographic signals released by muscle fibers prior to contraction. This results in a representation of the magnitude of activation for a given muscle. It does this by using electrodes which are placed on the skin overlying the muscle and detects changes in the electrical potential of the muscle fibers.

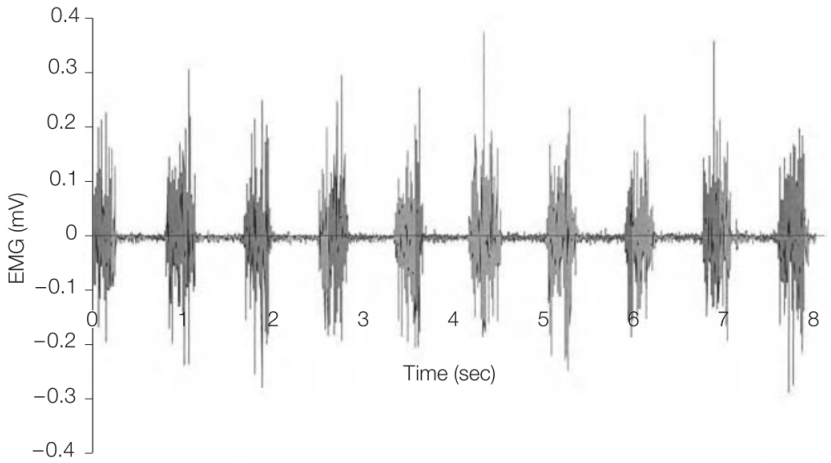


Figure 7: Figure showing the raw output of an EMG

A generic output is displayed in Figure 7 [29]. A limitation regarding EMG measurement is that recordings of dynamic contractions generally decrease the stability and reliability of signals. This is as a result of the rapid recruitment and de-recruitment of different motor units. Essentially, even if electrodes are based close to the belly of the muscle in question, it is possible that the detected signal may be disturbed by signals from other, sometimes distant muscles. This is especially important when recording potential from muscles that are obstructed by subcutaneous fat [31].

2.2.5 Experimental measurement summary

For the current research, experimental measurement was required to provide data that guided a simulation. The key requirements considered for the motion capture resources used in the current research are outlined below:

1. Must be operated remotely. Testing conducted at a genuine facility was more likely to produce reliable results.

2. Must be inexpensive and accessible. There was not sufficient funds available for a new or novel motion capture system to be sourced.

3. Must sample at a rate of 100 Hz or higher. The simulation required inputs at intervals of roughly 0.1 s and therefore a sampling rate of greater than 100 Hz was used.

4. For useful results to be obtained, the required output metrics must include: segment velocity/acceleration, angular velocity/acceleration and spatial coordinates. The positional trajectory data was the most important input for the modelling process [32].

5. Must output, or work in conjunction to, a system that outputs dynamic measurements such as ground reaction forces. This was important for the validation of the computed data.

When considering video analysis, while this form of analysis is affordable and available, it does not provide reliable kinematic data. Accurate kinematic feedback is a requirement of the analysis system decided upon. In addition, the cameras available do not offer a high enough frequency feedback, typical frequencies offered are approximately 60 Hz.

In terms of motion capture systems, whilst optical systems have been used extensively in literature for movement investigations, they are limited by expense and availability. Conversely, an inertial sensor based system was made available to the primary investigator of this study.

In an investigation using inertial motion sensors, Fisher [32] garnered invaluable kinematic results. However, there is little evidence of this investigation or others integrated a inertial motion capture system with dynamic (force) or EMG measurements.

EMG has been used in movement simulations as a means for validating the computed dynamics of the simulation [31]. However, the use of EMG is outside of the scope for this investigation. It would be best suggested for a project where there was a shared objective with a team specializing in the physiology of the skeletal muscles. A force plate is a suitable alternative when attempting to find empirical dynamic results.

2.3 Multibody simulation

Multibody simulation refers to the simulated movement of a system of segments or bodies that interface through a variety of different joints and prescribed conditions. Commonly used in robotics, the advantages, simplifications and implications of this approach for biomechanical analysis are outlined in this section.

Advantages and disadvantages for simulation based studies

It is challenging to accurately measure exact muscle forces using a motion capture or EMG data acquisition system [33]. A biomechanical simulation can compute muscle force and torque using built in algorithms on a predetermined rigid multibody system that is aligned as close as possible to reality. These force and torque computations are typically not available from a motion capture procedure. The simulation can take place as many times as necessary and manipulated to articulations that are not possible for humans to perform experimentally [40]. Furthermore, joint angles are prescribed which includes malleability to the investigation that is not available to typical movement investigations where joint articulations are usually represented by a complex combination of reference frames.

The primary pitfall of simulation based studies is the accuracy that the simulation possesses when compared to reality. This is exacerbated by simplifications that are required to reduce these complex movements into something that can be represented numerically [34].

2.3.1 Simplifications

Simplifications for properties of segments, joints and articulation are required to represent the human body mathematically. Key simplifications are outlined below:

Biological immeasurability

When developing a model of the human body, increasing the number of tendons, ligaments and muscles increases the complexity of the model. This is illustrated in Figure 8, where Delp et al. [35] used an Opensim model with 92 musculotendon actuators to analyze gait. Therefore, when representing a movement mathematically, a compromise needs to be reached between model accuracy and simplicity.

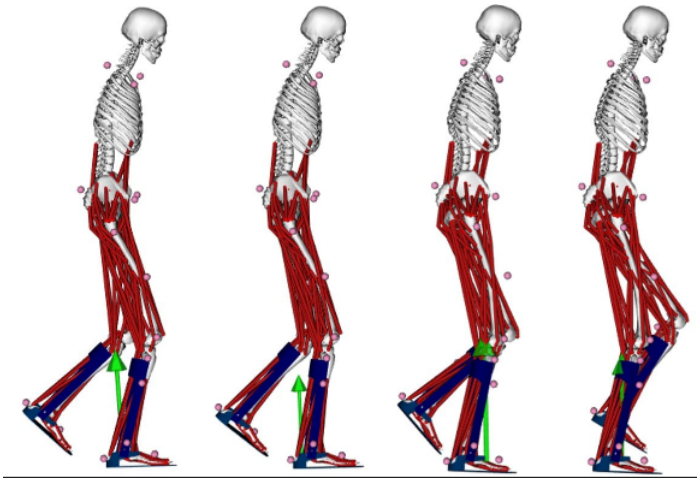


Figure 8: Opensim gait analysis

Segment inclusion

During motion, a number of the human body's muscles, bones and tendons are being recruited simultaneously to assist with the movement. Therefore, in addition to simplifying the exact material composition and geometric properties of body segments, the number of muscles and bones being represented needs to be limited. For instance, the vertebral column or spine will be modelled as one continuous beam as opposed to the 24 vertebral segments which is true for reality [36]. This simplification is detailed in Figure 9, where it is shown that increasing the number of segments aligns better with reality.

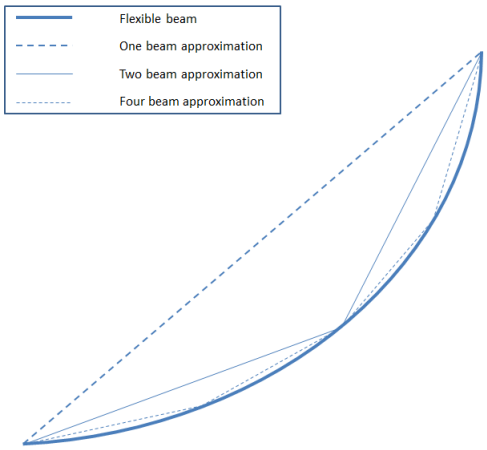


Figure 9: Diagram underlining the need for increased segments if the model is going to align accurately with real joints and segments

Rigid bodies

A further simplification is to assume that system is composed of rigid beams linked by joints. An implication of the rigid beam simplification is that the center of mass of a given rigid body is taken as a point mass. In addition, the joints or linkages are assumed to be frictionless.

Degrees of freedom

It is challenging to determine the exact degrees of freedom for the human body. The number of joints present results in an almost endless possibility of articulations. In any model, as soon as a joint between two segments is included, the degrees of freedom for the distal segment in relation to the proximal segment needs to be stipulated, in addition to a local coordinate frame. This can increase exponentially when attempting to represent the human body mechanically.

Other simplifications

A significant unknown for human movement modelling is the exact dynamics of muscle activation. An active muscle representation is challenging to accurately determine for simulation due to the uncertainty concerning the recruitment of the muscle resources during a given contraction. These variables can fluctuate for a number of reasons for a single athlete based on genetics, fatigue, stress, diet etc. The exact simplifications and approximations are made clear in the methodology.

2.3.2 Body segment properties

To analyze moments and forces on a given joint, the segment must be represented at least by a singular line with a mass and moment of inertia. The progression of which is described in Figure 10. If kinematic parameters or force/power need to be analyzed, the model segments increase in complexity into three dimensional shapes or representations [39].

When considering the properties of segments there are two important sections: geometry and mass/inertia.

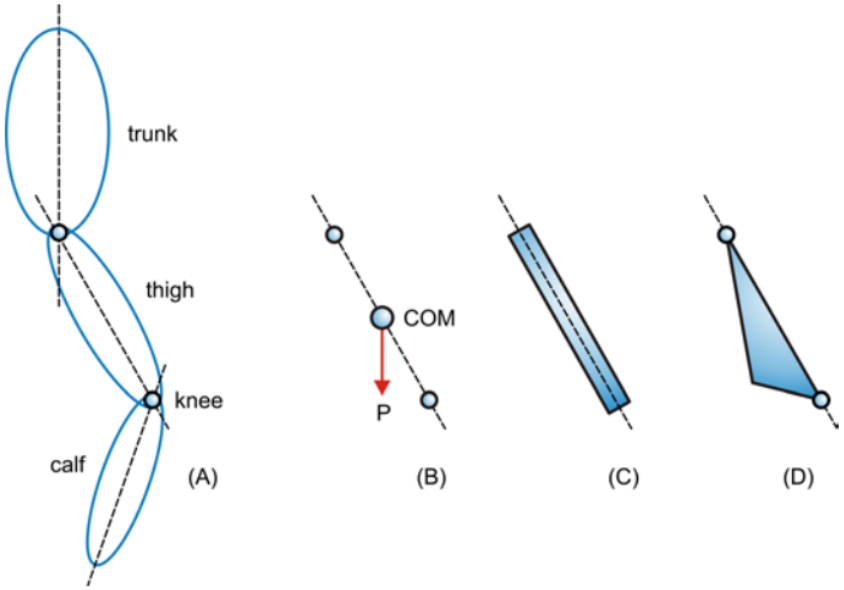


Figure 10: Diagram describing the different geometries of body segments when developing a model

Geometry

To be effective, motion capture systems attain approximations for the geometry of segments. These systems generally require measurements for calibration procedures that through the use of built in algorithms, generate the required measurements. A report by Karatsidis et al. [37], details the use of a least squares optimization method between the model and input marker positions. A mathematically-intensive technique such as least squares optimization is not a requirement of this study. The geometry is shown to be modelled sufficiently accurately in Section 5.

For biomechanical modelling, many of the required measurements are challenging to attain as they concern the bones and joints of the subject. The length of segments are a significant metric to the model as they play a role in the dynamic computations of torque.

Mass and Inertia

The literature study indicates numerous means for approximating properties for model segments. These methods include medical imaging techniques or empirical investigations on cadaver samples.

Two methods were suggested for the determining of segmental mass and inertia properties. The first uses regression equations determined by Zatiorsky [38], an example of which is shown in Equation 1. The equations take multiple segment measurements into account as coefficients to develop accurate approximations for segment properties [38].

$$Y = B_0 + B_1 X_1 + B_2 X_2 \qquad (1)$$

Where:
B_x =*Empirical coefficients*
X_1 =*Body mass (kg)*
X_2 =*Body height (cm)*

The second method investigated uses a general inertial value for the segment. The value used is rendered empirically with respect to the individuals anthropometric measurements. The mass is then obtained using the length of the segment. The inertia is taken from the proximal joint and is generally represented as a rod on a pin.

2.3.3 Anatomical planes of reference

The planes of reference or coordinate systems are vital for accurate translation of collected data. In addition, well defined coordinate systems facilitate a better understanding for the results. Figure 11 describes the coordinate frames used for descriptions of movements.

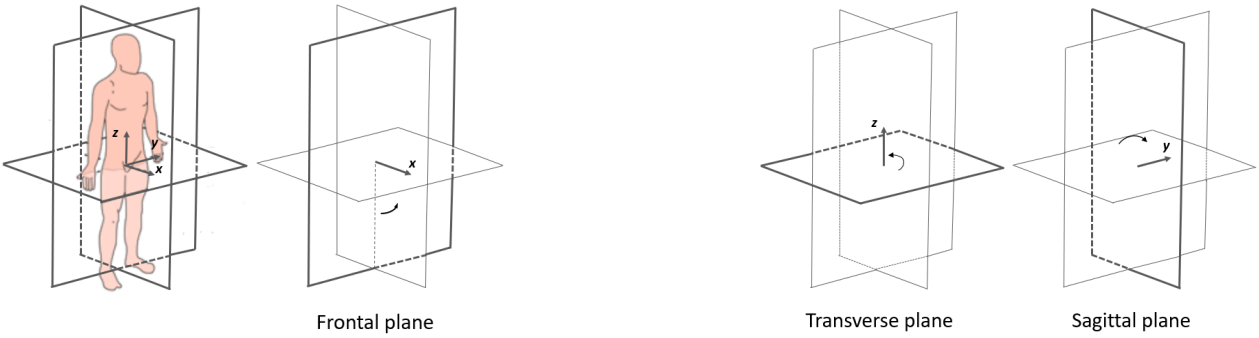


Figure 11: Diagram illustrating the anatomical frames of reference

- Abduction/adduction occurs in the frontal plane. Where abduction is the movement of segment away from the median line and adduction the movement of a segment towards.
- Rotation takes place in the transverse plane where the segment rotates about the z axis.
- Flexion and extension occurs in the sagittal plane and is described relative to the proximal segment. Flexion takes place where the angle decreases between the segments, extension where it increases.

In the sections that follow, the definitions described above for the anatomical frames of reference will be used [39].

2.3.4 Body joint properties

The primary points of consideration when concerning the joints of a rigid multibody model are the degrees of freedom (dof) prescribed to them. This is prescribed mobility and not to be confused with constraints of segments. The dof for joints can vary depending on joint function. This is described in Table 2.

Table 2: Significant joint properties*

Articulation description	**Function**	**Type**
Upper body		
Shoulder	3 dof, flex-ex, add-abd, rot	Ball-socket
Elbow	2 dof, flex-ex, sup-pro	Complex
Wrist	2 dof, flex-ex, add-abd	Complex
Metacarpophalangeal	3 dof, flex-ex, add-abd, rot	Ball-socket
Inter-phalange	1 dof, flex-ex	Hinge
Lower body		
Hip	3 dof, flex-ex, add-abd, rot	Ball-socket
Knee	1 dof, flex-ex	Hinge
Ankle	1 dof, dorsi-plantar	Complex
Subtalar	1 dof, sup-pro	Complex
Tarsals-metatarsal	2 dof (U)	Complex
Metatarsophalangeal	3 dof, flex-ex, sup-pro, rot	Ball-socket
Inter-phalangeal	1 dof	Hinge

*Note: dof = degrees of freedom, U = uncertain, flex-ex = flexion-extension, add-abd = add/abduction,rot = rotation, sup-pro = supine-pronate, dorsi-plantar = dorsi/plantarflexion

Each degree of freedom refers to an individual data point or angle, these angles are represented using the anatomical reference frame standards. Where joints are represented mathematically, friction is largely taken as negligible. Degrees of freedom are applied by bone geometry in conjunction with muscles and tendons.

Joint angles

Joint angles are described relative to the proximal segment. For instance, the relevant segments for the hip joint are the upper leg and the trunk [24]. This generates an angular position that can be described in one of the frames of reference described above.

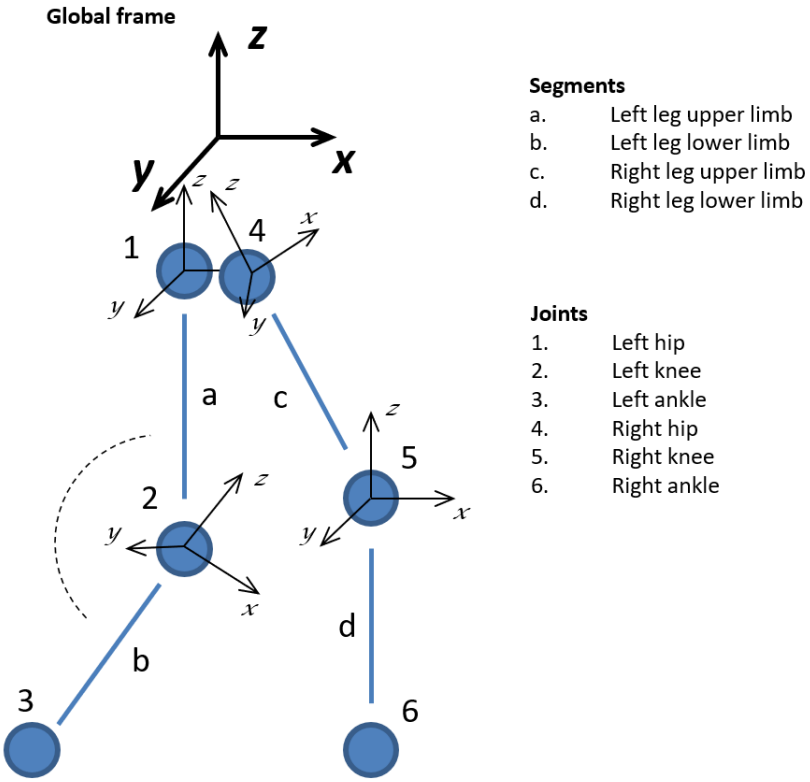


Figure 12: Diagram describing the joint angle categorization and the joint/segment organization for the methodology

In Figure 12 an example multibody model is provided to give a visual description of the segment-joint interface, including the relevant coordinate frames. The left knee joint is highlighted, represented as the angle between the left leg upper and lower limbs. The angle represented is a flexion angle, apparent due to the sagittal reference frame (XZ plane). The

figure includes a categorization of the local coordinate frames at the joints with reference to the global coordinate frame taken at the model CG.

Further considerations when concerning joints are the centers of rotation which are dependent on the efficacy of the anthropometric measurements and segment geometries. Another metric to be reviewed is the stiffness and damping coefficients of joints. It is not within the scope of this study to investigate these points thoroughly [39].

2.3.5 Segment hierarchy

The segment hierarchy is the decided upon organizing of the segments and joints into a multibody system that, when motion is prescribed, represents the required movement accurately. The segment hierarchy is an integral part of all movement investigations and has implications on the final results and analysis. The shoulder, elbow and wrist joints (upper body) are highly complex, with numerous degrees of freedom and poorly understood articulations as shown in Figure 13. Miller et al. [24] underlines that there is no universally accepted standard for the description of shoulder joint angles [24].

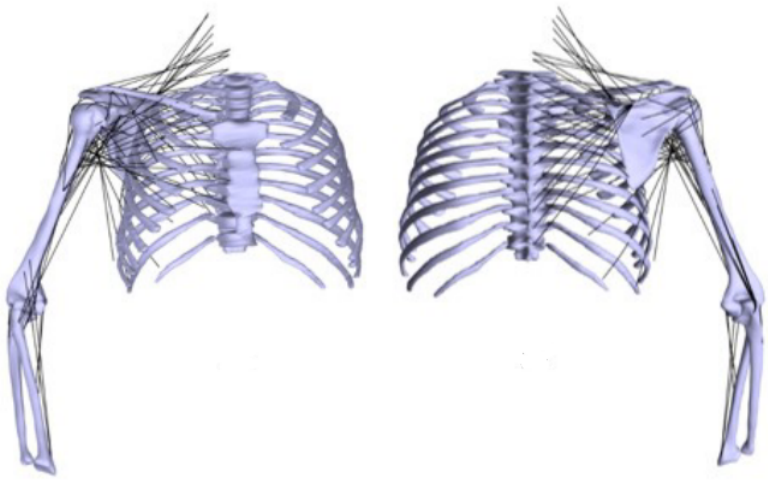


Figure 13: Diagram underlining the complexity of the shoulder joint

It is for these reasons that one might consider developing a lower body specific model as these segments and joints articulate in ways that are far more predictable and easier to represent. Once eliminating the upper extremities, there are still multiple considerations when

concerning the modelling of the trunk. These considerations have fundamental effect on the center of mass of the model, an approximation of which is shown in Figure 14.

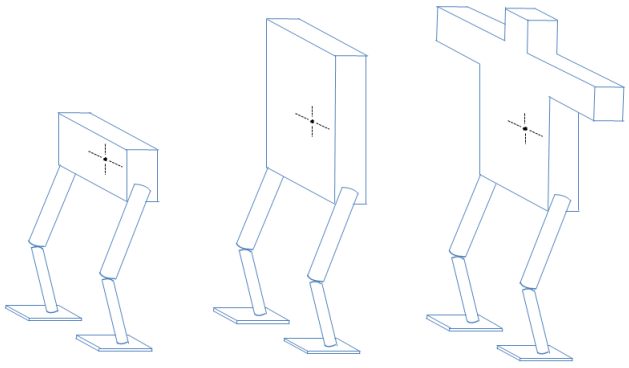


Figure 14: Diagram showing the options when modelling a lower body specific model.

2.3.6 Simulation kinematics

The kinematics of a multibody system concerns the motion of a point, body or system of bodies in the system. In this context the 'body' of multibody is defined as a rigid segment of which there are any number used to construct the mechanical system used.

Distinct from multibody dynamics, kinematics is particularly concerned with the portrayal of motion coordinates of spatial positions and velocities. It uses these descriptions in such a way that a simulation software may compute motion under prescribed conditions.

Forward and inverse kinematics

Multibody kinematics can be applied to a model in a forward or inverse manner. With knowledge of joint rotation, link connection and link length, forward kinematics can be used to determine the position of any segment in space.

Inverse kinematics is a more complex method for determining spatial coordinates. Given a collection of spatial quantities, the objective for inverse kinematics is to find the 'best fit' coordinates and velocities that satisfy both the spatial limitations and the system constraint equations [40].

The follow on section from multibody kinematics is the dynamics that initiates it. When a rigid multibody system has acceleration and mass/inertia there is dynamics taking place.

2.3.7 Simulation dynamics

Movement of a human body is as a result of a systemic chain of physiological processes that induce forces and torques on bones (rigid bodies). This results in reaction forces and an acceleration of the body/segment/joint [41].

Forward and inverse dynamics

Inverse dynamics is preferred when kinetic and kinematic input (joint angles/moments) is provided, most commonly through data by a motion capture system. The internal dynamic parameters (muscular forces) are then calculated or inferred using built in algorithms.

Forward dynamics is utilized when internal dynamic parameters are assumed or estimated. The kinematic or kinetic articulations that result from said input are then derived from the system algorithms. The role that forward or inverse dynamics can play in a simulation is described in Figure 15 by flow diagrams adapted from a description in a study by Wang [33].

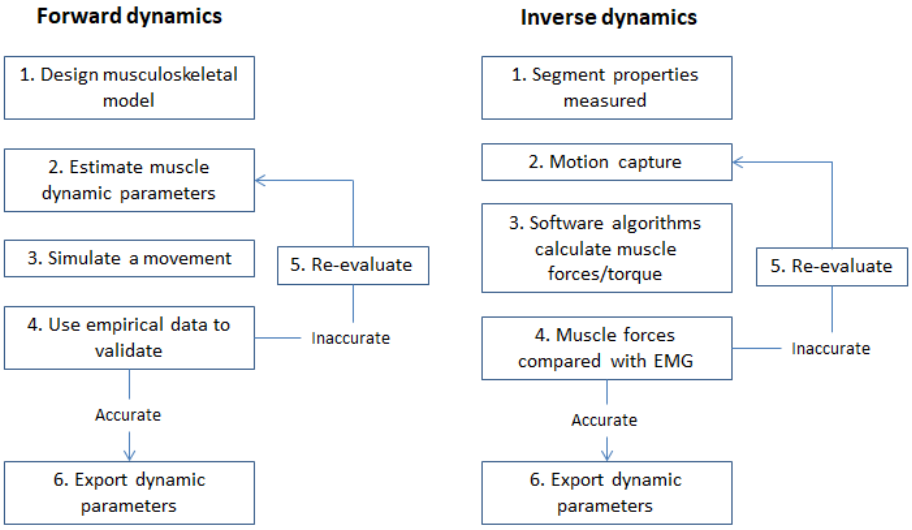


Figure 15: Flow diagrams describing the distinction between forward and inverse dynamics

Simulation actuation

The simulation uses the aforementioned principles to accurately actuate joints in a model. There are two types of actuation strategies:

1. Motion based actuation. In this strategy the motion is prescribed to a joint. This is known as a joint trajectory through the movement. The torque on a joint and the forces on segments are then computed.

2. Torque based actuation. Conversely, the torque for a joint is prescribed and the motion of the respective segments is inferred.

Torque based actuation would appear to be the most accurate, however the type of actuation is ultimately dependent on the type of experimental data that is collected [42].

Contact modelling

Equally important to the relative motion of segments is the interface of the model with external components. There are several approaches to contact modelling, depending on the application. Descriptions of these approaches are provided by Mathworks Inc. [43] and are displayed in Figure 16.

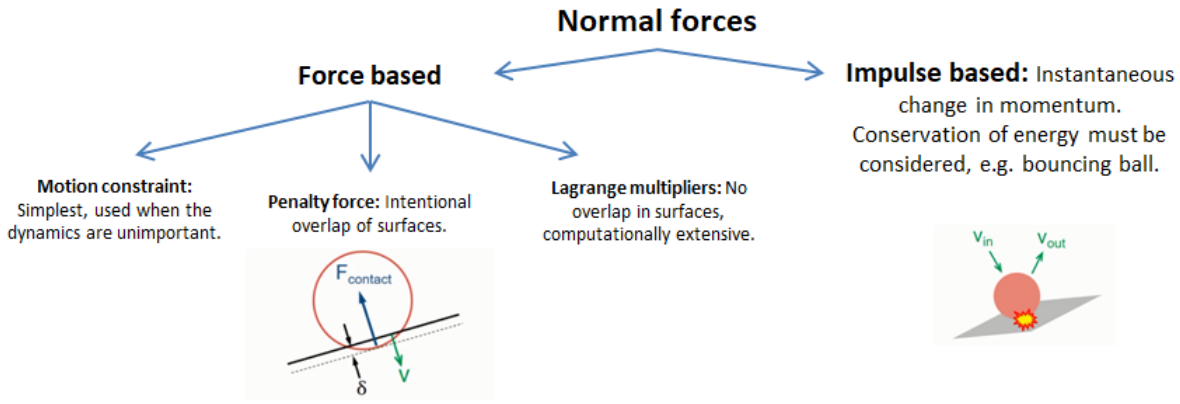


Figure 16: Figure depicting the type of normal forces when developing foot contact in a model

The impulse based approach is not detailed below as it is more specific to applications with elastic collisions.

- Motion constraint modelling takes place when the dynamics are unimportant. The motion of the interfacing segments is prescribed to a best approximation of friction force on the motion.
- The penalty force method allows an overlap of the interfacing segments. The friction is computed based on the overlap depth and the penetration velocity. This method allows for coefficients of friction to be modelled [43].
- The Lagrange multiplier approach is the most accurate considered, however it is computationally expensive and outside the scope of this investigation [44].

Contact modelling is a good means for providing validation for the model. If the normal or friction forces can be empirically collected, they can be compared to computed values of these same metrics.

2.3.8 Multibody modelling systems

Opensim

Opensim is an open source biomechanical simulation software that performs a variety of analyzes to investigate the performance of musculoskeletal models. The Opensim framework includes open source musculoskeletal models developed and published by researchers in a multitude of fields [40]. In the prosthesis or robotic field, Opensim has been used to design robotic systems that assist the motion of humans [41].

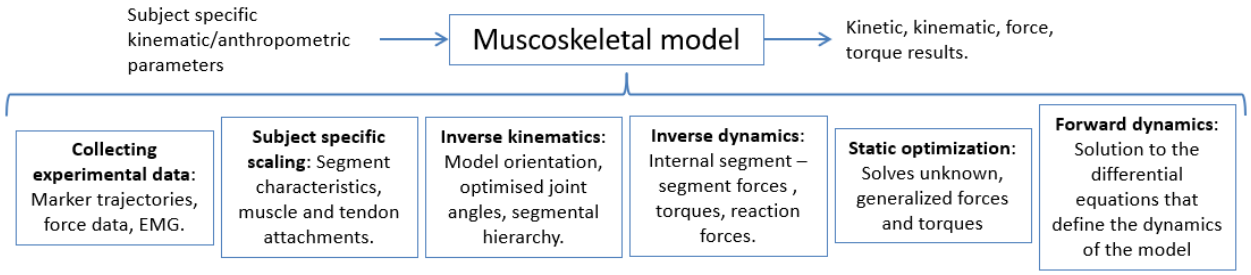


Figure 17: Flow diagram describing Opensim modelling process

The requirements for a multibody model in Opensim are detailed in Figure 17. What should be noted is the required marker trajectories and kinematic data. In addition, what is of importance is the ground reaction forces and EMG data required to actuate the model, indicating that Opensim uses a combination of motion and torque based actuation. [41].

A limitation of Opensim is that it is specific to high speed camera systems. It is not suitable to inertial sensor systems as there is no consensus on the standards for sensor number/placement/calibration [40].

Simscape Multibody

Simscape multibody provides a simulation environment for 3D mechanical systems and has most commonly been used to model complex robotic construction equipment and vehicle suspensions. Rigid bodies are generated using simple geometries developed through variables in a MATLAB environment or CAD generated parts can be imported and then assigned motion. The motion is assigned and dynamic results (torque/force) are inferred or vice versa [45].

A limitation of Simscape Multibody is that it is not specifically a human modelling software. This means that the accuracy of the simulation is dependent on how closely a human robot can be aligned to reality.

2.3.9 Multibody simulation summary

The multibody simulation section thoroughly researched relevant approaches to human movement modelling in literature. The simplifications to be taken into consideration were outlined. The importance of these simplifications was underlined and implementation is detailed in the methodology.

Furthermore, the strategy for the body segment approximations was discussed. The anatomical planes of reference and joint classifications were made clear to provide a framework for the body segments described.

Finally the kinematic and dynamic approaches to multibody simulation were discussed. Followed by a comparison of the software options available for use in the current research.

2.4 Literature search summary

The literature search was an integral part of the investigation and provided a foundation for the rest of the study. The three primary sections of the literature study are summarized below:

- Principles were researched in able-bodied shot put literature. Significant and necessary characteristics of shot put technique that are valid for able-bodied athletes were identified. The main biomechanical principles of able-bodied shot put athletes were found to be concerned with segment velocity, CG profile, feet sequencing and trunk rotation.
- Motion analysis literature was scrutinized to select a means of data collection for the benefit of a multibody simulation. The necessary simplifications are outlined in the methodology.
- Multibody simulation techniques and approaches were researched to provide understanding and context of a framework for simulation based studies on human movement.

Relevant sections of the literature search are referenced in subsequent sections of the current research. The next section details the research methodology, where the information and understanding gathered in this section was collated to develop a framework from which the problem statement can be justified.

3 Methodology

The methodology describes a complete means for achieving the objectives of this study. The research design is discussed below, which is followed by descriptions of the strategies for each of the respective sections for the body of the research.

3.1 Research design

Strengths and weaknesses for simulation based studies were outlined in Section 2.3. In the context of this investigation the advantages of a multibody simulation were twofold: the first advantage is that angles were prescribed in a controlled manner which meant an exact analysis was undertaken. The second advantage of the multibody simulation in this project were the computed results such as joint torque, friction/normal forces and segmental velocity.

Figure 18 is a flow diagram describing the methodology framework for the project. Each step provides unique outcomes that are essential for the overall functioning of the framework. These steps integrate to provide biomechanical information on the movement.

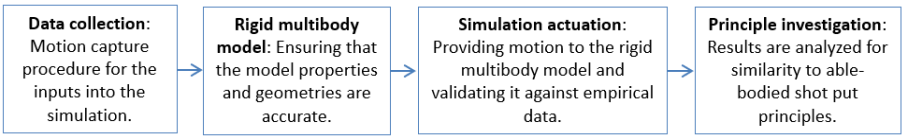


Figure 18: Flow diagram describing the framework used generically for simulation based studies.

- Data Collection. Data was collected through experimental motion capture in order for the simulation to be reliably realistic. This data was filtered appropriately for the purposes of the simulation.
- Rigid multibody model. The number of segments and necessary simplifications were determined. The athletes body measurements were translated accurately into geometries that could be used for the simulation. Accurate mass and inertia properties, along with joint properties were prescribed.
- Simulation actuation. The rigid multibody system developed in step two was actuated aligning with the data captured in step one. This actuation was validated using further empirical data collected.

- Principle investigation. The crux of the investigation, where key results were drawn from the simulation to find evidence on the aligning of the disabled athletes' movement with that of able-bodied counterparts.

The framework described is detailed in full in the rest of this section, beginning with the data collection and processing.

3.2 Data collection

This section includes the procedures for the motion capture and force plate data acquisition. Motion capture data was required so that the simulation could be validated and considered representative of a unique shot put movement.

3.2.1 Xsens MVN Analyze

Xsens MVN Analyze is an inertial sensor based motion capture system that can execute kinematic measurement of the entire body. The system uses a bespoke multibody model (avatar) and proprietary algorithms to estimate 3D joint kinematics based on feedback from the sensors [46]. This estimation is possible through the following processes:

- Anatomically defined segment lengths and axes,
- Sensors aligned to anatomical frames of reference and,
- Segments related to the global reference frame and adjacent segments [46].

A report by Chung et al. [47] designed with the purpose of validating the accuracy of the Xsens system, concluded that the data obtained from Xsens had good agreement with the VICON optical system (considered to be the gold standard) when measuring respective joint angle articulation [47].

3.2.2 FDM pressure walkway

An FDM pressure sensitive walkway was used for the validation process. The walkway was advantageous in that it allowed area for a complete shot put movement to take place. The instrument used (model 2), measures coordinate force and center of pressure (CoP) values.

The output from the pressure walkway in the form of a digital signal was directly acquired through a USB port. Digital acquisition software ensured that there was negligible cross talk, drift and signal interference. Considering linearity and hysteresis, the maximum error was less than 3% of the full-scale output signal. The walkway contains 15360 sensors with a 100 Hz sampling rate [48].

Particularly with the high impact loads concerned, extrinsic factors to the frequency needed to be considered. These factors primarily referred to the mounting surface. A rigid mounting surface was used in the testing which resulted in higher, more accurate frequency measurements obtained.

3.2.3 Data processing and analysis

The data flow for the investigation is shown in Figure 19. The data from this section was used as inputs into the simulation and validation.

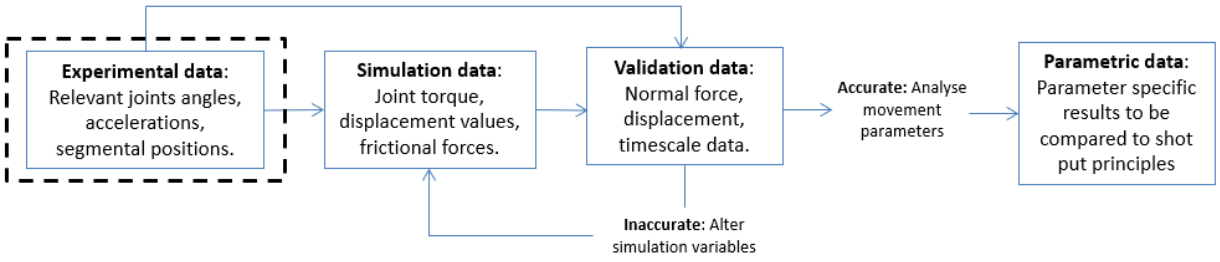


Figure 19: Diagram describing the flow of data gathered from the experiments and simulation.

Xsens MVN Analyze interfaces with MATLAB which is where the data was processed into relevant metrics (joint, segment data) and furthermore, the specific waypoint data which was required for the simulation. The analysis of the data collection was primarily concerned with generating data sets that were usable by the simulation. The implementation of the data in the simulation is detailed in two steps:

1. Movement timescale development

The movement timescale refers to the ordering and sequencing of the movement landmarks described in Section 2.1.1. An important step of the motion capture was to develop an identification standard for these movement landmarks, summarized in Table 3:

Table 3: Table detailing the approach used to identify significant landmarks of the shot put movement.

Movement landmark	**Identification approach**
TO	The first significant increase in the gradient of the velocity and displacement metrics for the right foot was identified. This denoted the initial glide movement.
RFL	The right foot produced a local maximum in acceleration upon landing from the initial glide.
LFL	The left foot making contact for the first time in the movement generated a local maximum for the left ankle acceleration.
SR	This landmark was identified through the global maximum in right wrist acceleration. The shot put release is the reference from which the data was aligned.

The timescale data was used in tandem with the joint trajectories analysis to aid in compatibility between the simulation and the motion capture data.

2. Joint trajectory development

The simulation required prescribed data at nine waypoints over the course of the shot put throw. More specifically, for each degree of freedom of a given joint, there needed to be nine different angles provided at regular intervals. The joint trajectories were guided by these waypoints and are essentially the profile that each of the joint angles took to collectively actuate the rigid multibody system. Linear interpolation between waypoints would have led to infinitely large accelerations and torques by virtue of impossible changes in joint velocity. Thus, a cubic spline function was used to develop smooth joint trajectories.

The outcomes of this section of the methodology were used in conjunction with the process detailed for the rigid multibody model to develop and actuate the simulation.

3.3 Rigid multibody model

The rigid multibody model is defined as the collection and organization of joints and segments used in the simulation. This was the first step in the simulation process and includes the modelling of the interfaces between segments, the joints and the contact plane. The main points in this section are as follows:

- Segment hierarchy. The number of and orientation of segments used in the rigid multibody model for the simulation.
- Segment properties. The geometry, mass and inertial properties for the chosen segments in the rigid multibody model.
- Joint properties. The degrees of freedom and range of movement available to the joints in the simulation.
- Contact plane. This includes the modelling of the friction and normal force computation.

3.3.1 Segment hierarchy

The segment hierarchy refers to the broad arrangement of the segments and joints in a multibody model. The simplifications necessary for the model are made clear in the segment hierarchy, where the complex combination of bones, joints and muscles present in the human body can be represented mathematically.

The segment hierarchy used in the current research was based on a lower body gait analysis developed by MATLAB using a bipedal walking robot with seven segments. The gait pattern was developed using a simplified linear inverted pendulum model which allowed for simple joints to be used (six hinge joints). These actuated the hips, knees and ankles for the robot [42].

The segment hierarchy in the current investigation needed to be more complex due to the intricacies of the shot put movement. To produce the movement required, the joint properties

needed to include increased degrees of freedom and the segment properties needed to include representative mass and inertia values. The segment hierarchy was chosen to be lower body specific as a result of the complexity in modelling upper body joints, more specifically the trunk (spinal vertebrae) and shoulders.

3.3.2 Segment properties

The segment properties were split into two sections: geometries and mass/inertia. All properties were based on the athlete's anthropometry (body measurements) and translated into the simplified geometries and properties used for the simulation. The body measurement standards used by Xsens (Table 4) were suitable for the geometry of each segment. Additional measurements required for the regression equations are detailed in Appendix A.

Table 4: Xsens measurement descriptions

Dimension	**Description**
Body height	Ground to the top of the head when standing upright
Shoulder height	Ground to C7 spinal process
Shoulder width	Right to left distal tip of acromion
Arm span	Standing with arms spread, the measurement between the tip of the left middle finger to the right middle finger taken across the back
Hip height	Ground to most lateral bony prominence of the greater trochanter
Hip width	Right to left of the anterior superior iliac spine
Knee height	Ground to lateral epicondyle of the femoral bone
Ankle height	Ground to distal tip of the lateral malleolus
Foot length	Length of heel to toe dimension

The mass and inertia characteristics used regression equations developed by Zatsiorsky and Seluyanov [49]. The equations along with the empirical coefficients and standard error are detailed in Appendix A. Meaningful insight in the design of the prosthesis was not included in the scope of this investigation. The dimensions and properties of the prosthesis used in the simulation are detailed in Section 5.

3.3.3 Joint properties

Simscape Multibody offers numerous types of joints, each providing different combinations of degrees of freedom and articulation. A key step of the simulation was to determine the correct combination of joints that, when the waypoints were applied, led to an accurate representation of the movement. Table 5 describes the types of joints offered by Simscape.

Table 5: Simulation joint types

Joint block	**Joint primitives**						
6DoF joint	Px	Py	Pz				S
Bearing joint			Pz	Rx	Ry	Rz	
Bushing joint	Px	Py	Pz	Rx	Ry	Rz	
Cartesian joint	Px	Py	Pz				
Gimbal joint				Rx	Ry	Rz	
Revolute joint			Pz				
Spherical joint							S

Joint blocks are assigned a variety of joint primitives, which determine the potential behaviour of the joint in the context of the rigid multibody system [50]. For the purposes of the current research, there were three different types of joint primitives considered:

- Prismatic (P). Enables linear translation along a single axis (x, y, z). A given joint block could simultaneously employ up to three prismatic primitives.
- Revolute (R). Enables rotation about a single axis (x, y, z) and needs to articulate each rotation individually.
- Spherical (S). Enables rotation about any 3D axis and thus is advantageous compared to the revolute joint when more than one rotation is required simultaneously [50].

The type, properties and configuration of each joint are included in the results. The Xsens body measurement standards were used for the joint centers of rotation.

3.3.4 Contact plane

The contact plane and normal forces are a significant element of the simulation, providing the basis for ground reaction forces and by extension the joint torque data. The back-end computation for the normal and friction forces was resolved using the MATLAB contact forces library.

The chosen classification of normal force modelling used a penalty force method. This allows the bodies to penetrate minimally, where normal forces are then computed based on the penetration depth and velocity [51]. The following parameters needed to be prescribed prior to the simulation:

- Normal force parameters. This included contact stiffness and damping which were set to default for the simulation.
- Friction force classification. The stick-slip model was used for the friction forces. The stick-slip representation indicates that two sliding objects will alternate between kinetic and static friction when interfacing. The permutations of this model was computed by the MATLAB contact forces library. The coefficients of static and kinetic friction were selected as well as the critical velocity.
- Sensing. This determined what measurements could be extracted. Including the normal and friction forces for the movement as well as the separation distance of the solid bodies.
- Contact points. The foot was modelled as a rectangular prism. The contact points were located at each of the four corners.

The efficacy of the normal force model and the associated parameters is reflected in the validation of the model.

3.4 Simulation actuation

In this section, the method for providing motion to the simulation is described in addition to the validation approach used. The associated research instruments and data is detailed below:

3.4.1 Simscape Multibody

Simscape multibody provides a simulation environment for 3D mechanics and has been commonly used to model complex robotic applications and suspension systems. It is a MATLAB toolbox that combines with the MATLAB and Simulink environments. It includes control block diagrams or state machines both relying on simple MATLAB code. Typical implementations include electric, hydraulic or thermal applications [42].

Figure 20 describes the procedure for developing a simulation using Simscape. Rigid bodies are generated using simple geometries or CAD generated parts which can be imported and then assigned motion. The motion in the form of joint trajectories is prescribed from which dynamic results (torque/force) are computed. Alternatively torque on joints can be prescribed in which case the motion is then calculated.

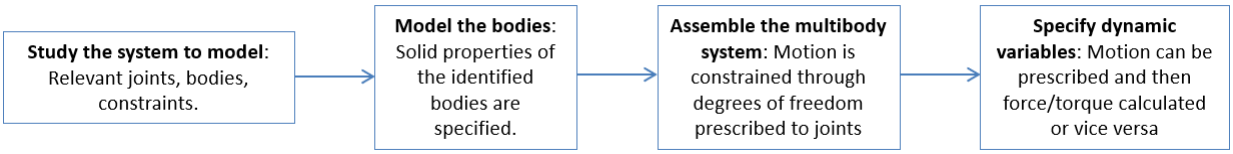


Figure 20: Simscape flow diagram for developing a biomechanical model

A limitation of Simscape Multibody was that it is not specifically a human modelling software. The accuracy of the simulation was dependent on how closely a human model could be approximated to a robotic simulation.

3.4.2 Actuation and validation data

Taking the data from the motion capture and transferring it into the simulation meant that the simulation had empirically accurate joint articulations. The data was adjusted and fitted with respect to the following simulation based directives:

- Differing coordinate systems. The coordinate systems had alternate reference frames and joint classifications, which meant that no one angle could be transposed identically from the experiment into the simulation.
- Degrees of freedom. The mocap system generated many more angles than what was required by the simulation (see Table 6). These angles influenced one another and altered the values that were included in the simulation.

- Contact forces. The simulation was modelled using a cuboid representing the foot and a modified blade as the prosthesis. In reality however, feet offer many more segments that aid in balance and force transmission.

The data was entered using insight from video analysis and the Xsens GUI. Table 6 shows the joint degrees of freedom captured by Xsens compared with the degrees of freedom used by the simulation. Most notable are the knee and ankle joints which are simplified significantly.

Table 6: Lower body joint data comparison

Xsens		**Simulation**	
Joint	**Function**	**Joint**	**Function**
Pelvis	3 DF	Pelvis	3 DF
Hip	3 DF	Hip	3 DF
Knee	3 DF	Knee	1 DF
Ankle	3 DF	Ankle	3 DF
Ball of foot	3 DF	N/A	
Total (left and right)			
	27		17

3.4.3 Actuation validation and analysis

The analysis of the actuation and validation of the simulation was concerned with two comparisons: firstly, the comparison of computed and motion capture joint trajectories and secondly, the comparing of simulated normal forces at the contact plane interface to those measured using the FDM pressure walkway.

Joint trajectory analysis

The primary joints in the rigid multibody model that were analyzed are:

- Right ankle joint (3 dof)
- Right knee joint (1 dof)
- Right and left hip joints (3 dof each)

- Trunk rotation (3 dof)

A total of 13 dof were formulated and compared. The strategy for this section was to display that the articulation of the simulation represents the movement accurately.

Validation analysis

The simulation actuation required validation to legitimize the parametric study. The validation used motion capture and force plate data. The data used for validation was split into the following categories:

- Normal force validation refers to the comparison of empirical and computed normal force data. The profile, values and timing of significant landmarks were compared.
- Displacement validation concerns the displacement path/trajectory of the athlete CG in the x and z direction. There is evidence in the study by Coh et al. [42] of both the x and z displacement metrics being used as a performance principle for athletes using the glide technique.

The pressure walkway collected data at 200 Hz and the simulation at approximately 560 Hz [52]. Therefore, the computed normal force data set was reduced linearly to fit the force plate data. Evidence from able-bodied literature indicates that displacements of 1.5 m and 0.8 m to 1.2 m in the x and z directions respectively are typical [10].

3.5 Principle investigation

There were two levels of analysis for the investigation:

- Simulation results. This analysis detailed computed results from the simulation of characteristics and metrics which are important to the selected shot put principles but were not applicable to a parametric study.
- Parametric results. Significant movement parameters were identified to analyze principles that lend themselves to a given parameter or movement characteristic which was then altered iteratively.

The analysis approach integrated to provide a thorough biomechanical investigation for the disabled athlete.

3.5.1 Simulation results

The simulation results offered insight into principle outcomes of the movement. Below is a description of the key principles and their results to be analyzed using the simulation.

Segment velocity. The velocity of individual segments was investigated to determine if the segments aligned with the principle governing their integration detailed in Section 1.1.2. The points to be scrutinized for this principle were twofold. Firstly, that segment velocity increases sequentially as the movement 'cascades' up the body to release. Secondly, the lower extremity segments should remain fixed at release to offer a stable base from which the upper extremities can extend effectively.

X displacement profile. This is the profile or trajectory of the CG visualized in the XY plane. It is beneficial to have a consistent direction through the preamble to the throw.

Z displacement profile. Similarly to the x displacement profile, this principle concerned the trajectory of the CG observed in the XZ plane. Able-bodied literature indicates that a sinusoidal shape is beneficial. The release height was also highlighted by this result.

The above principles described, and their relationship to the results, are separate to the parametric study described in the next section. This is due to the fact the principles highlighted do not lend themselves to a particular movement parameter.

3.5.2 Parametric study

A parameter is defined as a characteristic of the movement that is testable/changeable and significant to the efficacy of the movement. For each of the parameters below, the principle to be outlined by a parameter is indicated, a brief description is given, followed by the testing strategy used. The expected results are also detailed.

Knee flexion - initial glide principle

The knee flexion parameter concerns the flexion and extension that enables the initial glide of the movement. This is an important principle of the shot put throw preamble. The flexion and extension takes place prior to TO at approximately 0.1 s in the movement. The knee

flexes in preparation for the extension. This is displayed in Figure 21.

The strategy for testing this parameter was to vary the flexion range and thus the extension torque and velocity. There were five tests of flexions at intervals of 15°.



Figure 21: Schematic describing the knee flexion parameter

The key results observed for this parameter were the friction force results (at TO), and resultant variations to the extension velocity and torque. The glide distance (x) and height (z) were highlighted to evaluate the efficacy of the glide movement.

The reasoning for this parameter was to determine if the flexion and extension used by the athlete is optimal in terms of the results computed. There is limited details on numeric targets for this principle in literature, the efficacy was judged entirely on the displacement metrics.

Hip abduction parameter - delivery stance principle

The delivery stance principle is significant because it can extend or limit the acceleration path of the shot put during the movement. The strategy for this parameter was to vary the abduction angle for each of the legs. This resulted in the overall combined abduction angle increasing or decreasing at the point in the movement where the left foot lands and the delivery stance takes place. This is described in Table 7.

Table 7: Table of prescribed angles used for the hip abduction parameter

Test #	Left abduction angle(°)	Right abduction angle(°)	Overall abduction angle(°)
1	30	10	40
2	35	15	50
3*	40	20	60
4	45	25	70
5	50	30	80

Able-bodied literature indicates that a delivery stance of 1.1 m to 1.3 m is effective. This offered a numerical benchmark from which to compare the delivery stance of the athlete in question. The outcomes of this parameter were also analyzed to detect the friction force and torque implications of differing delivery stances used.

Trunk rotation velocity - trunk rotation principle

Trunk rotation is an important principle of the entire shot put preamble. The trunk was the upper-most segment of the model used and thus represented the final segment articulated for the shot release.

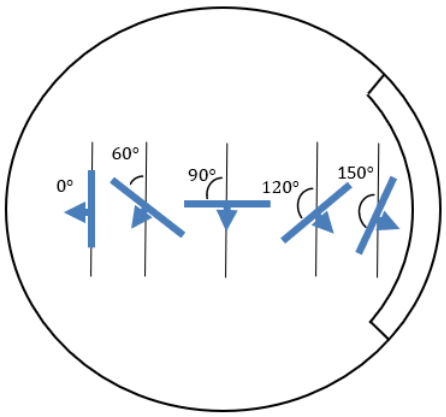


Figure 22: Schematic describing the trunk rotation velocity parameter

The strategy for testing this parameter was to vary the joint trajectory of the trunk segment. This resulted in a variety of velocities at different stages of the movement. The trajectories

of each iteration are included in the results. There were four different tests using unique trajectories. The reasoning for this approach was to observe if there is a rotation technique that is more effective than the one used by the athlete and if so, what the implications of that technique are.

This principle has been used as an indicator to pre-empt back injury for shot putters [53]. A large rotation was expected (100° to 150°), shown in Figure 22. It was also important to observe the effect this had on the other metrics investigated such as friction and release velocity [10]. The linear velocity of the right shoulder was calculated to approximate a release velocity and was used as a measure of rotation efficacy.

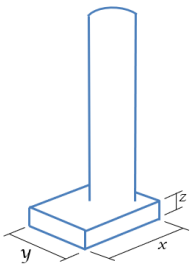
Prosthesis parameters

The prosthesis parameters were not aimed at providing design information for the prosthesis but rather the optimal utilization of the current prosthesis and the relevant variables that influence effective utilization. They did not lend themselves to any of the principles, but yielded important information on the influence of the prosthesis.

Contact surface parameter

The contact surface refers to the surface area of the prosthesis that interfaced with the contact plane. This was altered by modifying the prosthesis geometry. The dimensions used are illustrated in Figure 23 with geometries detailed in Table 8.

Table 8: Table detailing geometries of contact surface used



Test #	x (m)	y (m)	z (m)	Area (x10^{-3} m^2)
1	0.075	0.05	0.07	3.75
2	0.11	0.075	0.07	8.25
3	0.15	0.1	0.07	15
4	0.195	0.125	0.07	24.1
5	0.225	0.15	0.07	32.8

Figure 23: Contact surface parameter

The strategy for this parameter was to change the geometry of the part of the prosthesis that makes contact with the contact plane.

Coefficients of friction

The coefficients of friction (static/kinetic) parameter refers to the interface of the prosthesis with the contact plane. The aim was to observe the effect of varying the friction parameters for the contact model used in the simulation.

Table 9: Table of the friction coefficients to be used for the friction parameter

Test #	**LFL**	**SR**	**Interface**
1	0.1	0.02	Ice - ice
2	0.16	0.1	Carbon - carbon
3	0.6	0.5	PVC - asphalt
4	0.8	0.7	Wood - asphalt
5	0.9	0.8	Rubber - asphalt

The strategy for this parameter was to use the coefficients of well studied interfaces [54] and then observe the effect on the friction force computation. The coefficients used are detailed in Table 9. The friction results were expected to increase proportionally with increased coefficients of friction. This test also plays the role of investigating the efficacy and accuracy of the friction laws used in the simulation.

3.5.3 Principle investigation summary

Table 10: Table summarizing investigation approach using the simulation.

Result	Method	Interpretation	Principle
Segment velocity	Velocity time graphs of the segment velocities were computed. One for the left leg/prosthesis, trunk and shoulders. The other graph containing the right leg segment velocity through the simulation.	The graphs were inspected to determine if the segments aligned with principles governing their integration found in literature. Namely, that the velocity increases sequentially up the body and the lower extremities provide a stable base for upper body extension.	Integration of segments
z displacement profile	Displacement-time graph of CG displacement in the XZ plane.	Graph was analyzed in order to determine if the profile aligned with the sinusoidal trajectory found to be beneficial in literature. Maximum displacement occurring at release.	CG displacement, release height
x displacement profile	Displacement-time graph of CG displacement in the XY plane.	The consistency of direction was key for the interpretation of the graph.	CG displacement

Parameter	Method	Interpretation	Principle
Initial glide	Knee flexion prior to jump was altered in 15° increments. Graphs included angle trajectory, friction force, and knee flexion torque vs time. Other results included the displacement of the glide movement.	As there is no numerical evidence of this parameter in literature, the effectiveness of a given glide movement was judged on it's torque results and it's successful displacement.	Feet placement
Delivery stance	The combined hip abduction angle was altered in 10° increments. Graphs included the hip abduction torque and the right and left leg friction as well as the combined hip abduction angle joint trajectory.	The primary interpretation required for this parameter is for the comparison of the numerical delivery stance values found in literature versus the results computed by the simulation.	Feet placement
Trunk rotation	The trunk rotation angle trajectory was altered using four different rotation techniques. Graphs included velocity and friction versus time.	There is limited evidence in literature of this parameter. An effective trunk rotation was thus judged as one were the translational velocity reached a maximum at the point of release.	Feet placement, release velocity
Prosthesis parameters	The friction vs time graphs were used for both parameters. Each parameter concerned the contact interface.	The friction results were analyzed in order to determine the efficacy of the respective parameters used by the athlete in question. This parameter also played a role in validating the contact model used.	

Through the analysis of the simulation outlined in Table 10, meaningful observations were outlined that provide insight into the mechanical intricacies of the movement. This aided in aligning the movement to the depth of able-bodied literature present.

3.6 Limitations and ethical considerations

This section details the limitations for the study based on the equipment available and the scope of the simulation. The primary limitations were:

1. The complexity of the model when comparing it with the real life movement. The legitimacy of the simplifications made to overcome this are a key point of consideration when analysing and discussing the data.

2. There is evidence in past movement investigations of a lack of accuracy on the part of Xsens when investigating movements including high accelerations.

3. The validation of the simulation relied on the comparison of the force plate data to the computed normal force results generated by the simulation. Thus, the effectiveness of this validation and the efficacy of the simulation will be impacted by how well these data sets can aligned.

The above limitations had an affect on the reliability of the findings. Attempts were made to mitigate their effect so that accurate and meaningful results were obtained.

3.6.1 Ethical considerations

Ethical clearance was needed to ensure that the research was conducted in a responsible and ethically accountable way for the benefit of the athlete in question. In addition, ethical clearance ultimately ensures that this research will lead to beneficial outcomes and increased legitimacy of findings.

The ethical clearance used in this project was required for the one research participant and aligns with the guidelines set up by the University of Witwatersrand and furthermore the research integrity standards set out by The Hong Kong Principles for assessing researchers. The University's Ethics Committees are registered with the National Health Research Ethics Council (NHREC) of the Department of Health. The ethics retrospective acknowledgement certificate for this research is found in Appendix D.

3.7 Conclusion

The final part of the methodology provides a framework for the body of the report. As the method was followed correctly and not impaired by the aforementioned limitations, the body of the project or the results and analysis section described in Figure 24 refined the objectives and provided conclusions.

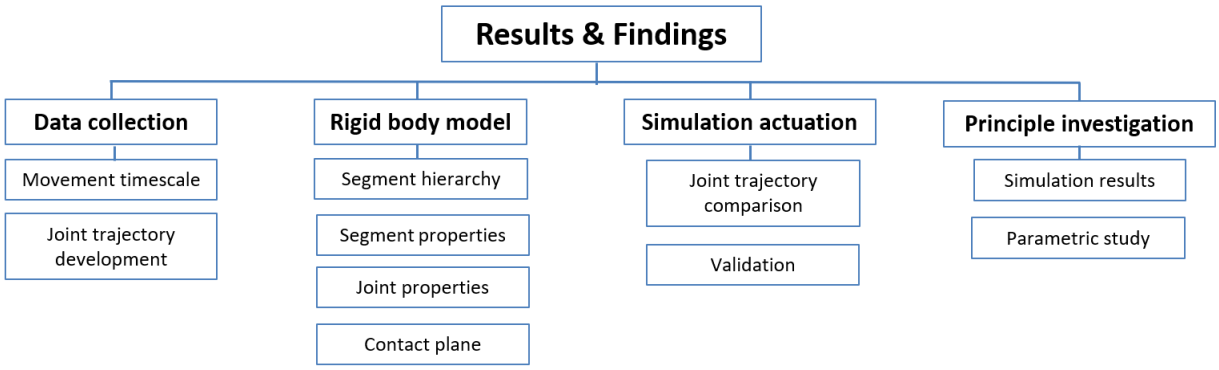


Figure 24: Structure of the results and analysis section

The body is split into the four primary categories of the methodology and includes discussion and conclusions in each section.

4 Data collection

The data collection procedure took place at a genuine shot put facility used for competition. Two important steps were required in the data collection which provided actuation and control to the model: the movement timescale and the joint trajectories. These steps are detailed below.

4.1 Movement timescale analysis

Segment kinematic data was used to determine the sequencing and timing of significant movement landmarks in the movement. The timescale was generated through averages of these landmarks identified in the data collection process. The kinematic results are illustrated in Figure 25 and 26.

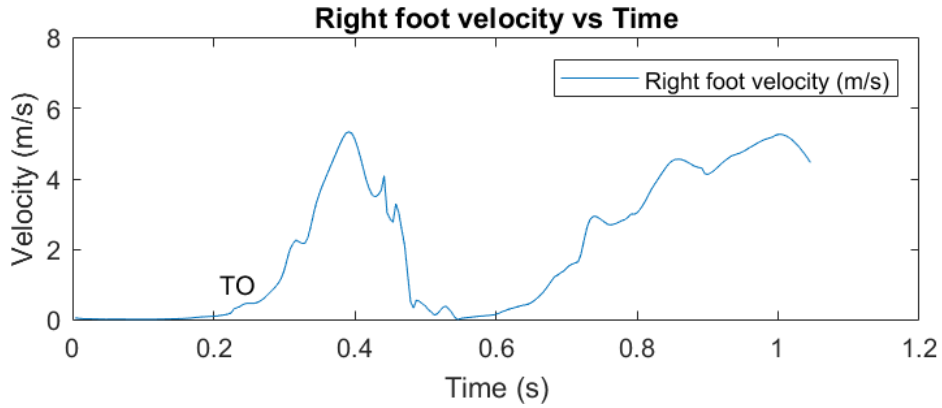


Figure 25: Graph displaying the right foot displacement and velocity metrics.

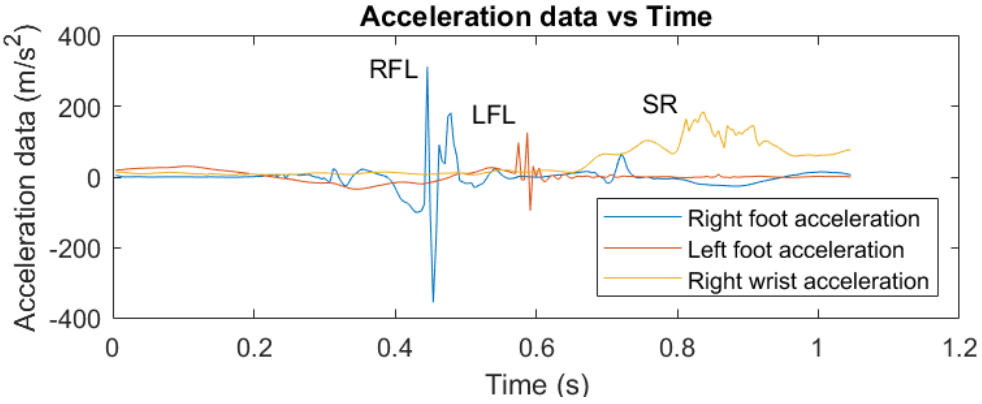


Figure 26: Graph displaying acceleration data for relevant segments.

Using the identification techniques described in Table 3 (Section 3), the significant movement landmarks were identified. The results are detailed in Table 11 with the mean used by the simulation.

Table 11: Timescale empirical values

Throw #	**TO(s)**	**RFL(s)**	**LFL(s)**	**SR(s)**
1	0.10	0.31	0.43	0.65
2	0.17	0.34	0.45	0.65
3	0.11	0.29	0.38	0.65
4	0.14	0.31	0.40	0.65
5	0.17	0.32	0.43	0.65
6	0.22	0.36	0.46	0.65
7	0.21	0.37	0.48	0.65
Average	0.16	0.32	0.44	0.65

The final averaged landmarks were confirmed using the Xsens GUI. The timing analyzed in this section was a vital step for prescribing actuation to the simulation.

4.2 Joint trajectory analysis

The joint trajectory analysis was an integral part of the study where the waypoints for the simulation were measured and processed. A waypoint is described as a distinct angle for a given joint. Each joint is given nine waypoints at regular intervals through the movement which, when connected, resulted in a joint trajectory. The trajectory analysis is split into two collections of segments: the first being the right leg segments of ankle, knee and hip. The second is the left hip and trunk segments.

Right leg segments

The trajectories were generated by applying a cubic spline filter to nine waypoints acquired through the motion capture data. The graphs below include the joint trajectories of the right leg, each representing a degree of freedom for a given joint.

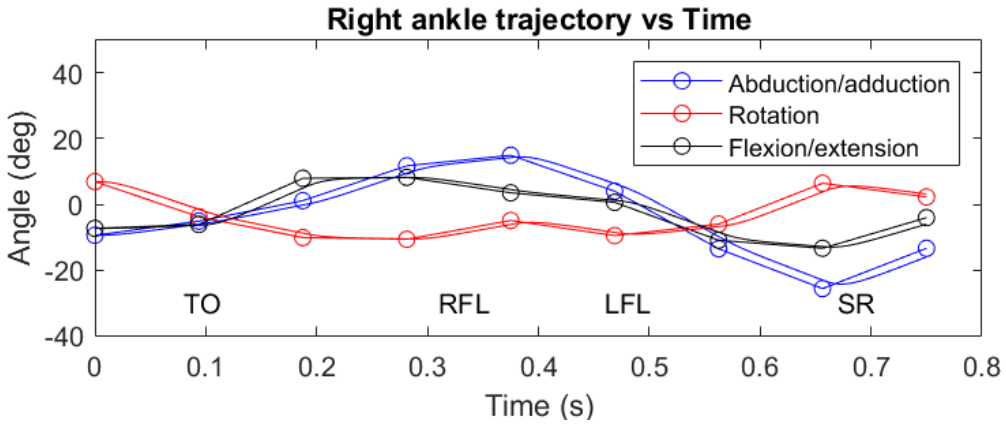


Figure 27: Graph displaying the filtered data collected for the right ankle.

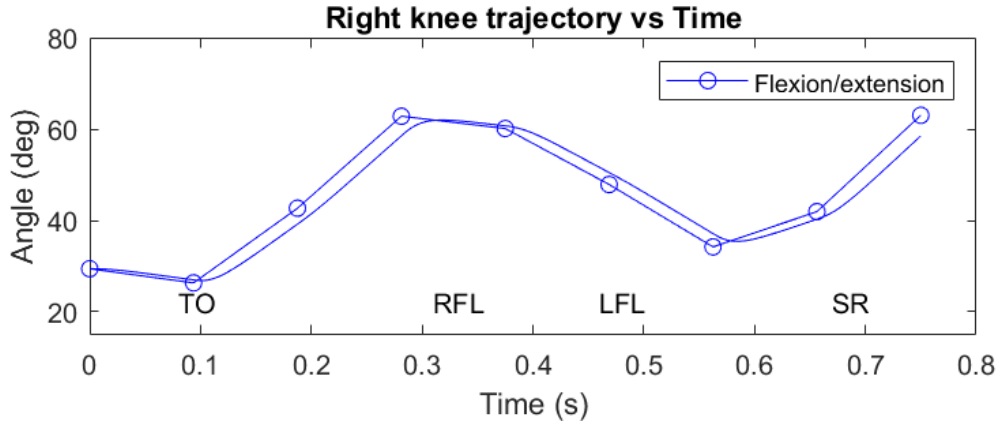


Figure 28: Graph displaying the filtered data collected for the right knee.

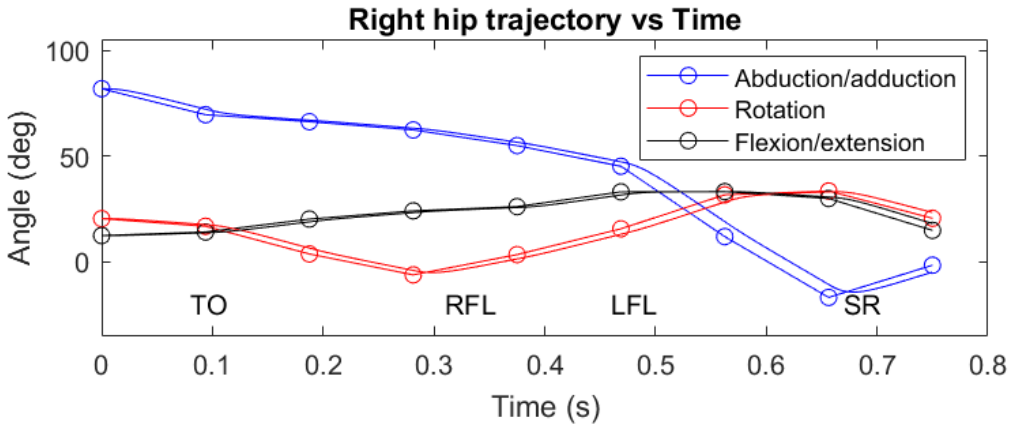


Figure 29: Graph displaying the filtered data collected for the right hip.

Important observations made on the segment trajectories are outlined below:

- The right ankle (Figure 27) undergoes substantial abduction that reverses to adduction in the second half of the movement, after the right foot contact is made (RFL). This could be as a result of the pivoting that is required to rotate the trunk for the throw.
- The right knee (Figure 28) is simplified to only have motion in the flexion/extension or sagittal coordinate plane. Between waypoints 2 and 4 the extension that allows take off (TO) can be seen.
- The right hip (Figure 29) has pronounced adduction in the beginning of the movement that moves to abduction rapidly after waypoint 4 to generate a powerful release.

For the first half of the simulation the right leg was the only collection of segments activating movement. In the second half of the movement, the CG of the athlete is shifted over the left leg (and prosthesis) whilst the trunk rotates and right arm extends for release.

Left hip and trunk joint trajectories

The remaining joints that were free for articulation are the pelvis (actuating the trunk) and the left hip joints. The trunk segment represents the entire upper half of the body and thus the pelvis joint represents the pivoting in the movement generated by the upper body.

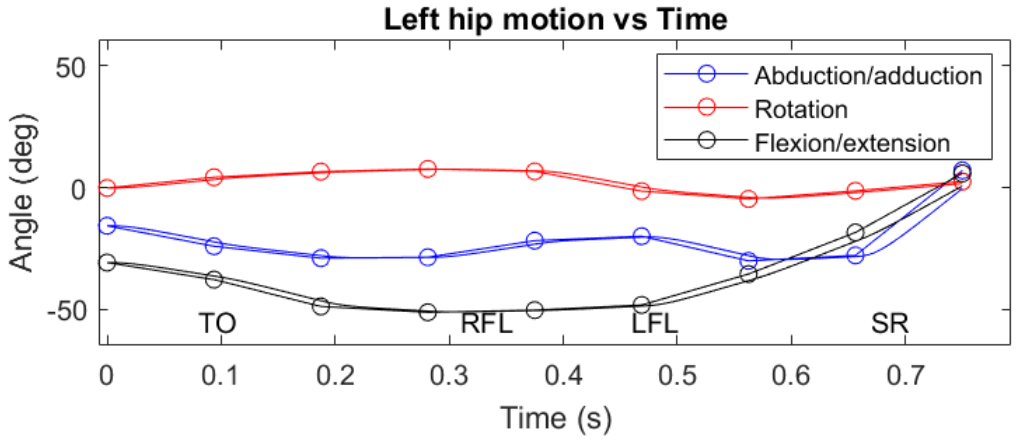


Figure 30: Graph displaying the filtered data collected for the left hip.

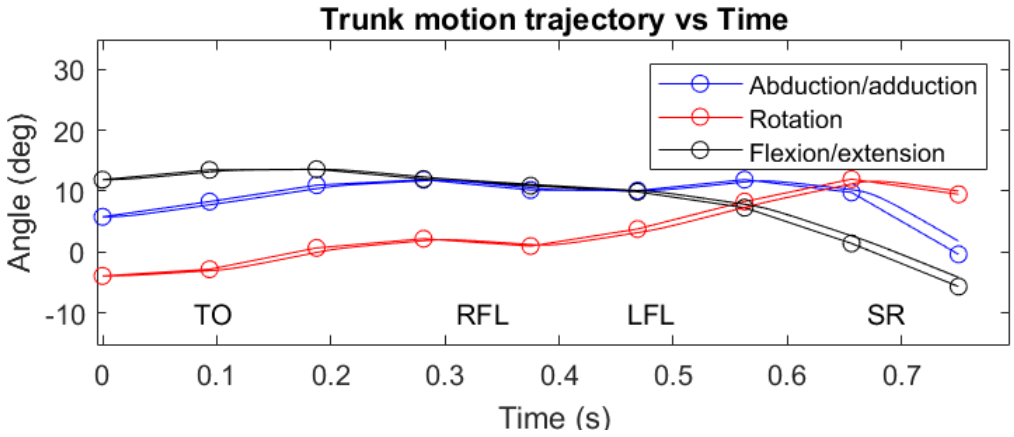


Figure 31: Graph displaying the filtered data collected for the pelvis segment.

Important analysis is underlined below for each of the joints.

- The flexion/extension of the left hip (Figure 30), starts in the extended position or negative with respect to the y axis. It then flexes and becomes positive throughout the movement. It increases substantially from waypoint 5, indicating at its importance in activating the trunk and upper body for an eventual powerful release.
- The motion capture representation of the trunk movement (Figure 31) did not correspond with what was expected. In the second half of the movement the entire trunk/torso pivots on the right foot to generate momentum for a powerful throw. The rotation was expected to be approximately 40° to 50°. However, the captured data displays rotation of not more than 30°. This could indicate that the other joints i.e. hips and ankles compensate for the apparent lack of pelvis articulation.

Table 12 specifies the exact values for the joints from the joint trajectories for each of the waypoints.

Table 12: Waypoint data

	Waypoints									Range	
Joint	**1**	**2**	**3**	**4**	**5**	**6**	**7**	**8**	**9**	**Lower**	**Upper**
Right ankle											
Ab/add	-9.4	-5.1	1.1	11.7	14.9	4.0	-13.5	-25.59	-13.36	-25.59	14.91
Flex/ext	-7.3	-6.1	7.9	8.2	3.5	0.6	-10.9	-13.36	-4.04	-13.36	8.24
Rot	6.9	-3.8	-10.1	-10.6	-4.9	-9.5	-6.0	6.43	2.24	-10.64	6.86
Right knee											
Flex/ext	29.4	26.3	42.7	62.9	60.2	47.9	34.2	41.95	63.10	26.27	63.10
Right hip											
Ab/add	81.9	69.6	66.3	62.4	55.0	45.2	11.9	-16.87	-1.63	-16.87	81.86
Flex/ext	12.4	14.1	20.2	24.1	26.1	33.1	33.2	29.95	14.86	12.39	33.15
Rot	20.4	16.8	3.7	-6.2	3.4	15.6	31.7	33.48	20.58	-6.17	33.48
Left hip											
Ab/add	-15.6	-24.0	-28.9	-28.5	-21.7	-19.9	-30.0	-27.76	7.10	-29.97	7.10
Flex/ext	-30.7	-37.7	-48.7	-51.1	-50.2	-48.1	-35.4	-18.35	5.88	-51.06	5.88
Rot	-0.1	4.3	6.6	7.7	6.7	-1.4	-4.6	-1.29	2.54	-4.58	7.67
Pelvis/trunk											
Ab/add	5.8	8.3	11.0	11.9	10.2	10.1	11.9	9.80	-0.35	-0.35	11.93
Flex/ext	-3.9	-2.8	0.7	2.2	1.0	3.8	8.3	11.98	9.49	-3.88	11.98
Rot	11.9	13.5	13.6	12.0	10.9	9.9	7.3	1.43	-5.64	-5.64	13.62

4.3 Data collection conclusion

The results were generated using the Xsens motion capture system at a competition level shot put facility. Timing of the movement landmarks was obtained through the processing of kinematic data captured using the Xsens MVN Analyze system. Joint data was averaged over seven shot put throws. For each joint dof, the averaged data was split into nine distinctive waypoints at regular intervals for motion to be prescribed in the simulation. The joint data was smoothed using a cubic spline function.

The problem statement required this part of the investigation to ensure that the motion data collected was translated into discrete waypoints to be prescribed for the simulation. This process was successful, offering an accurate foundation from which to prescribe motion.

The accuracy of inertial sensor based motion capture systems when measuring fast moving, distal segments (such as the hand or foot) was a concern. Particularly for joints with complex articulations such as the ankle and hip.

The section that follows describes the development of the rigid multibody model. This was the collection of joints and segments that, when the data collected was prescribed, accurately represented the shot put movement in the simulation.

5 Rigid multibody model

This section details the methods of measurement used in the simplification of segments for the rigid multibody model used for the simulation. The number of rigid bodies used, along with their dimensions, were carefully determined through the consideration on the computation limitations as well as the athlete anthropometry. The rigid multibody model included seven segments connected by a variety of joints. The details for which are described in this section.

5.1 Anthropometric measurements

Anthropometric measurement served three purposes in the development of the simulation. The first was to provide input for the motion capture calibration procedure. The second was to develop accurate segment geometries for the rigid multibody model (Section 5.2). The third purpose was to provide information for the regression equations which computed the inertial properties required for the simulation (Section 5.3). The collected measurements are detailed in Table 13.

Table 13: Table detailing the values for the anthropometric measurements used

Segment	Measurement	Value
1	Length (cm)	26
	Width (cm)	14
	Body fat (%)*	23.6
2	Length (cm)	43
	Lower diameter (cm)	26
	C1 (proximal diameter (cm))	40
	C2 (distal diameter (cm))	30
	C3 (maximal diamater (cm))	42
3	Length (cm)	50
	Lower diameter (cm)	46
	C1 (distal diameter (cm))	46
	C2 (proximal diameter (cm))	70
	C3 (median diameter(cm))	58
4	Pelvis circumference (cm)	110
	Bispinous breadth (cm)	30
	Body fat (%)	23.6
5	Length (cm)	35
	Lower diameter (cm)	52
	C1 (distal diameter (cm))	52
	C2 (proximal diameter (cm))	74
	C3 (median diameter (cm))	63

5.2 Segment geometries

The segment geometries section details the values for the dimensions of the rigid bodies used for the model. The most important approximations in this section were the values used for the lengths of segments as these have the greatest effect on the computed torque values. The dimensions of the Simscape model given in centimeters are illustrated in Figure 32.

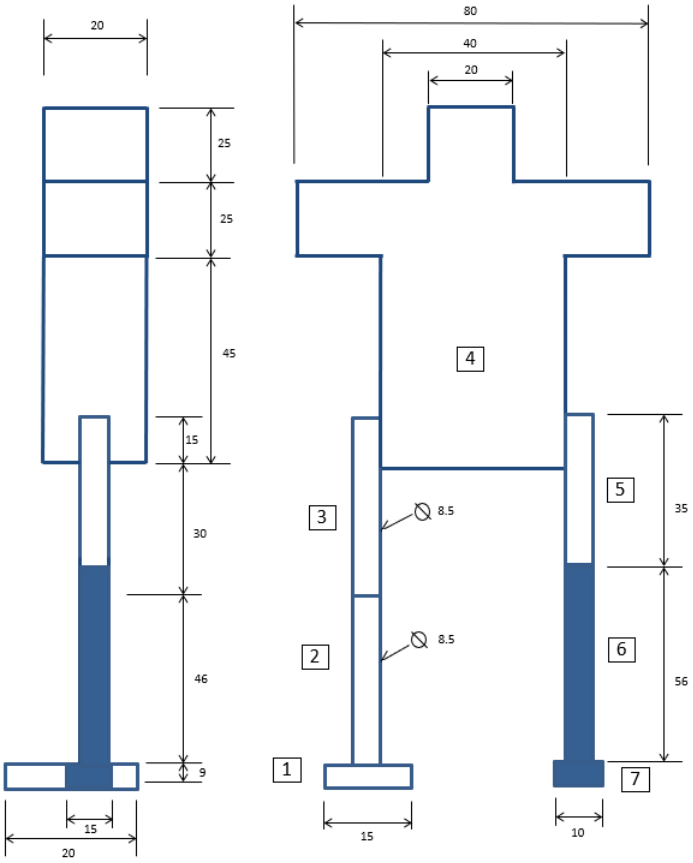


Figure 32: Diagram detailing the geometries of relevant segments

5.2.1 Definitions

1. Right foot
2. Right lower leg
3. Right upper leg
4. Upper body
5. Left upper leg
6. Prosthesis
7. Prosthesis interface

5.3 Inertial properties

Inertial properties were assigned to each segment. The accuracy of these properties was dependent on the anthropometric measurements and regression equations used. The collection of segmental masses when summed were equal to the overall mass of the athlete and thus it was expected that the experimental normal forces would be comparable to the simulated normal forces. Calculated values for these properties are detailed in Table 14.

Table 14: Table of inertial properties of segments. * CoM taken from the proximal end of a segment ** Rod moment of inertia about proximal end

Segment	**Mass (kg)**	**CoM (cm)***	**Inertia** $(kg.cm^2)$ **
1	1.1	15.6	50.8
2	4.9	17.2	684.2
3	21.7	22.1	4342.2
4	78.0	55.1	448 000.0
5	15.1	13	3050.2
6	3.0	12.1	6075.0
7	0.3	0.075	67.5

5.4 Joint properties

The joints provided the model with degrees of freedom necessary to numerically simulate the movement required. The Simscape Multibody representation of joints depicted in Figure 33 were selected in accordance to the degrees of freedom available for each joint in reality. A trial and error process was used to determine the capabilities and the correct combination of joints thereafter. The validity of the combination decided upon was reflected in the success of the investigation.

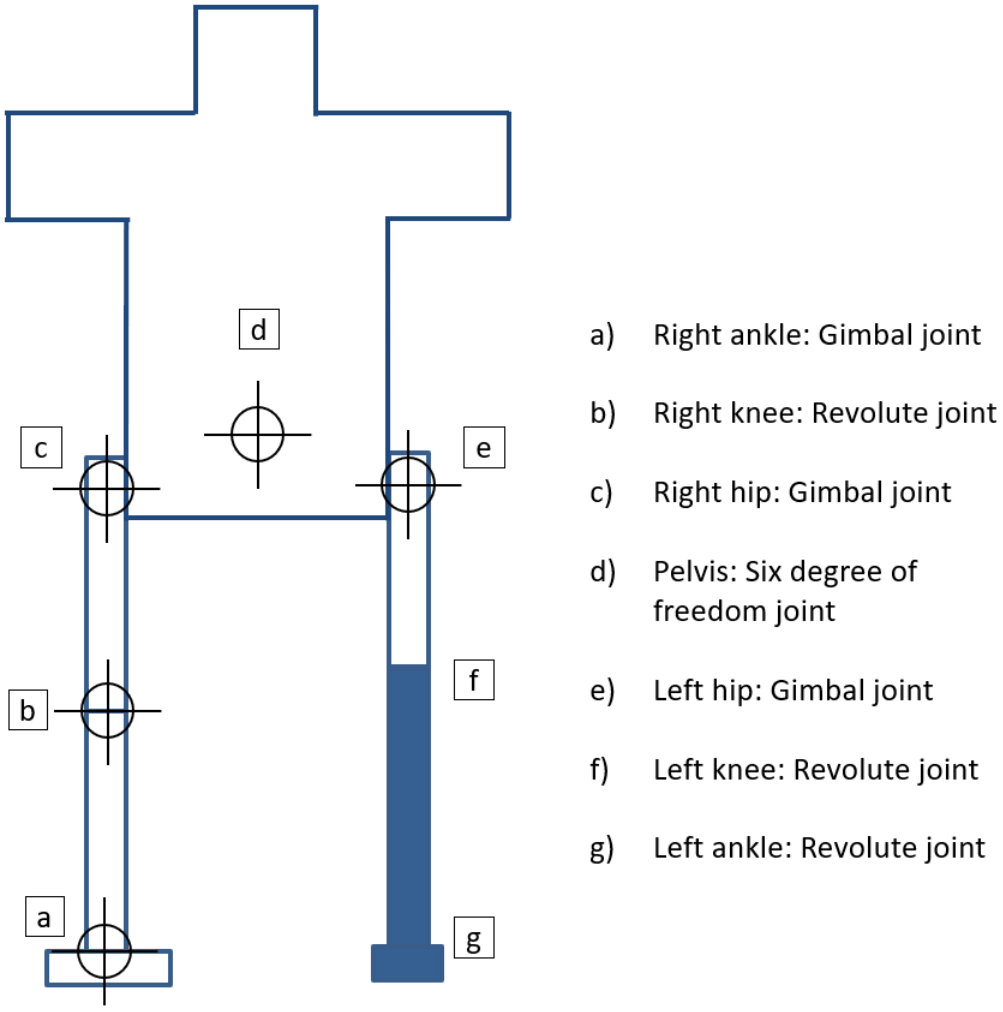


Figure 33: Diagram detailing type and location of joints in the rigid multibody model

5.5 Rigid multibody model conclusion

The rigid multibody model required simplified body properties of the athlete in question. These simplifications included adjustments to the geometry, inertial properties and the joints that were used for the model.

The accuracy in representation was important so that the computed movement was useful in comparison to the able-bodied movement principles found in literature and thereafter, to observing the modifications necessary as a result of the influence of the prosthesis. Discussion points concerning the simplifications are outlined below:

More representative segments

Medical imaging techniques or the input of a medical professional are significant steps that could have resulted in more accurate measurements and simplifications. The exact influence of more accurate measurements is unknown, but can only be beneficial for the simulation. A further recommendation would be to create more representative segments using CAD software such as Solidworks which would result in more accurate segment properties and simulation results.

Prosthesis material investigation

Due to intellectual property commitments made by the athlete with respect to the prosthesis design company, it was impossible in this investigation to make a thorough analysis into the design of the prosthesis. It is recommended to use an investigation such as this to analyze the forces and torques on a prosthesis in order to aid the design process. This could include a material investigation or a finite element analysis process that would support the composition and manufacturing of prostheses for these unique movements.

Trunk modelling

The trunk movement is articulated through 33 vertebrae which is challenging to model accurately. However, the trunk is an important component of many movements where it plays the role of an interface between the upper and lower collections of body segments. There is potential for future investigations to model the action of the trunk in a measured approach. This would mean including joints that represented each or a multitude of vertebrae in the spine. For instance, to represent the entire lumbar, thoracic and cervical combinations of vertebrae as one joint each.

The next section details the actuation and validation of the simulation which was influenced by this section. This essentially validates the means and methods of measurement and simplification used for the simulation development.

6 Simulation actuation and validation

This section of the results is split into two parts:

- Joint trajectory analysis
- Simulation validation

6.1 Joint trajectory comparison

A joint trajectory is the profile of the change of angle for duration of the movement. Despite the efforts to ensure that the simplifications are accurate, the differences in the simulation are such that the prescribed motion needed to be altered from the motion capture data. The purpose of this analysis is to underline notable similarities and differences in each data set.

6.1.1 Right leg joints

The joints of the right leg include the ankle (3 dof), knee (1 dof) and hip (3 dof). For each joint, the simulated trajectory (solid line) is compared to the experimentally captured trajectory (dotted line). This is followed by significant observations for each joint.

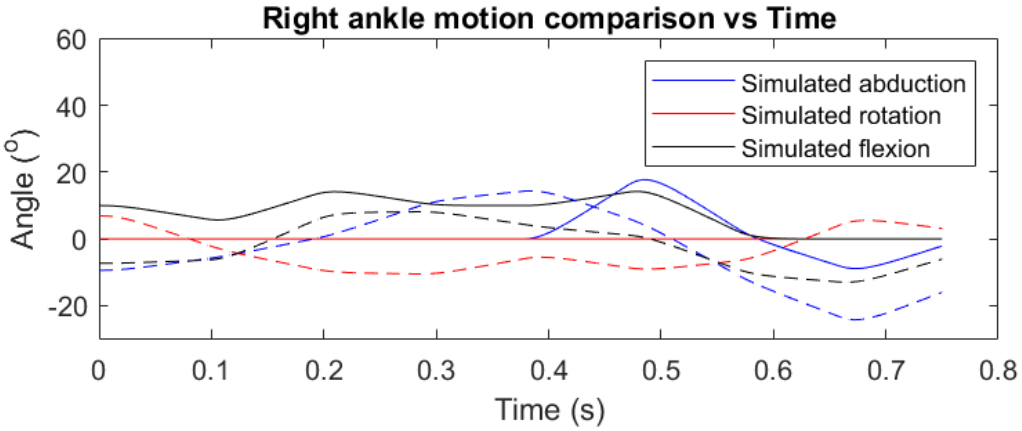


Figure 34: Right ankle motion trajectory

The abduction profile of the simulated trajectory illustrated in Figure 34 is comparable to the captured trajectory. The only significant difference is an offset of 0.2 s (x axis) and 7° (y axis). Ankle abduction/adduction is important for moving laterally, necessary in the second half of the movement.

The flexion/extension profile of the simulated ankle joint trajectory is similar to the captured trajectory. In both, the extension at 0.1 s denoting the initial glide movement is apparent. As is the flexion (0.2 s to 0.5 s) that follows as the athlete prepares for eventual release and extension.

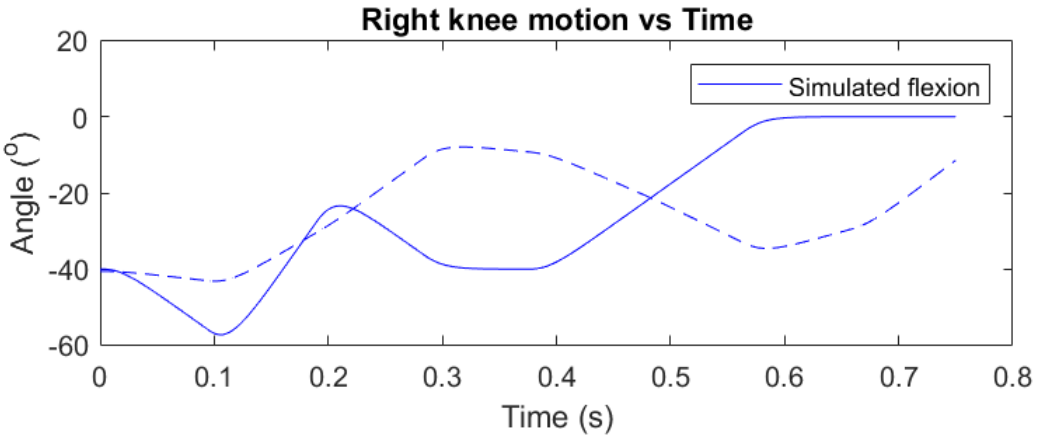


Figure 35: Right knee motion trajectory

The knee joint (Figure 35) was simplified to only articulate flexion/extension. Similarly, to the abduction/adduction of the ankle, there is an offset of 15° and 0.15 s lag for the simulated joint. What is apparent in both the captured data and the simulated results, is the extension at 0.1 s denoting the initial glide and the flexion and extension in the second phase of the movement that allows for the release.

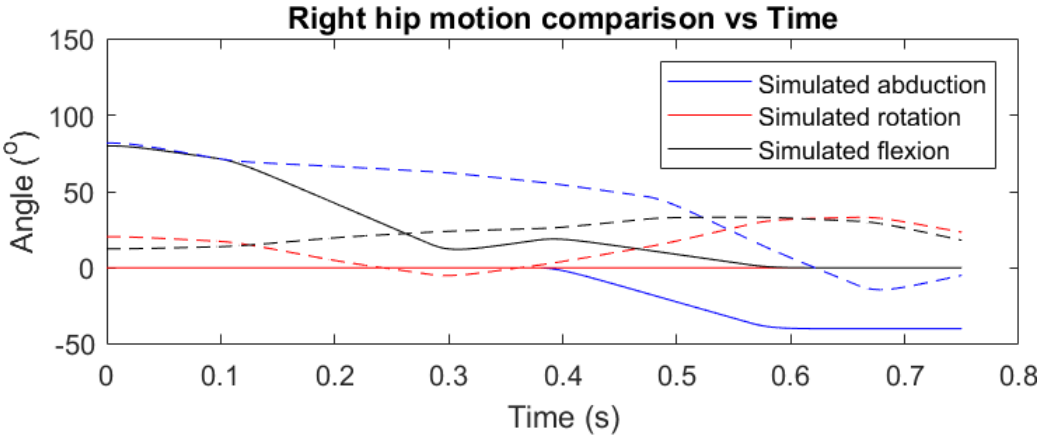


Figure 36: Right hip motion trajectory

The simulated right hip motion (Figure 36) differed significantly to the captured motion where flexion/extension is seen to be inverted. This is apparent in the manner by which the simulated angle is decreasing (flexion) whilst the captured angle increases (extension) during the movement. This disparity could be due to the coordinate systems of Xsens and the simulation not aligning optimally.

An important observation is the way that the ankle, knee and hip operate simultaneously for flexion/extension. This does not exactly align with the integration of segments principle; however, the principle refers to segment velocity and not joint velocity. This is detailed further in the principle investigation (Section 7).

6.1.2 Left hip and trunk joint motion

The trunk (pelvis) and left hip were both modelled with three degrees of freedom.

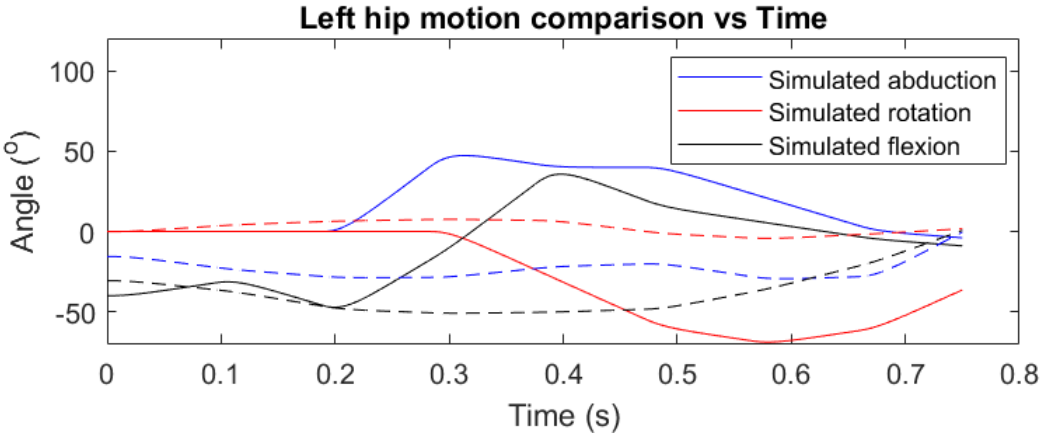


Figure 37: Left hip motion trajectory

Similarily to the right hip, the simulated left hip data (Figure 37) differs when compared with the data collected on the left hip. The profiles of the abduction/adduction and rotation curves are similar to their counterparts. However, the simulated flexion/extension profiles are not alike.

Thus, the trajectories for both joints could not be directly translated into the simulated movement. Two reasons are provided for these deviations:

- Misalignment of coordinate systems. The algorithm used to generate the hip joint in the Xsens motion capture system could use a subtly different coordinate system when describing hip motion.
- Joint complexity. The hip joint has three degrees of freedom and is influenced by trunk rotation and the opposite hip. For these reasons, it is difficult to accurately capture the articulation of the hip for any motion capture system.

Similarly to the hip joints, the trunk or pelvis movement differs significantly to that introduced by the motion capture. With the only exception being the abduction/adduction of the trunk. An explanation for this is that the pelvic joint is being used to represent the entirety of the trunk in the simulation, including each of the vertebra and the shoulders.

6.2 Normal force validation

For this validation strategy the normal force data for the simulation was compared to the collected data from the pressure walkway, illustrated in Figure 38.

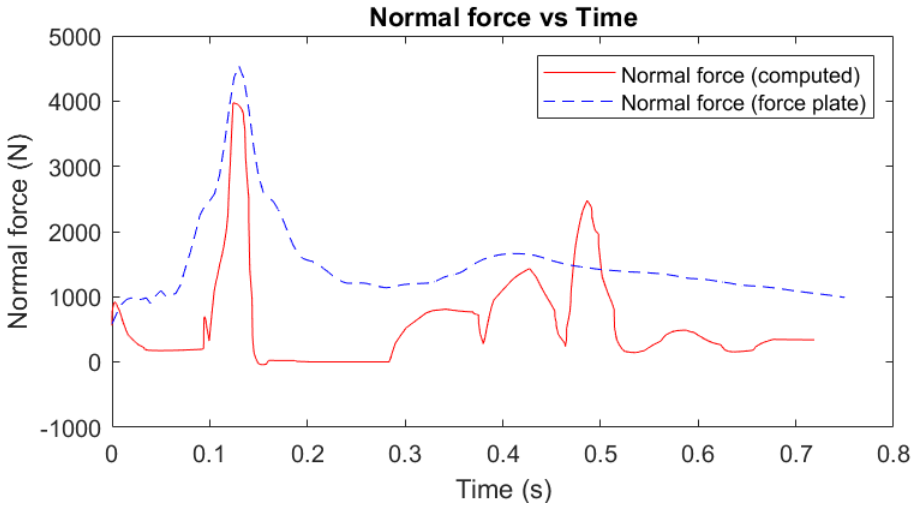


Figure 38: Graph displaying the computed normal force in comparison to one of the experimental data sets.

Table 15 reflects the average of three successful experimental throws from the force plate and compares them to the computed values at significant landmarks.

Table 15: Normal forces at significant landmarks.

	Ti	**TO**	**RFL**	**LFL**	**SR**
Force plate normal force (N)	853	4475	1160	1520	1315
Simulated normal force (N)	880	3981	811	2346	540

Referring to Table 15, the following analysis underlines important observations of the normal forces at each respective timescale landmark:

- T_i. Before the movement has started, the athlete is balanced on one leg. This should be an accurate representation of the standard normal force opposing the weight of the athlete. In this, the two representations are incredibly similar, differing by only 27 N.
- **TO**. The take off of the athlete generates a maximum normal force in both the computed and experimental normal forces. This maximum was used to align the two data sets.
- **RFL**. The right foot landing or impact does not generate a notable maxima for either normal force representations. This result is unexpected despite the correlation in results.
- **LFL**. Left foot landing. Here, the entire weight of the athlete has returned to the force plate and shifts from the right onto the left foot. This is accompanied by a flexion of the right leg which results in the second maximum. It is at this point in the comparison where the computed forces differ most significantly to the empirical values.
- **SR**. The shot release produces an unremarkable local maximum in the data. This could be as a result of the extension having left the lower body and moved onto the upper body.

The normal force data sets had a mean deviation of 837 N and a percentage deviation 50.8 %. This could be as a result of differences in the movement, but is more likely as a result of poor approximations on the part of the normal force computation. The profile of the two normal force graphs however, is remarkably similar, which is encouraging for the accuracy of the simulation.

The normal force computation was also used to identify the timing of significant landmarks. Table 16 details the comparison of values at these points in the movement. The shot release (SR) was not identified as a result of the simulation being lower body specific.

Table 16: Timescale of significant landmarks in the shot put movement

	T_i	**TO**	**RFL**	**LFL**	**SR**	T_f
Motion capture timescale (s)	0	0.16	0.32	0.44	0.65	0.75
Simulated timescale (s)	0	0.12	0.33	0.49	N/A	0.75

Normal force is a direct computation of the simulation and thus was a good metric for this comparison. A pertinent observation here is that the time intervals between each landmark were more pronounced in the simulation. The transition being approximately 0.05 s longer for both the TO-RFL and RFL-LFL transitions.

The accuracy of individual landmarks was encouraging for the validity of the simulation. Particularly considering the simplified segments of the simulated rigid multibody system, it was unreasonable to expect perfect accuracy in the comparison of significant landmarks.

6.3 Displacement validation

A comparison of the CG displacement for the athlete is included as a broader proof of the accuracy of the movement. The results for the x/z CG displacement are included in Figures 39 and 40.

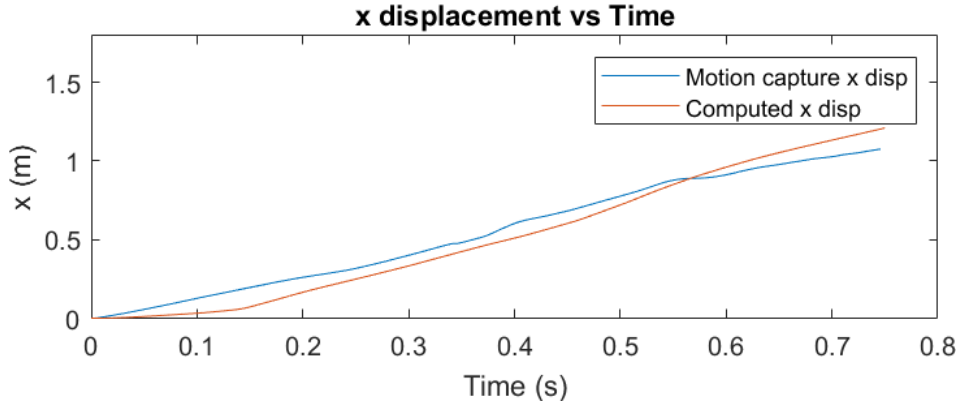


Figure 39: Graph displaying x displacement comparison

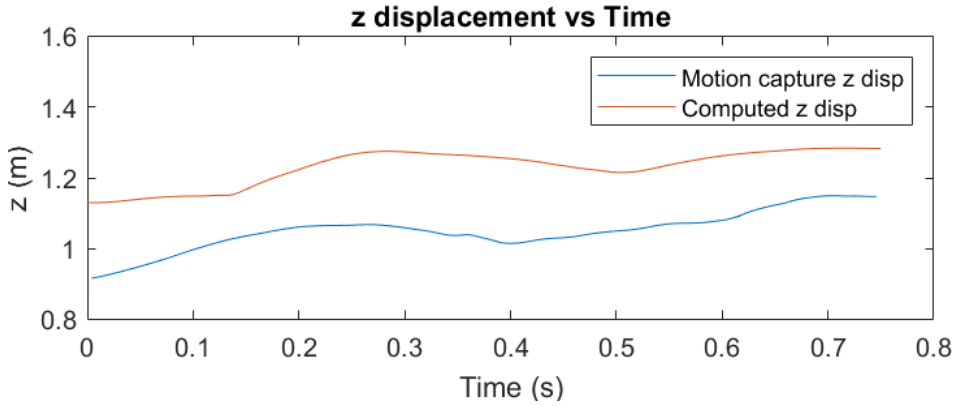


Figure 40: Graph displaying z displacement comparison

The three main points of analysis for this section are as follows:

- The CG x displacement metric (Figure 39) for the simulation is closely alike to that of the motion capture. This indicates that the joint articulation of the simulation is displacing the athlete to approximately the same value during the movement (1.1 m). The greatest difference between the two data sets at any point being 0.13 m indicates at the effectiveness of simulation at aligning with this metric.

- Illustrated in Figure 40, the CG z displacement for the two data sets is incredibly similar which is encouraging concerning the validation of the simulation. There is a consistent 0.15 m offset between the two profiles. This could indicate at an error in the rigid multibody model properties.

- The velocity of the respective data sets is almost identical on observation. This means that, despite the slight difference in timing of significant landmarks, the overall movement of the simulated athlete is valid.

The displacement validation proved the similarity in these metrics for both data sets. The percentage deviation for the respective x displacement data sets was 12.1 %, with a mean deviation of 0.11 m. This result indicates at an almost identical velocity of simulation when compared to reality. Analysis of displacement for each individual segment could lead to a more authentic validation but is beyond the scope for this section.

6.4 Actuation and validation conclusion

The validation of the simulation described in this section explored multiple facets of the overall movement which affirm the quality of the simulation. These are summarized below:

- Accurate input data - the joint data used for the simulation is backed up by data collected of the movement. Deviations and similarities were outlined and significant landmarks of the movement were highlighted.
- Comparable normal forces - the computed normal force graph displayed a similar profile to that of the data collected.
- Similar displacement and velocity - the displacement and velocity of the athlete is almost identical to that of the simulation.

This validation was a vital step to substantiate the claim that a disabled movement can be aligned to able-bodied counterparts. The successful validation affirms the framework developed in the previous sections for the rigid multibody model and prescribed motion.

The primary concern regarding the validation section is the behaviour of the computed normal forces. The human body has a complex means of balancing and modulating contact with a given plane. This is challenging to model in a simulated environment, with simplified body segments. In addition, the approach used required a stiffness and damping coefficient to be assigned to the contact plane. These metrics needed to be altered delicately to develop the required results. These considerations could have had a significant impact on the results.

The section that follows uses the simulation to investigate the thesis statement and compare the results to able-bodied shot put literature. From this, meaningful conclusions on the influence of the prosthesis were made.

7 Principle investigation

The two levels of analysis for the principles are:

- Simulation results
- Parametric study

Observations and relevant analysis are provided for each level of investigation.

7.1 Simulation results

This section refers to the results for the ideal collection of joint trajectories and model properties that applied to the most accurate representation of the movement. The graphs illustrate relevant results that were computed by the simulation. Not included in the parameter investigation, these results are still beneficial and meaningful conclusions are drawn from them.

7.1.1 Segment velocity

The segment velocity results were processed and illustrated as a result of the shot put principles regarding the integration of segments and the extension of the distinct body systems during different phases of the movement.

Right leg segments

The right leg segments include the right foot, lower leg and upper leg. The results are displayed in Figure 41 with relevant landmarks indicated.

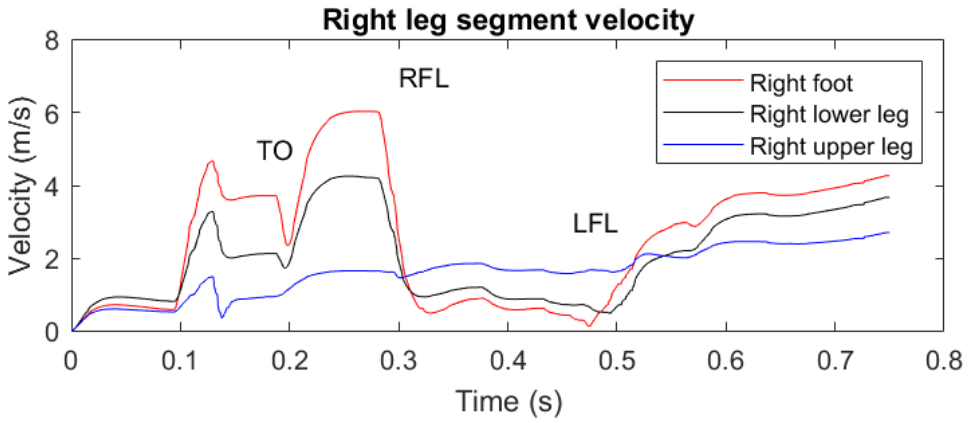


Figure 41: Right leg segments velocity

The results aligned with what was expected from literature concerning the principles governing the integration of segments. Prior to the right foot landing (< 0.3 s), the right leg segments operate in a sequential manner and are activated collectively before the movement proceeds onto other body systems such as the left leg, trunk and eventually the throwing arm. The segments are almost stationary for approximately 0.2 s in the movement (0.3 s to 0.5 s). This supports the principle that the lower segments should provide a stable base for the extension of the upper body. The segments are not motionless however, and it can be speculated that it would be more beneficial if the segments were completely stationary.

Left leg and trunk segments

The left leg and trunk segments include the prosthesis, upper leg, trunk and an approximation of the shoulders. The results are displayed in Figure 42 and observations at relevant landmarks are highlighted.

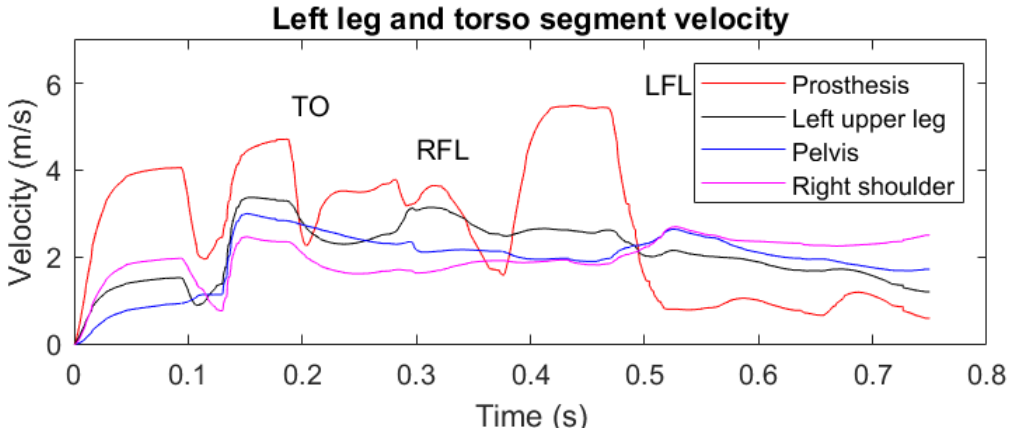


Figure 42: Left leg and trunk segment velocity

A key observation in the results is that the prosthesis has a varied velocity during the movement, particularly in comparison with the result of the segments. This contrasts with the right leg segments, where the activation of the segments happened collectively.

The velocity for these segments correlates more loosely with what was expected from this principle in able-bodied literature. This could be as a result of an issue within the preparation and actuation for the simulation, however, it is more likely that the lack of adherence to the principle indicates toward the influence of the prosthesis. More specifically, that the

prosthesis makes it challenging to a.) activate segments sequentially and b.) keep lower body segments stationary at the critical moment of release.

7.1.2 CG displacement profiles

The CG profile results were processed and illustrated as a result of the evidence of CG principles referenced in literature in the XZ and XY planes.

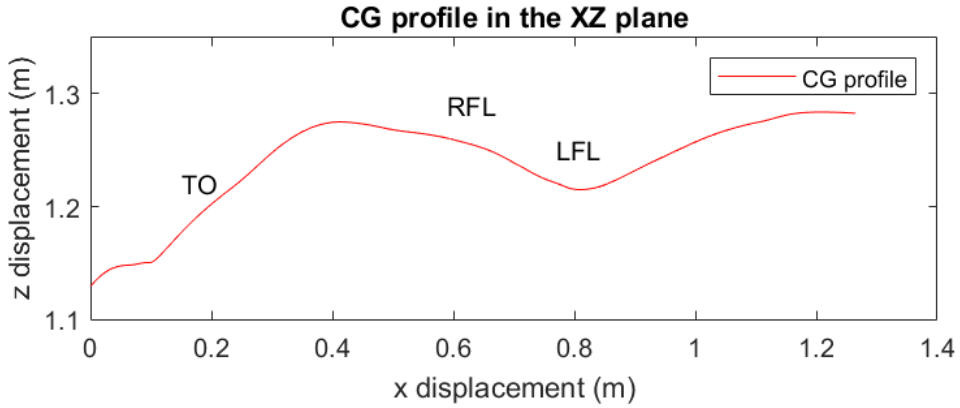


Figure 43: CG profile depicted in the XZ plane

Of the two planes investigated, the XZ is referenced most often in literature. It also produced more relevant results where it correlated well with what was expected from able-bodied principles. This is illustrated in Figure 43, where it follows a clear sinusoidal shape. The maximum displacement is taken at release.

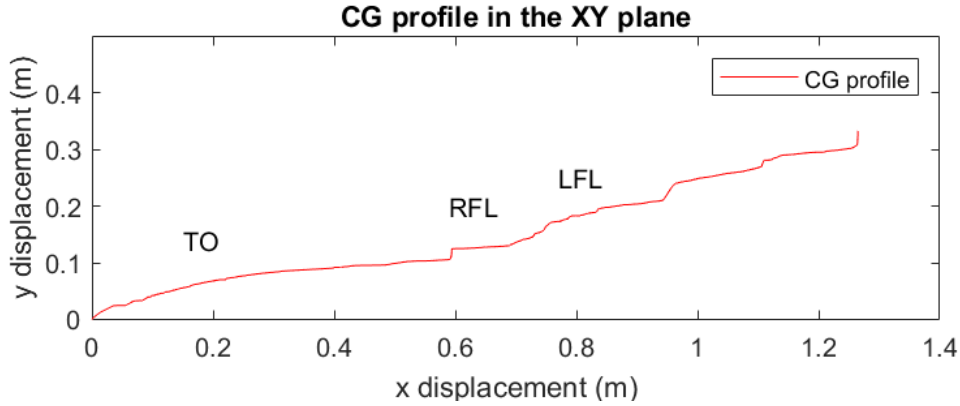


Figure 44: CG x displacement

The computed x displacement behaved well in the simulation results, particularly with what was expected through the literature search. Noteworthy evidence from Figure 44 is that a consistent direction is maintained. The deviation in the y axis is minimal. This does not exactly correlate with any evidence from literature but it is a point of consideration for this and future investigations.

Overall the simulation results and principles highlighted above behaved well in their correlation with what was expected through able-bodied principles. In addition, important contributions were raised concerning the influence of the prosthesis.

7.2 Parametric results analysis

The strategy for this analysis was to investigate the able-bodied shot put principles by varying the prescribed motion to pertinent movement parameters. Each parametric test is described in terms of its importance to the movement, the testing method, and its relevance to shot put principles found in literature.

7.2.1 Knee flexion during initial glide

There were five alternate knee flexion angles investigated, illustrated in Figure 45. This parameter underlined the initial glide or small jump that is initiated at TO, this is designated by a label in Figure 45.

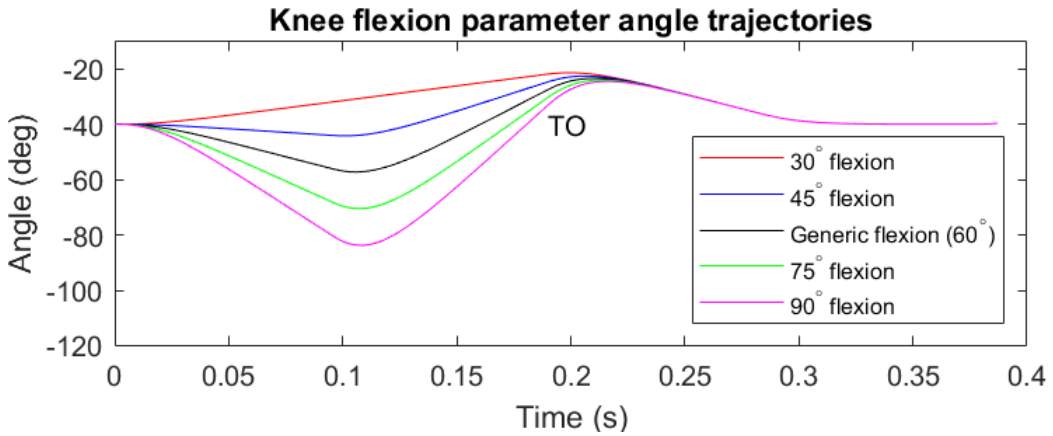


Figure 45: Graph displaying knee flexion trajectories used for the knee flexion parameter.

The goal for this parameter was to identify flexion angles which result in suitable extension and thus displacement. Flexion angles were excluded due to an ineffective glide displacement, or inefficient friction and torque implications. The friction and torque results for each flexion angle are illustrated in Figure 46 and 47 respectively.

Friction force

The effectiveness of translation in the x direction was dependent on the friction forces elicited. The results of which are illustrated in Figure 46.

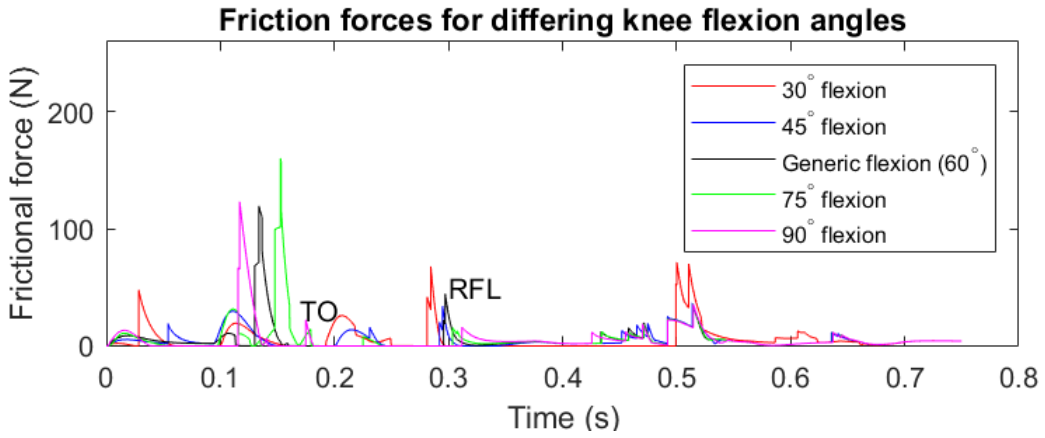


Figure 46: Graph displaying friction forces for varying knee flexion angles.

Notably, the friction increases in proportion to the torque results. This was unsurprising as both torque and friction are dependent on the normal force. The friction increased uniformly with the flexion angle until the 90° flexion where it was notably less than the previous test. This indicates that there is a limit to the benefits of an increased initial flexion angle and an effective flexion range.

Torque

The torque results for the five knee flexion tests are illustrated in Figure 47.

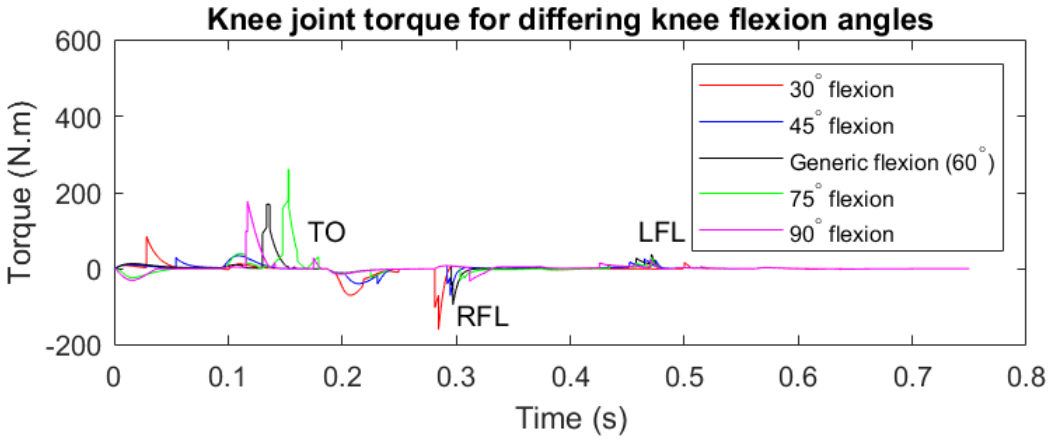


Figure 47: Graph displaying knee joint torque required for varying knee flexion angles.

There were three primary torque observations. The first point is that torque increased with the flexion angle. This was anticipated but encouraging for the validity of the torque computation of the simulation. The second observation was that the knee and hip joint experience the majority of the torque in comparison with the ankle in all tests. This was appropriate due to the muscular resources available to these two joints, in addition to the superior moment arm available to both. Lastly, the 90° flexion does not generate significant torque in any of the right leg joints. This indicates that there is a limit to the torque returns for increased friction.

Table 17: Table detailing results based on a varying knee flexion range during the initial glide movement. * indicates the generic flexion used by the athlete.

Flexion #	**Flexion angle (^{o})**	**Torque (N.m)**			**Friction force (N)**	**Displacement (m)**	
		Ankle	**Knee**	**Hip**		**x**	**z**
1	30	17.2	71.0	85.4	47.8	0.25	0.01
2	45	10.2	36.9	34.6	29.7	0.29	0.02
3*	60	45.8	161.2	169.8	119.5	0.44	0.04
4	75	66.9	223.3	261.4	160.1	0.38	0.05
5	90	8.0	182.0	177.5	122.9	0.20	0.05

Displacement

The displacement results detailed in Table 17 were the most accurate means for determining the glide efficacy of a given flexion angle. From this result it is evident that the 60° and 75° flexion results in torque and friction that propels the athlete sufficiently in the x and z directions. Tests 1, 2, and 5 can be excluded due to the lack of displacement in the x direction, indicating at an ineffective initial glide movement.

Able-bodied literature does not indicate at an ideal displacement for the initial glide movement. However, as discussed in Section 2.1.3, it is a well accepted principle of the shot put movement. The parameter also provided insight into a flexion/extension based movement, the hip abduction parameter provides insight into an abduction/adduction movement.

7.2.2 Hip abduction for delivery stance

There were five incrementally increasing abduction angles investigated in this parameter. The delivery stance is established at the LFL landmark and provides a base from which the release ultimately takes place. The combined abduction angles used during the test are illustrated in Figure 48.

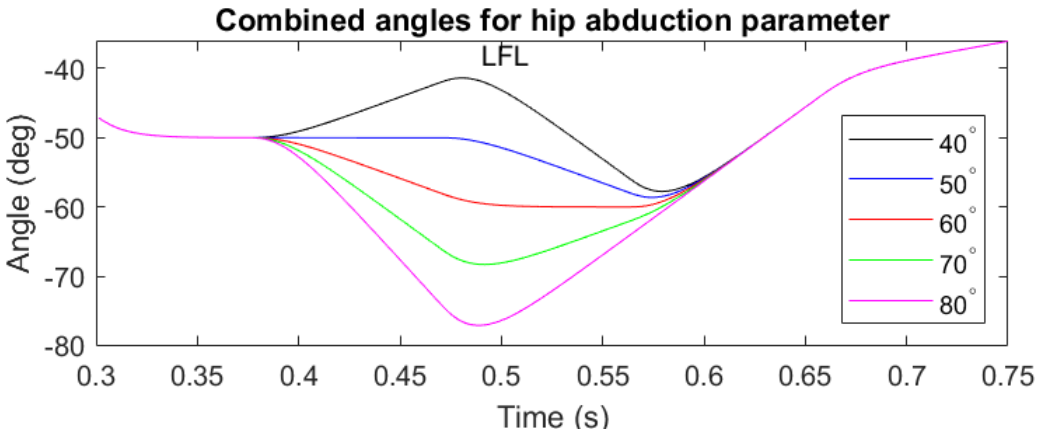


Figure 48: Graph displaying the combined hip abduction angles used in the hip abduction parameter

The goal for the testing of this parameter was to observe the implications of differing abduction angles on the torque and friction metrics. Furthermore, with delivery stance values

taken from literature, the results provide information on the friction and torque variance when concerning these able-bodied values.

Friction and torque results

Notably, the torque on each leg was inversely proportional to the friction force acting on it. This is evident in Table 18. A further observation is the torque on the left leg increased significantly (approx. 180 N.m) with the increasing abduction angle. Likewise, the torque on the right leg decreased (less significantly) with an increased abduction angle.

This data holds true to the principles governing segment velocity, where the torque data peaks at the point of the delivery stance. This indicates at muscle activation in the hips at that point. Furthermore, this activation recedes for the rest of the movement as the hips stabilize to form a base for a powerful release.

Table 18: Table detailing the results of the hip abduction parameter taken at the left foot landing (LFL) landmark, approximately 0.49 s.

Abduction angle #	**Angle**	**Friction force (N)**		**Abduction torque (N.m)**		**Delivery stance (m)**
		Right	**Left**	**Right**	**Left**	
1	40	51.6	29.4	-1.8	55.0	0.92
2	50	48.9	62.0	-3.3	46.2	1.16
3	60	37.5	78.4	-4.9	23.8	1.17
4	70	35.0	116.8	-53.6	7.4	1.22
5	80	37.3	189.8	-139.9	15.7	1.31

Delivery stance

The delivery stance is an essential principle that was scrutinized by this parameter. The accepted range of delivery stance values found in literature is approximately 1.1 m to 1.3 m. This range is incredibly alike to the delivery stances generated in this parameter (Table 18) and their associated hip abduction angles. Three key observations are summarized below:

- The generic delivery stance computed by the simulation (1.17 m) would be considered to be on the lower end of the able-bodied delivery stance spectrum. This is undoubtedly as a result of the influence of the prosthesis.
- The friction increases in proportion to the delivery stance. This occurs opposite to the direction of the release and is detrimental if excessive. A trade off is then required between extending the delivery stance (and the acceleration path) against the friction required to overcome it.
- The correlation between the computed delivery stances and the ones found in literature is encouraging for the validity of the simulation and the claim that able-bodied principles can be aligned to fit a disabled movement.

If able-bodied literature is to be utilized in the case of this parameter, a wide delivery stance is beneficial for the efficacy of a throw to increase the path of acceleration for the shot during the movement preamble. The increase in friction force opposing this is exponential which indicates that an abduction angle close to 60° is beneficial as the friction has not increased to the point of having an inverse effect on the movement.

7.2.3 Trunk rotation for release velocity

There were four different rotations investigated for the trunk rotation parameter. This investigated if there was any notable impact on the rest of the movement where different rotations were used. The primary result concerns the friction force and velocity metrics generated at movement landmarks during the throw. The four different rotations are shown in Figure 49 followed by angular velocity results (Figure 50). Significant values are detailed in Table 19.

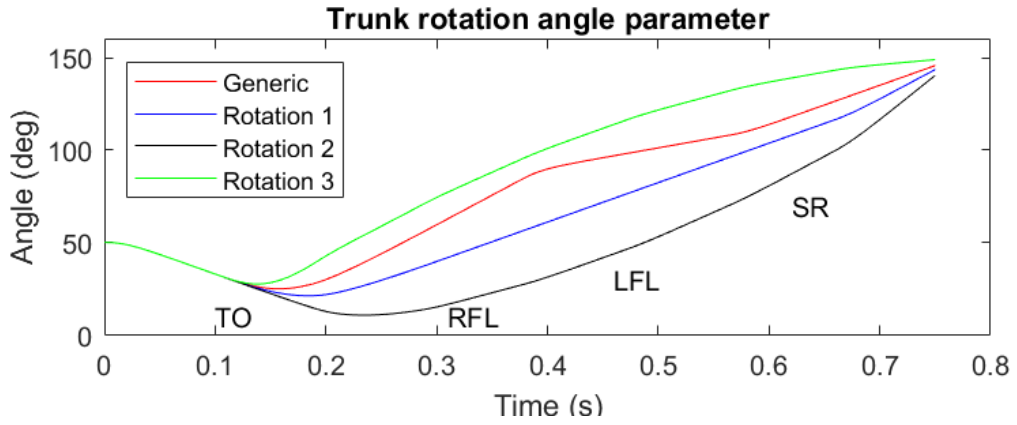


Figure 49: Trunk rotational trajectories used for the trunk rotation parameter

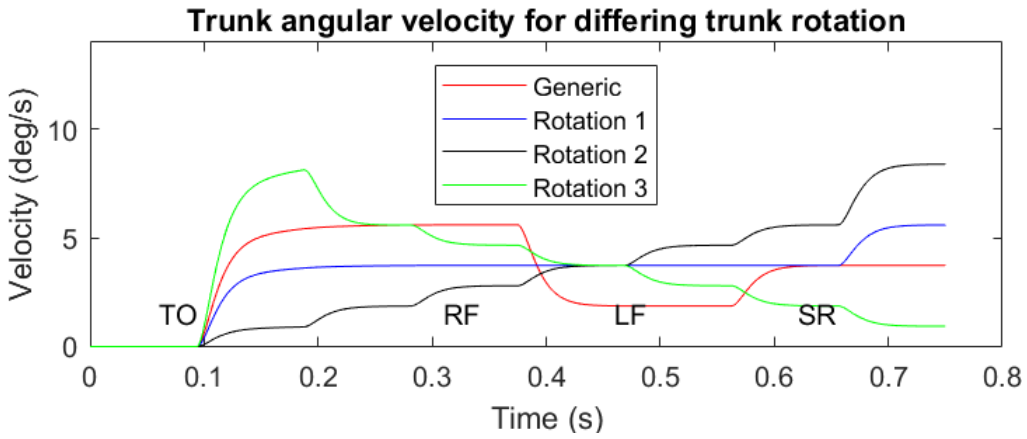


Figure 50: Graph displaying the trunk angular velocity for differing trunk rotation

Table 19: Table of local maximums denoting throw landmarks for varying trunk rotations. FF = Friction force, AV = Angular velocity

	TO (0.12s)		**RFL (0.3s)**		**LFL (0.49s)**		**SR (0.69s)**		**Release velocity**
Rotation #	FF (N)	AV (°/s)	FF (N)	AV (°/s)	FF (N)	AV (°/s)	FF (N)	AV (°/s)	**(m/s)**
1*	160.1	5.1	8.1	5.5	15.6	5.6	11.9	3.7	0.026
2	126.6	3.4	8.1	3.7	37.0	3.7	12.0	3.7	0.026
3	126.6	0.9	7.4	1.5	36.8	4.6	11.6	5.6	0.039
4	153.9	7.7	9.8	5.7	53.4	5.4	6.4	1.9	0.013

The principle concerning the integration of segments indicates that as the trunk (pelvis) is the last segment in the lower body, the rotation where the trunk reaches a maximum angular velocity would be most ideal, this is rotation number three. For this rotation, the friction results (Table 19) are comparable to the preceding rotations meaning that this rotation could provide the friction necessary to provide the muscular force of a throw. However, this does not correlate with the generic rotation.

Trunk rotation is a vital principle of the shot put throw. This is underlined in Section 2.1.4. However, in this instance, developing a parameter to corroborate this principle proved to be challenging. There are intricacies in the shot put movement that may require a more in depth knowledge of the movement to accurately model or interpret the results.

7.2.4 Prosthesis property parameters

The geometry and friction coefficient properties were varied in this parameter to provide insight into the nature of the prosthesis's influence. This is important when considering the need to investigate the modifications to the movement that are necessary as a result of this influence.

The prosthesis is independent of the other segments in that it has different properties and a simplified joint interface which means that the properties and trajectory of the prosthesis was malleable whilst being tested. Table 20 details the results of this parameter at the left foot landing (LFL) and shot release (SR) landmarks, as this is where the prosthesis influences the movement.

Table 20: Prosthesis parameters. *denotes the generic geometry and friction coefficients used.

Varying prosthesis geometries		
	Friction force (N)	
Test #	LFL	SR
1	39.2	14.4
2	48.6	9.3
3*	40.0	11.9
4	33.0	13.6
5	36.7	8.0

Varying friction coefficients		
	Friction force (N)	
Test #	LFL	SR
1*	35.4	11.9
2	31.0	10.4
3	22.3	7.5
4	4.6	3.1
5	0.9	0.5

Prosthesis contact surface geometry

The contact surface parameter investigated if increased contact area with the ground during the final part of the movement would increase the friction or torque significantly and therefore have a considerable influence on the efficacy of the movement.

The results of this parameter did not follow an obvious pattern. This is evident in the varied friction results irrespective of the geometry used evident in Figure 51. The geometry used in Test 5 reflects the surface area of an able-bodied athlete's shoe. The decreased friction force could be as a result of the simulation not interfacing with the increased geometry accurately.

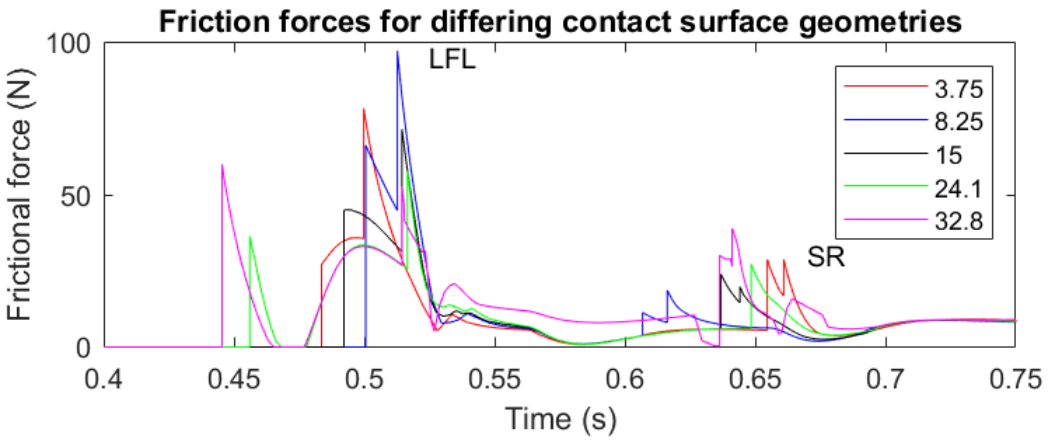


Figure 51: Graph displaying the friction force variance for differing prosthesis surface areas. * legend units: x$10^{-3}m^2$

For an effective test, the movement would have to be altered suitably in each rendition of the geometry test to ensure that the contact surface interfaces consistently with the contact plane. However, the movement alterations would have to be standardized and measurable for it to be a fair test. This difficulty was a setback to the testing of this parameter.

Prosthesis friction coefficient

The second property tested was the friction coefficients for the prosthesis. This investigated the changes in friction force by varying coefficients, the approach is visualized in Figure 52.

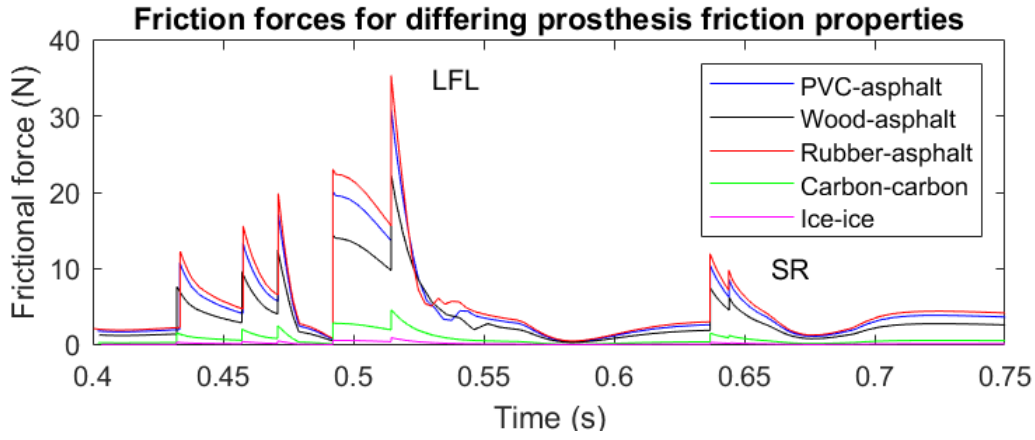


Figure 52: Graph displaying the friction force variance for differing prosthesis friction properties

The contact surface used by the prosthesis most closely reflects the friction coefficients of an athletic shoe on the same surface. While excessive friction would undoubtedly hinder the movement of the athlete, this parameter indicates that the surface used by the athlete in question aims to maximise this variable..

It was evident through these results that the athlete requires a measure of friction at shot release for an effective throw. This was clear in that the coefficients of friction assumed for the athlete in question result in the largest friction computation. Despite not offering any crucial principle information, this parameter played the important role of validating the contact force model used.

7.3 Principle investigation conclusions

Simulation and parameter investigation results were accurately depicted and analyzed in this section to provide substantiation to shot put principles from able-bodied literature used by the athlete in question. Pertinent results were identified, and analyzed for key observations.These are summarized below:

- The segment velocity results provided substantiation for the principles concerning the integration of segments in the shot put movement. The right leg segments aligned well with these principles, the left leg did not, which indicates at the influence of the prosthesis..
- The CG profile results correlated well with the same principles from able-bodied athletes. This also validated the contact model and the joint trajectories used in the simulation.
- Insight into the torque dynamics of the knee flexion movement during the initial glide was significant. The results indicate that a flexion of 60° to 75° provides a suitable initial glide based on the result jump displacement. The prosthesis has no influence on this movement.
- Evidence from the testing of the combined hip abduction angle for the delivery stance principle indicates that a 60° angle is advantageous when concerning the friction and torque results. This resulted in a delivery stride width of 1.17m which is found to be on the lower end of the widths expected from able-bodied principles.

- The prosthesis parameters provided important results on the influence of the prosthesis. Importantly, the parameters also provided an opportunity to validate the contact model used.

It is clear through the principle investigation that the movement abides relatively closely to the principles governing the able-bodied movement. The deviation from the principles of able-bodied athletes is undoubtedly due to the influence of the prosthesis, the exact manner of which was investigated by the analysis. This is summarized in Table 21.

Table 21: Table highlighting the influence of the prosthesis for individual principles.

Principle	**Able bodied athletes**	**Disabled athlete**
Initial glide	There was little evidence for a value for the initial glide. However, the importance is well underlined to provide linear momentum for the release.	An initial glide of approximately 0.4∼m, with a height off the ground of 0.04∼m was seen to be most advantageous
Delivery stride	Evidence was provided in literature of a delivery stride of between 1.1∼m and 1.4∼m. The delivery stride plays an important role of providing a stable base from which to release.	The delivery stride principle is most influenced by the prosthesis. The results indicate at a shortened delivery stride width as a result of a lack of stability.
Trunk rotation	The trunk rotation is the crux of a powerful and effective release. A rotation of approximately 150 has been observed in able-bodied athletes.	The trunk rotation results did not cooperate well with the simulation. However, it is evident that a gradually increasing rotational velocity is advantageous.
Segmental velocity	Evidence in literature indicates that the segments get activated sequentially, cascading upward for the eventual release. This means that movement initiation begins with the right foot and ends with the right hand.	The segmental velocity results aligned well with what is evident in able-bodied sports research. Particularly in prior to the left foot landing (<0.46 s). After the left foot lands, the influence of the prosthesis is evident as it interrupts the sequential activation of segments.
Displacement profile	The profile in the XZ plane indicates at a sinusoidal shape. The profile in the XY plane maintains uniformity such that no energy is wasted in a different direction.	The displacement profile of the athlete correlated well with the principles outline from able-bodied research. This indicates that the prosthesis had little effect on this principle.

The primary recommendation for this part of the project would be to include a more intensive parameter search. Unfortunately, the parameters available to be tested were only made clear when an understanding of the limitations for the simulation were established. This could mean that there should be an extensive literature search and discussion with the athlete and coaches after the simulation is completed with reference to the exact capabilities of the simulation. Or there could be an entirely different investigation into how best to use multi body simulations for an irregular movement.

Comparative study

The current research aimed to investigate the influence of a prosthesis by aligning the movement to that of able-bodied individuals in literature. These investigations in the literature search typically use empirical models based off optical motion capture systems. This produces a degree of difficulty in the alignment of the disabled movement to able-bodied principles found in literature. A comparative study may have provided more in depth information where two simulations could have been built representing an able-bodied and disabled athlete respectively.

The principle investigation provided a thorough means of understanding an irregular movement and offered a scientific foundation which otherwise was not present. Dynamic results, such as friction forces and joint torques, were computed which are not offered in literature. The next section offers broad conclusions for the entirety of the analysis and amalgamates the body of the investigation, including the validation and motion capture procedures.

8 Conclusion

8.1 Summary of investigation

The movement investigation framework developed in this study determined the relevance of able-bodied shot put research on a shot put movement when influenced by a lower limb prosthesis. This was accomplished as follows:

Significant shot put movement principles were identified from able-bodied literature. The main biomechanical principles of able-bodied shot put athletes were found to be concerned with segment velocity, CG profile, feet sequencing and trunk rotation.

Motion data was captured using an Xsens MVN Analyze system to provide accurate prescribed joint and segment data for the simulation. Using this data with regression equations found in literature, an accurate, simplified rigid multibody model was developed for use in the multibody simulation.

The model was validated using data acquired from the FDM Pressure Walkway. This was compared to computed normal forces from the simulation. The validation also included a CG displacement comparison and the timescale of relevant movement landmarks determined through the motion capture procedure. These comparisons led to an acceptable simulation and validation of the accuracy of the rigid multibody model and its movement.

The results of the validated simulation were used in two different applications. The first being the simulation results section, where pertinent shot put principles were examined against the simulated movement results. The second application was in a parametric study where significant movement parameters were identified and tested to observe similarities to able-bodied shot put and the influence of the prosthesis on the movement.

8.2 Summary of findings

The findings are split into three sections: validation, shot put principles and prosthesis influence. Important points with regards to the validation of the simulation are outlined below:

- The profile of the simulated CG correlated very well with the same principle found in literature. Particularly in the z direction, where the profile follows the sinusoidal shape found to be beneficial in literature.
- The efficacy of the contact force model was validated in accurate normal/friction force values. Importantly, the initial glide parameter provided an effective jump or displacement which also underlines the efficacy of the contact model.
- The delivery stance parameter of the simulated movement fell within the range of delivery stride widths found to be effective in literature.
- Most importantly, the normal force computation provided comparable values and profiles with the empirical normal force data acquired using a pressure walkway.

Using the validated simulation, the simulation results and parametric study provided invaluable analysis for the study of able-bodied shot put principles found in literature:

- The right leg segment velocity aligned well with the integration of segments principles. The left leg (and prosthesis) did not align well. This is undoubtedly as a result of the influence of the prosthesis.
- The CG profile results correlated well with the same principles from able-bodied athletes. More specifically, the CG profile of the simulated movement followed a sinusoidal profile in the XZ plane, the importance of which is underlined in able-bodied shot put literature.
- The knee flexion results for the initial glide indicate that a flexion of 60° to 75° provides a suitable initial glide based on the result jump displacement.
- The hip abduction parameter indicated that a 60° combined angle is advantageous when concerning the delivery stride principle. This results in a delivery stride of approximately 1.1 m.

- The prosthesis parameters provided invaluable results on the influence of the prosthesis (detailed below). In addition, this parameter set up discussion points for the simulation of human movement.

Points concerning the influence of the prosthesis are as follows:

As described, the left leg segment velocity results did not align well with able-bodied shot put principles. This is very likely as a result of the action of the prosthesis on the left leg in the movement. Secondly, the simulated delivery stance of the athlete in question was on the lower end of the able-bodied delivery stride spectrum. This undoubtedly points toward the influence of the prosthesis on this part of the movement.

The implications of these two points are mitigated by the athlete in practice. However, it is invaluable that the exact nature of the influence was identified.

8.3 Conclusions

The current research successfully developed a framework to investigate the degree to which able-bodied research can be adapted to the use of a disabled athlete where the movement has been significantly influenced by the presence of a prosthesis. This analysis provided an important foundation from where the exact influence of the prosthesis could be investigated.

The outcome of this investigation is that disabled athletes need not view their movement in isolation to the principles of movement of their able-bodied counterparts. This is despite the significant influence of the prosthesis, and the adaptations required to be made to the movement that renders it different to their able-bodied peers.

The able-bodied shot put principles coupled with the multibody simulation developed to investigate these principles, has been proven to be a significant progression to remedy the paucity in disabled sports research for the athlete in question. The most significant areas of influence on the movement by the prosthesis are where stability is required in the delivery stride and release. This is evident in a shortened delivery stride width and a decreased rotational velocity to able-bodied counterparts.

The segmental velocity of the disabled athlete, along with the displacement profiles align well with what is found in able bodied literature. Providing credence to the claim that disabled athletes can rely on able-bodied research. For a disabled athlete, the evidence from this

study would indicate the segmental velocity should be attain a local maximum sequentially, cascading up the body until release occurs. Furthermore, in the XY plane, the profile of the CG maintain uniformity of direction, whilst a sinusoidal shape should be observed in the XZ plane.

It is evident from this investigation that there is significant scope for disabled sports science to investigate a given movement due to the influence of the prosthesis. This influence, whilst hindering the overall efficiency of the movement, adds another element to the training and movement science for disabled athletes. A further significant outcome from the current investigation is the assertion that the principles identified from able-bodied research can be considered as fundamental theory for disabled athletes for any given projectile sport. This inference is made due to the fact that the disabled athletes movement aligned well to these principles, despite the significant influence of the prosthesis.

8.3.1 Recommendations for future work

The points that follow are relevant areas in the investigation which could be altered or extended in future work.

A distinct validation movement framework where specific movements are used solely for the purpose of validating the model is ideal. This is contrasted with the process used in the investigation where the shot put movement was used to validate the model. This movement is not repeatable or measurable to the same degree that a more simple movement would be. A good example would be to use a series of single leg squats. The single leg squat is a part of the shot put movement and can be repeated for a large sample to develop a reliable source of data that would be contrasted to the simulation values. This was not able to be undertaken or corrected in the investigation due to availability constraints on the athlete under investigation and its importance was only fully realized retrospectively.

Investigations such as these underscore the inherent intelligence of the human body. This goes beyond simple motor function and extends to the body's ability to intuitively balance itself throughout a complex movement. This is known as proprioception and is challenging to replicate on a simulated level. Measures need to be put in place to substitute for this ability. However, these measures have effects that influence the entire movement and introduces more complexity into an already elaborate compilation of factors. As discovered in

this investigation, the simplifications necessary in multibody human movement simulations can introduce more complexity than they remove.

Therefore, the nature of the movement needs to be considered when developing a simulation. Fewer simplifications are needed to compensate for movements that are already straightforward. Movements such as this could include weightlifting, gymnastics or cycling. These movements operate under strict constraints that would be better suited to a simulation process.

An important advantage of simulation based studies is the novel computed results from the simulation. For multibody robotic and human simulations, this is most pronounced by the joint torque data. The results of investigations such as this one could have a positive impact on the realm of new age prostheses that are essentially bionic. The torque results could be used as prescribed measures for servo motors and the like. Undoubtedly the simulations would need to be incredibly complex with an integrated understanding of the individuals disability along with the interface and capability of prosthesis components.

References

[1] S. K. S. Yadav. Advantage of biomechanics in sports. *International Journal of Applied Research*, 2(5):669–670, 2016.

[2] World Para Athletics. Rules and regulations 2018-2019. *World Para Athletics*, page 23, 2019.

[3] G. Laurence. Shot put history - where did it begin? *Ezine@Articles*, 2010.

[4] J. Lanka. *Chapter 21; Shot putting*, volume 4 of *The encyclopedia of sports medicine*. Blackwell Sciences Ltd, 2000. Biomechanics in sport.

[5] P. G. Brolinson, M. Rogers, and J. Edison. *Functional and Kinetic Chain Evaluation of the Hip and Pelvis*. Springer, 2017.

[6] G Marhold. Biomechanical analysis of the shot put. *Baltimore: University Park Press*, pages 502–509, 1973.

[7] W. Schaa. Biomechanical analysis of the shot put at the 2009 iaaf world championships in athletics. *New Studies in Athletics*, 25(3/4):9–21, 2010.

[8] M. R. Broer; R. F. Zernicke. *Efficiency of Human Movement*. Harcourt College Publishers, 2009.

[9] M. Zatsiorsky, G. E. Lanka, and V. Shalmanov. Biomechanical analysis of shot putting technique. *Exercise and Sport Sciences Reviews*, 9(1):353–389, 1981.

[10] M. Coh and M. Supej. Comparative biomechanical analysis of the rotational technique. *Collegium antropologicum*, pages 250–251, 2008.

[11] A. Lees, T. Asai, T. B. Andersen, H. Nunome, and T. Sterzing. The biomechanics of kicking in soccer: A review. *Journal of Sports Sciences*, 28(8):805–817, 2010.

[12] D. Greenwood, K .Davids, and I. Renshaw. The role of a vertical reference point in changing gait regulation in cricket run-ups. *European Journal of Sport Science*, 16(7):794–800, 2016.

[13] C.B. Blackwood, T.J. Yuen, B.J. Sangeorzan, and W.R. Ledoux. The midtarsal joint locking mechanism. *Foot Ankle Int.*, 26(12):1074–1080, 2005.

[14] Vicon Motion Systems Limited. Oxford foot model 1.4 release notes june 2012. *VICON*, Version 1.4, 2012.

[15] A. Lenz. The optimal angle of release in shot put. *Durham University*, pages 3–5, 2010.

[16] K. Bartonietz and A Borgstöm. The throwing events at the world championships in athletics. *New studies in athletics*, 10(4):43–63, 1995.

[17] P. J. Worthington, M. A. King, and C. A. Ranson. Relationships between fast bowling technique and ball release speed in cricket. *Journal of Applied Biomechanics*, 29:78–84, 2013.

[18] A. Mero and P. Komi. Body segment contributions to javelin throwing during final thrust phases. *Journal of Applied Biomechanics*, 10(2):166–177, 2016.

[19] W. Schaa. Biomechanical analysis of the shot put at the 2009 iaaf world championships in athletics. *New Studies in Athletics*, 25(3/4):15–17, 2010.

[20] G. Terzis, T. Kyriazis, G. Karampatsos, and G. Georgiadis. Muscle strength, body composition, and performance of an elite shot-putter. *International Journal of Sports Physiology and Performance*, 7(4):394–396, 2012.

[21] C Sugumar. Physical education a biomechanical analysis of the shot put performance. *Global Journal for Research Analysis*, 3(5):118–119, 2014.

[22] R. Shumaker and H-C Chen. *Multimedia and Video Analysis for Sports*. Springer Science, 2010.

[23] I. Kakadiaris and C. Barron. Model based motion capture. *University of Houston*, page 326, 2006.

[24] A. Miller. An upper extremity biomechanical model: Application to the bicep curl. *Grand Valley State University*, page 30, 2007.

[25] R. Tranberg. Analysis of body motions based on optical markers. *University of Gothenburg*, page 14, 2010.

[26] J. T. Zhang, A. C. Novak, B. Brouwer, and Q Li. Concurrent validation of xsens mvn measurement of lower limb joint angular kinematics. *Queens University*, page 1, 2013.

[27] Xsens. *MVN User Manual*. Xsens, revision v edition, 2018.

[28] M. Schepers and M. Giuberti. Xsens mvn: Consistent tracking of human motion using inertial sensing. *Xsens Technologies*, pages 1–7, 2018.

[29] G. Grimshaw and A. Burden. *Sports & Exercise Biomechanics*. Taylor & Francis Group, 2006.

[30] A. C. Fry, T. J. Herda, A. J. Sterczala, et al. Validation of a motion capture system for deriving accurate ground reaction forces without a force plate. *Big Data Analytics*, 2016.

[31] A. D. Kaye and S. F. Davis. *Neurophysiological Assessment, Mapping, and Monitoring*. Springer, 2014.

[32] C. Fisher. State estimation of a cheetah spine and tail using an inertial sensor network. *University of Cape Town*, page 11, 2012.

[33] W. Wang. Unit 6 - computer simulation. *University of Dundee, Distance Learning Section*, page 1, 2012.

[34] G. A. Korn. *Advanced Dynamic-system Simulation: Model-replication Techniques and Monte Carlo Simulation*. John Wiley & Sons, 2007.

[35] S. Delp, F. Anderson, and A. Arnold et al. Opensim: Open-source software to create and analyze dynamic simulations of movement. *IEEE Transactions on biomedical engineering*, 54(11):1940–1950, 2007.

[36] W. Wang. *Unit 2. Modelling Techniques*. Distance Learning Section, University of Dundee, 2012.

[37] A. Karatsidis et al. Estimation of ground reaction forces and moments during gait using only inertial motion capture. *Sensors (Basel)*, 17(1):75, 2017.

[38] P. Kudzia. Estimating body segment inertial parameters of the human body using a microsoft kinect. Master of applied science, Queen's University, Kingston, Ontario, Canada, 2015.

[39] L. S. Persad. Musculoskeletal modelling of the shoulder during cricket bowling. *Department of Bioengineering, Imperial College London A*, page 23, 2016.

[40] P. Eastman and M. Sherman. *Simbody and Molmodel User's Guide*. Stanford University, second edition, 2011.

[41] A. Seth, M. Sherman, and J. Reinbolt. Opensim: A musculoskeletal modeling and simulation framework for in silico investigations and exchange. *Procedia IUTAM*, 2:212–232, 2011.

[42] MATLAB and Simulink Robotics Arena. Modeling and simulation of walking robots. *Mathworks*, 2020. https://www.mathworks.com/videos/modeling-and-simulation-of-walking-robots-1576560207573.html.

[43] MATLAB and Simulink Robotics Arena. Introduction to contact modeling, part 2. *Mathworks*, 2017. https://www.mathworks.com/videos/matlab-and-simulink-robotics-arena-introduction-to-contact-modeling-part-2-1502716250563.html.

[44] S. Brunßen, S. Hueber, and B. Wohlmuth. Contact dynamics with lagrange multipliers. *Solid Mechanics and its Applications*, 1970.

[45] MathWorks. *Simscape Multibody User Guide*, volume 17. The MathWorks Inc., 1 Apple Hill Drive, Natick, 2020.

[46] T. Zhang, A.C. Novak, B. Brouwer, and Q. Li. Concurrent validation of xsens mvn measurement of lower limb joint angular kinematics. *Physiological Measurement*, 34:63–69, 2013.

[47] W. M. Chung, S. Yeung, W. W. Chan, and R. Lee. Validity of vicon motion analysis system for upper limb kinematic measurement. *Hong Kong Polytechnic University*, 2011.

[48] Zebris Medical GmbH. The zebris fdm system— gait and roll-off analysis in practice. *The World of Biomechanics*, 2012.

[49] V.M. Zatsiorsky and V.N. Seluyanov. Mass-inertial characteristics of the segments of the human body and their relationship with anthropometric landmarks. *Voprosy Antropologii*, 62:91–103, 1979.

[50] Simscape Multibody Documentation. Modeling joint connections. *Simscape Inc.*, 2020. https://www.mathworks.com/help/physmod/sm/ug/joints.html.

[51] Mathworks inc. Spatial contact force: Apply contact forces between a pair of connected bodies in simulation. *Mathworks: Help Center*, 2020. https://www.mathworks.com/help/physmod/sm/ref/spatialcontactforce.html.

[52] Bertec Corporation, Leeds, United Kingdom. *Bertec Force Plates*, version 1.0.0 edition, 2012.

[53] P. J. Worthington. A biomechanical analysis of fast bowling in cricket. *Loughborough University Institutional Repository*, page 31, 2010.

[54] Engineers Edge. Coefficient of friction equation table and chart. *www.engineersedge.com*, 2004. http://www.engineersedge.com/coeffients-of-friction.htm.

9 Appendices

9.1 Appendix A - Regression equations for inertial properties

Appendix A details the techniques used for determination of mass and inertia properties for each of the simplified segments used in the rigid multibody simulation.

Main anthropometric measurements*

Segments	**Length (distance between anthropometric landmarks)**		**Circumference, **** the level of measurement
	From	**To**	
Foot	Acropodion	Pternion	Metatarsus
Shank	Tibiale	Sphyrion	Maximum calf
Thigh	Iliospinale anterior	Tibiale	Below the gluteal fold
Hand	Stylion	Dactylion	Metacarpus
Forearm	Radiale	Stylion	Maximum circumference
Upper arm	Acromion (the arm is abducted 90°)	Radiale	Maximum circumference
Head and neck	Vertex	Cervicale	Maximum circumference
Thorax	Cervicale	Xiphion	Immediately below the breast nipples (in men)
Abdomen	Xiphion	Omphalion	At the level of the omphalion
Pelvis	Omphalion	Iliospinale anterior	At the level of the trochanterions

*The length measurements from this table are used mainly for segmentation purposes. They characterize the length of the segments whose inertia properties are determined.

**A tape is perpendicular to the longitudinal axis of a segment.

Best predictive regression equations for estimating inertia properties of body segments in males

Coefficients of linear multiple regression equations

$$Y=B_0+B_1X_1+...+ B_nX_n$$

Inertia properties of the foot

Parameter	B_0	B_1	B_2	B_3	R	σ
Mass, kg	–0.6286	0.066	–0.0136	0.0048	0.723	0.099
CoM, cm	–1.267	0.519	0.176	0.061	0.711	0.92
I_s, kg cm^2	–91.17	5.25	–0.335	0.386	0.810	6.0
I_f, kg cm^2	–89.1	4.788	0.477	0.271	0.835	5.0
I_l, kg cm^2	–11.9	0.77	0.047	0.243	0.518	2.8

CoM position is determined from the end of the second toe.

X_1 –length of the foot, cm. The length is measured as a projected distance between the rearmost point on the heel and the tip of the most prominent toe (in overwhelming majority of the subjects it was the second toe).

X_2 –maximal width of the foot; cm. The width is measured as the distance between the heads of the first and the fifth metatarsals.

X_3 – body fat, kg. Estimated from the skinfold measurements.

Inertia properties of the shank

Parameter	B_0	B_1	B_2	B_3	R	σ
Mass, kg	–6.017	0.0675	0.0145	0.205	0.963	0.121
CoM, cm	0.0937	0.396	0.064	–0.041	0.645	1.1
I_s, kg cm^2	–1437	28.64	3.202	21.6	0.964	24.3
I_f, kg cm^2	–1489	28.97	6.48	21.5	0.968	23.1
I_l, kg cm^2	–194.8	0.214	–3.64	8.9	0.583	20.5

CoM position is determined from the tibiale.

X_1 – length of the shank, cm.

X_2 – lower diameter of the shank, cm (the projected transversal distance between the tips of the malleoli).

$X_3 = \frac{C_1 + C_2 + C_3}{3}$, where C_1 is the proximal circumference of the shank, cm; C_2 is the distal circumference of the shank, cm; and C_3 is the maximal circumference of the shank, cm.

Inertia properties of the thigh

Parameter	B_0	B_1	B_2	B_3	R	σ
Mass, kg	–17.819	0.153	0.23	0.367	0.933	0.572
CoM, cm	–3.655	0.478	–0.07	0.088	0.800	0.99
I_s, kg cm^2	–6729	87.8	50.3	75.3	0.893	206
I_f, kg cm^2	–6774	88.4	38.6	78.0	0.896	205

The CoM position is determined from the iliospinale.

X_1 is the projected length of the thigh measured from the iliospinale to tibiale in the supine position, cm.

X_2 is the lower diameter of the thigh, i.e. the maximal horizontal distance between the tips of the inner and outer tuberosities of the femur (the femoral epicondyles), cm.

$X_3 = \frac{C_1 + C_2 + C_3}{3}$, where C_1 is the distal circumference of the thigh measured 10 cm above the center of the patella, cm; C_2 is the proximal circumference of the thigh measured approximately 2 cm below the gluteal furrow landmark (the gluteal fold), cm; and C_3 is the median circumference of the thigh measured in the middle between the C_1 and C_2 measurements, cm.

9.2 Appendix B - General model parameters

Appendix B provides the MATLAB code used for input variables into the block diagram model (Appendix C).

```
%% General parameters

world_damping = 0.25;
world_rot_damping = 0.25;

%% Inputs
SPPeriod = 0.75;
time = wpspace(0,SPPeriod,9)';
lankle_motiona = deg2rad([0, 0, 0, 0, 0, 0, 0, 0,
0]');
lankle_motionr = deg2rad([0, 0, 0, 0, 0, 0, 0, 0,
0]');
lankle_motionf = deg2rad([0, 0, 0, 0, 0, 0, 0, 0,
0]');
lknee_motionf = deg2rad([0, 0, 0, 0, 0, 0, 0, 0,
0]');
lhip_motiona = deg2rad([0, 0, 0, 50, 40, 40, 20, 0,
-5]');
lhip_motionr = deg2rad([0, 0, 0, 0, -30, -60, -70,
-60, -30]');
lhip_motionf = deg2rad([-40, -30, -50, -10, 40, 15,
5, -5, -10]');
rankle_motiona = deg2rad([0, 0, 0, 0, 0, 20, 0, -
10, 0]');
rankle_motionr = deg2rad([0, 0, 0, 0, 0, 0, 0, 0,
0]');
rankle_motionf = deg2rad([10, 5, 15, 10, 10, 10, 0,
0, 0]');
rknee_motionf = deg2rad([-40, -60, -20, -40, -40, -
20, 0, 0, 0]');
rhip_motiona = deg2rad([0, 0, 0, 0, -10, -20, -40,
-40, -40]');
rhip_motionr = deg2rad([0, 0, 0, 0, 0, 0, 0, 0,
0]');
rhip_motionf = deg2rad([75, 70, 50, 20, 20, 10, 0,
0, 0]');
%sixdof_motion = deg2rad([0, 0, 20, 40, 60, 80,
100, 120, 150,]');
```

```
sixdof_motion = deg2rad([0, 0, 30, 60, 90, 100,
110, 130, 150,]');
% sixdof_motion = deg2rad([0, 0, 45, 75, 100, 120,
135, 145, 150,]');
% sixdof_motion = deg2rad([0, 0, 5, 15, 30, 50, 75,
105, 150,]');
sixdofx_motion = deg2rad([0, 0, 0, 0, 0, 0, 0, 0,
0,]');
sixdofy_motion = deg2rad([-50, -30, -10, 0, 0, 0,
0, 0, 0]');



ActData =
cubspl(sixdof_motion,sixdofx_motion,sixdofy_motion,
lankle_motiona,lankle_motionr,lankle_motionf,lknee_
motionf,lhip_motiona,lhip_motionr,lhip_motionf,rank
le_motiona,rankle_motionr,rankle_motionf,rknee_moti
onf,rhip_motiona,rhip_motionr,rhip_motionf,gaitPeri
od);

%% Contact/friction parameters
constiff = 1000;
condamp = 7500;
u_k = 0.8;
u_s = 0.9;
u_vth = 0.1;
height_plane = 0.025;
plane_x = 25;
plane_y = 3;
contact_point_radius = 0.01;

%% Foot parameters
foot_x = 5;
foot_y = 4;
foot_z = 1;
rfoot_x = 28;
rfoot_y = 15;
```

```
rfoot_z = 7;
lfoot_x1 = 7.5;
lfoot_y1 = 15;
lfoot_z1 = 7;
lfoot_x2 = 11;
lfoot_y2 = 7.5;
lfoot_z2 = 7;
lfoot_x3 = 15;
lfoot_y3 = 10;
lfoot_z3 = 7;
lfoot_x4 = 19.5;
lfoot_y4 = 12.5;
lfoot_z4 = 7;
lfoot_x5 = 22.5;
lfoot_y5 = 15;
lfoot_z5 = 7;
foot_offset = [1 0 0];
lfoot_offset1 = [1.25 0 0];
lfoot_offset2 = [2 0 0];
lfoot_offset3 = [2.5 0 0];
lfoot_offset4 = [3 0 0];
lfoot_offset5 = [3.7 0 0];
rfoot_offset = [6 0 0];
foot_mass = 1.1;

%% Leg parameters
leg_radius = 0.75;
leg_radius1 = 4;
lower_leg_length = 10;
rlower_leg_length = 46;
rupper_leg_length = 45;
llower_leg_length = 56;
lupper_leg_length = 35;
lower_leg_inertia = 684;
lower_leg_mass = 4.9;
upper_leg_length = 10;
upper_leg_density = 4342;
upper_leg_mass = 21.7;
```

```
%% Torso parameters
torso_y = 8;
torso_x = 5;
torso_z = 8;
torso_y1 = 40;
torso_x1 = 20;
torso_z1 = 30;
torso_y2 = 40;
torso_x2 = 20;
torso_z2 = 80;
torso_y3 = 40;
torso_x3 = 20;
torso_z3 = 50;
torso_y31 = 20;
torso_x31 = 20;
torso_z31 = 20;
arm_mass = 6.5;
head_mass = 9.7;

t_off_z = -2;
t_off_x = -1;

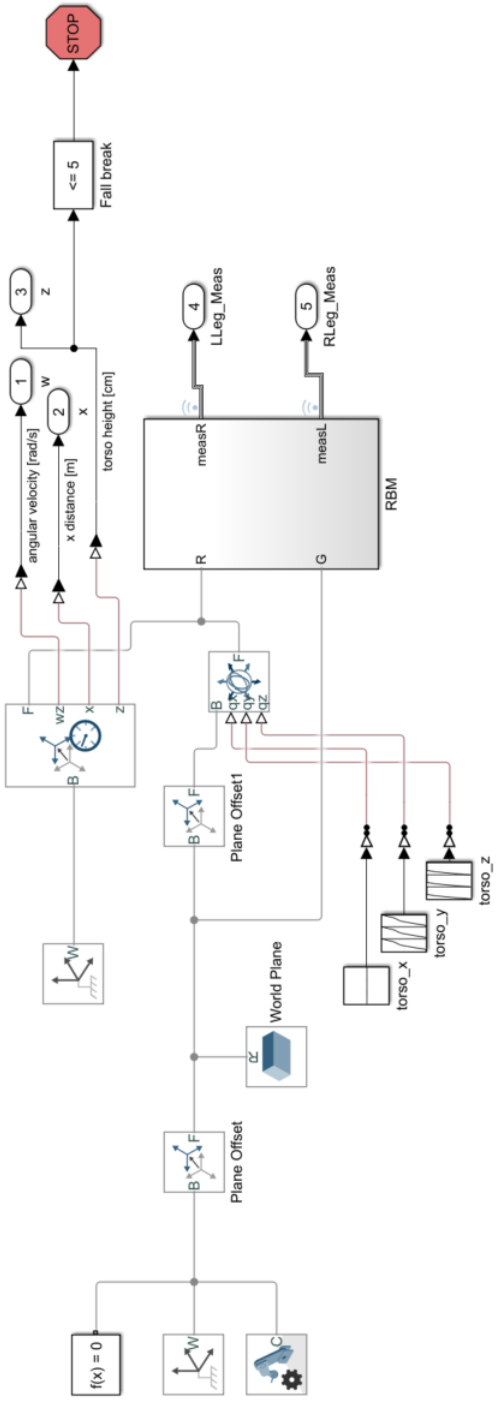
ih = lfoot_z1 + llower_leg_length +
rupper_leg_length + ...
    torso_z1/2-10;
inh1 = lfoot_z1 + llower_leg_length +
lupper_leg_length + ...
    torso_z/2;

%% Joint parameters
joidam = 0.001;
joistiff = 0.001;
timcon = 0.01; %0.025;
```

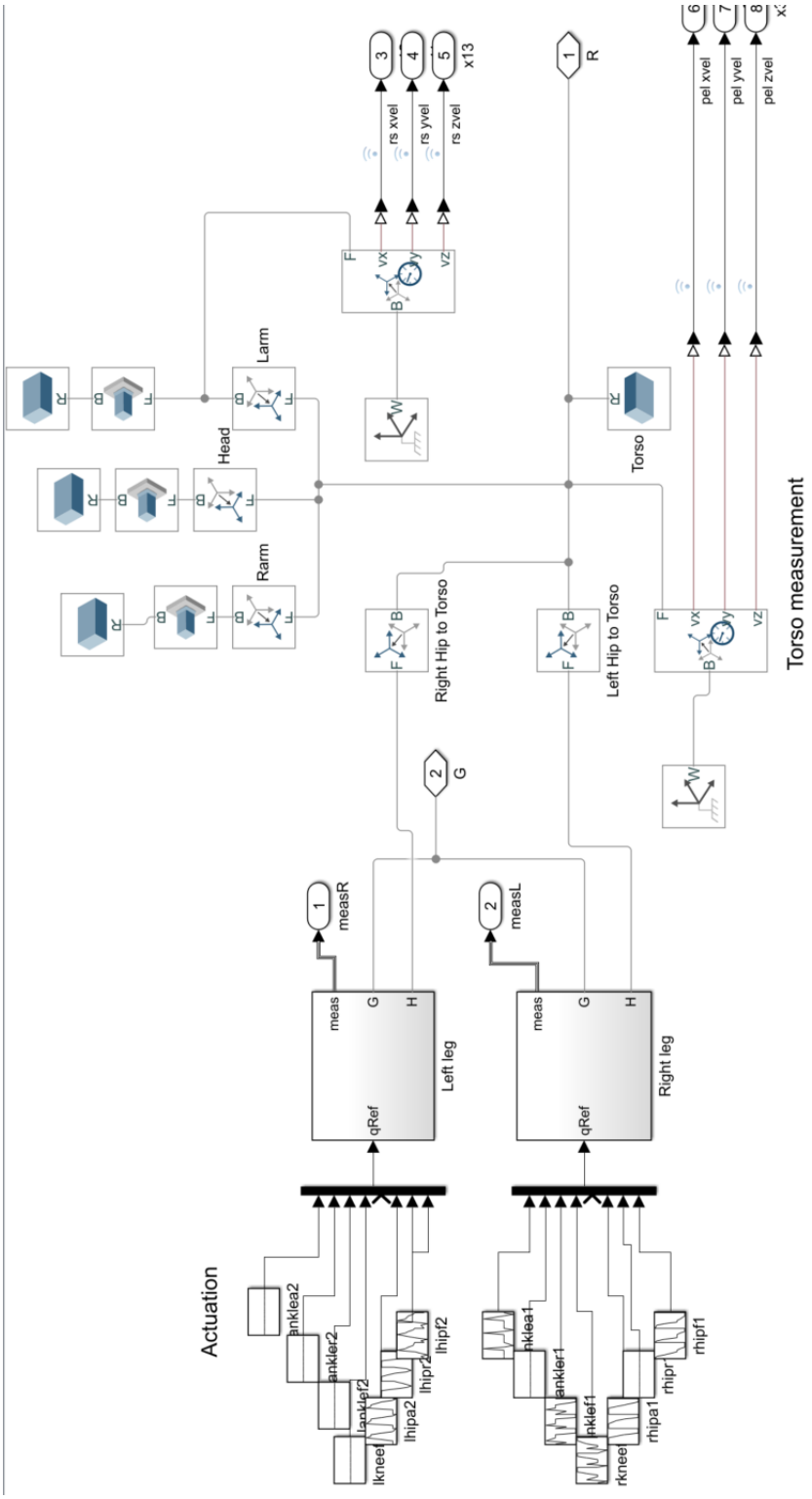
9.3 Appendix C - Simscape Multibody block diagram interface

Appendix C shows images of the world view as well as relevant subsystems for the torso and left/right legs in Simscape Multibody.

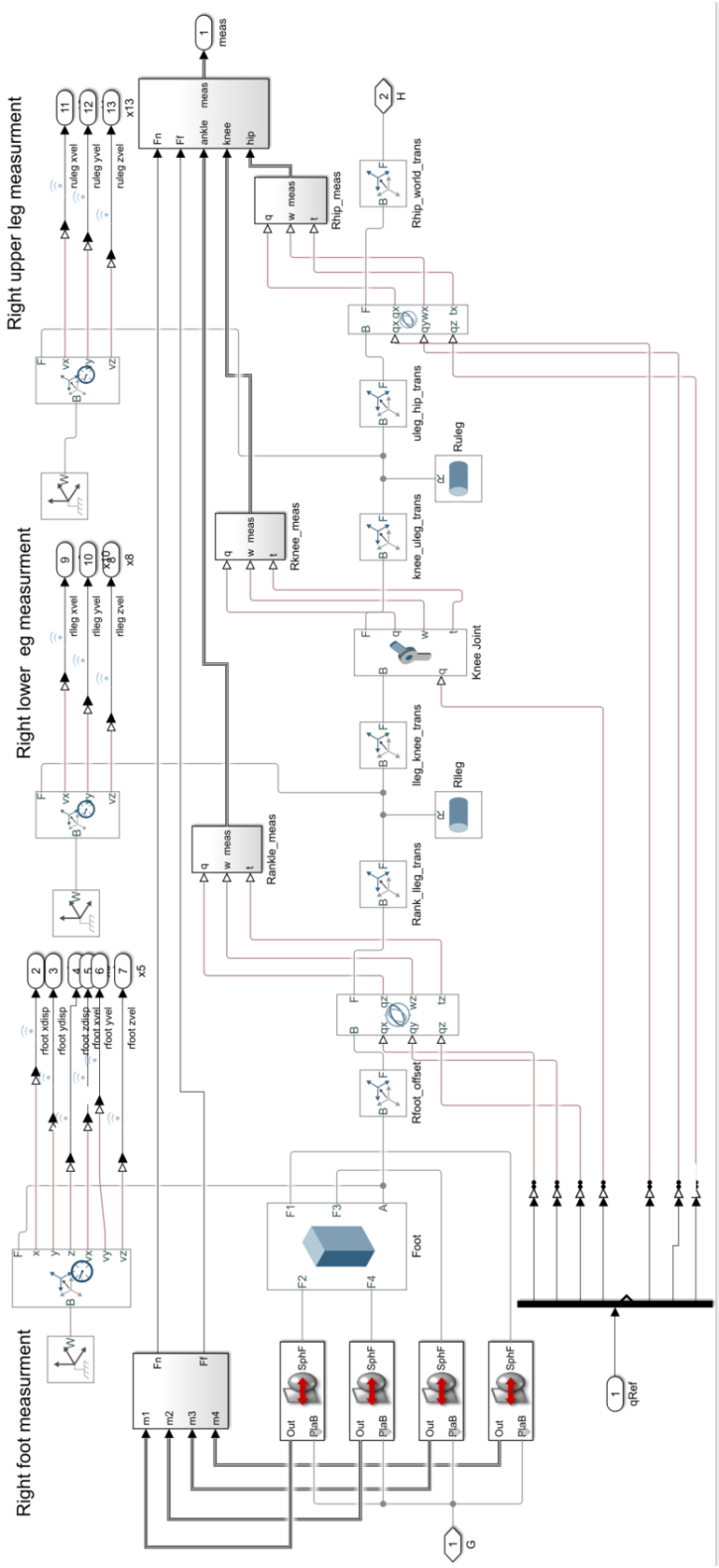
9.3.1 World plane



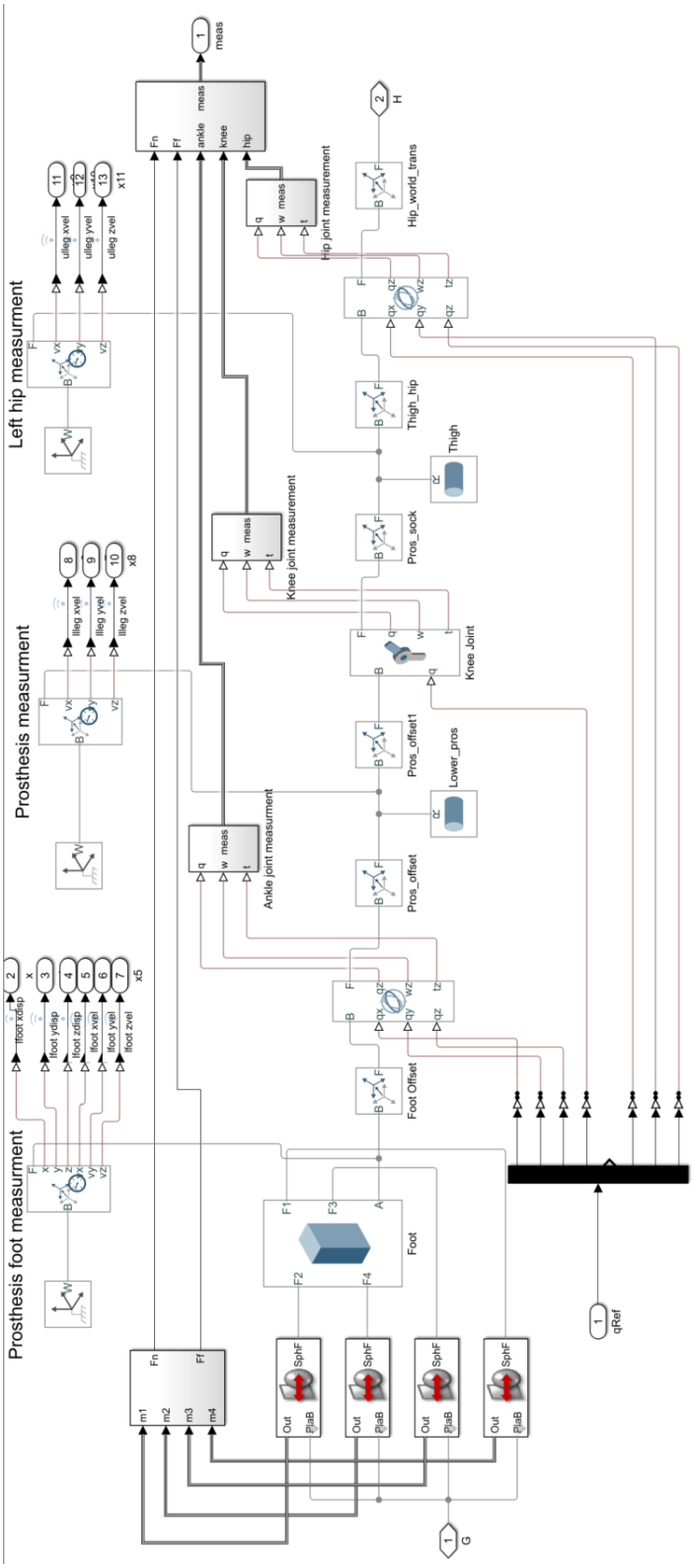
9.3.2 Torso subsystem



9.3.3 Right leg subsystem



9.3.4 Left leg subsystem



9.4 Appendix D - Ethical clearance

Research Office

UNIVERSITY OF THE WITWATERSRAND, JOHANNESBURG

ACKNOWLEDGEMENT OF RETROSPECTIVE APPLICATION FOR ETHICS CLEARANCE
R14/49

CERTIFICATE OF RETROSPECTIVE ACKNOWLEDGEMENT
PROTOCOL NUMBER H19/10/41

PROJECT	Testing parameters of a shot put movement when influenced by a lower limb prosthetic
INVESTIGATORS	Mr N Boulle
DEPARTMENT	Mechanical and Aeronautical Engineering
DATE CONSIDERED	18 October 2019
EXPIRY DATE	16 January 2023
DECISION OF THE COMMITTEE*	Retrospective Acknowledgement

NOTE:
- **The HREC (Non-Medical) acknowledge receipt of this retrospective ethics clearance application.**
- **The HREC (non-medical) found no ethics problems.**
- **This acknowledgment is valid for three (3) years.**

DATE 17 January 2020 **CHAIRPERSON** .....
(Professor J Knight)

cc: Supervisor: Ms T Mangera

DECLARATION OF INVESTIGATOR(S)

To be completed in duplicate and **ONE COPY** returned to the Secretary at Room 10004, 10th Floor, Senate House, University.

I/We acknowledge that appropriate permission should have been sought, this acknowledgement does not entitle the applicant to conduct further research under this protocol number.

Signature

PLEASE QUOTE THE PROTOCOL NUMBER IN ALL ENQUIRIES